(12)

PREDICTION OF CRACK GROWTH IN AQUEOUS ENVIRONMENTS

Final Technical Report

July 1986

By: L. E. Eiselstein, M. C. H. McKubre,
and R. D. Caligiuri

Prepared for:

OFFICE OF NAVAL RESEARCH
800 N. Quincy Street
Arlington, VA 22203

Attn: Dr. A. J. Sedriks
Materials Science Section

SRI International Project No. PYU-4333

Reference: N00014-82-K-0343

SRI International
333 Ravenswood Avenue
Menlo Park, California 94025-3493
(415) 326-6200
TWX: 910-373-2046
Telex: 334486

UNCLASSIFIED
SECURITY CLASSIFICATION OF THIS PAGE

REPORT DOCUMENTATION PAGE

1a. REPORT SECURITY CLASSIFICATION: Unclassified	1b. RESTRICTIVE MARKINGS: None
2a. SECURITY CLASSIFICATION AUTHORITY	3 DISTRIBUTION / AVAILABILITY OF REPORT: Unlimited
2b. DECLASSIFICATION / DOWNGRADING SCHEDULE	
4 PERFORMING ORGANIZATION REPORT NUMBER(S): PYU-4333	5. MONITORING ORGANIZATION REPORT NUMBER(S)
6a. NAME OF PERFORMING ORGANIZATION: SRI International; 6b. OFFICE SYMBOL (If applicable)	7a. NAME OF MONITORING ORGANIZATION: Office of Naval Research
6c. ADDRESS (City, State, and ZIP Code): 333 Ravenswood Avenue, Menlo Park, CA 94025	7b. ADDRESS (City, State, and ZIP Code): 800 N. Quincy Street, Arlington, VA 22203
8a. NAME OF FUNDING / SPONSORING ORGANIZATION: Office of Naval Reaearch; 8b OFFICE SYMBOL (If applicable)	9 PROCUREMENT INSTRUMENT IDENTIFICATION NUMBER: N00014-82-K-0343
9c. ADDRESS (City, State, and ZIP Code): 800 N. Quincy Street, Arlington, VA 22203	10. SOURCE OF FUNDING NUMBERS: PROGRAM ELEMENT NO. / PROJECT NO / TASK NO / WORK UNIT ACCESSION NO

11 TITLE (Include Security Classification)
Prediction of Crack Growth in Aqueous Environmenta

12 PERSONAL AUTHOR(S)
L. E. Eiselstein, M.C.H. McKubre, and R. D. Caligiuri

13a TYPE OF REPORT	13b. TIME COVERED	14 DATE OF REPORT (Year, Month, Day)	15 PAGE COUNT
Final	FROM 4/82 TO 6/86	July 1986	116

16. SUPPLEMENTARY NOTATION

17 COSATI CODES		
FIELD	GROUP	SUB-GROUP

18 SUBJECT TERMS (Continue on reverse if necessary and identify by block number)
Stress corrosion, corrosion fatigue, AC Impedance, tranamission line model, Ti-6Al-4V, HY-80 steel, predictive model

19 ABSTRACT (Continue on reverse if necessary and identify by block number)

The report describea the resulta of a research program to simultaneously determine the mechanical and electrochemical process that occur within and near the tip of active stress corrosion and corrosion-fatigue cracks. Electrochemical/mechanical impedance analysis is one of the few techniques with this capability. Our approach was to make electrochemical/mechanical impedance measurements on HY80 ateel in 3.5 wt% NaCl solutions under corrosion-fatigue conditiona. The data were then analyzed by means of an AC transmission line model to determine the distribution of electrochemicsl and mechanical states within the crack and st the crack tip.

The bulk (uncracked) electrochemical parameters were measured for both HY80 and Ti-6Al-4V by AC impedsnce techniquea. The electromechanical impedance of HY80 was measured and found to be sensitive to crack wall area at frequencies above 1 Hz and more sensitive to the crack tip at mechanical frequencies below 0.1 Hz. A DC transmiaaion line model of the growing corrosion-fatigue cracks constructed from data on HY80 undergoing corrosion-

20 DISTRIBUTION / AVAILABILITY OF ABSTRACT: ☐ UNCLASSIFIED/UNLIMITED ☒ SAME AS RPT ☐ OTIC USERS	21 ABSTRACT SECURITY CLASSIFICATION: Unclassified
22a NAME OF RESPONSIBLE INDIVIDUAL: Dr. A. J. Sedriks	22b TELEPHONE (Include Area Code): (202) 767-6380; 22c OFFICE SYMBOL: Materials Science

DD FORM 1473, 84 MAR — 83 APR edition may be used until exhausted. All other editions are obsolete.

SECURITY CLASSIFICATION OF THIS PAGE
UNCLASSIFIED

19. ABSTRACT (concluded)

fatigue was used to predict crack growth rates and potential and chemistry distributions within the crack. The predicted crack growth rates were in reasonable agreement with the experimentally measured values. The model also predicted a reasonable ΔK threshold for crack growth. At present the model treats the crack tip region rather simply, but several more realistic models exist that could be easily incorporated.

The results of this program have shown that a technique combining AC impedance, electrochemical/mechanical impedance, and transmission line modeling offers the potential to determine both the mechanical and electrochemical processes that occur within stress corrosion and corrosion-fatigue cracks. At present, it is one of the few techniques with this capability. The results did not conclusively show that the combination of AC impedance, electromechanical impedance, and transmission line modeling can be used to quantitatively predict crack growth rates because the transmission line model was not used to reproduce the electromechanical impedance. We recommend additional effort to use the transmission line model in conjunction with the electromechanical/electrochemical impedance to obtain the critical mechanical and chemical parameters at the crack tip. It is clear that, with more modeling and experimental work on a wider variety of materials, load cycles, and aqueous environments, the electrochemical/mechanical technique developed in this program can become an important research tool.

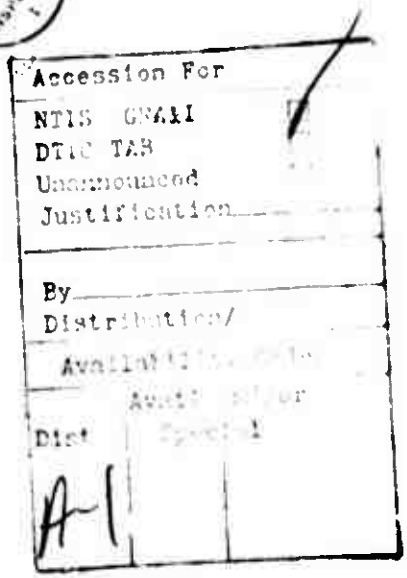

CONTENTS

ACKNOWLEDGMENTS..... ix

LIST OF ILLUSTRATIONS..... v

LIST OF TABLES..... vii

1. INTRODUCTION..... 1

    1.1 Background..... 1
    1.2 Program Objectives..... 3

2. DEVELOPMENT OF THE DISCRETE TRANSMISSION LINE MODEL..... 5

3. EXPERIMENTAL METHODS AND RESULTS..... 13

    3.1 Test Materials and Environment..... 13
    3.2 Electrochemical/Mechanical Experiments 13
        3.2.1 Planar Electrode Experiments..... 19
        3.2.2 Mechanically Loaded Cracked Electrode Experiments..... 29
        3.2.3 Electrochemical Mechanical Impedance Experiments..... 43

4. APPLICATIONS OF THE DISCRETE TRANSMISSION LINE MODEL 53
   TO CRACK GROWTH PREDICTION

    4.1 Overview..... 53
    4.2 Assumptions..... 55
    4.3 Equations..... 56
    4.4 Implementation..... 60
    4.5 Results..... 64

5. CONCLUSIONS 77

REFERENCES 79

APPENDICES

A IMPEDANCE DATA MANAGEMENT AND CONTROL PROGRAM..... A-1

B DIFFUSION IN AN ANGULAR CRACK..... B-1

C DC TRANSMISSION LINE MODEL..... C-1

ILLUSTRATIONS

Figure		Page
1	Transmission Line Model for a Crack in an Aqueous Environment	6
2	Interfacial Impedance Element; Randles' Equivalent Circuit	8
3	Microstructure of Alloys Tested	16
4	Measured and Calculated Impedance Spectra for a Bed of 600-μm Graphite Spheres	18
5	Experimental Configuration for AC and DC Test on Plane Parallel Electrodes	20
6	Tafel Plot for a Plane Parallel Electrode of Ti-6Al-4V Exposed to 3.5 wt% NaCl and 25°C, Voltage Sweep Rate = 0.01 mV s^{-1}	21
7	Mott-Schottky Plot for a Plane Parallel Electrode of Ti-6Al-4V Exposed to 3.5 wt% NaCl at 25°C	23
8	Impedance Locus Plot for a Plane Parallel Electrode of HY80 Exposed to 3.5 wt% NaCl at 25°C	24
9	Reduced Admittance Versus $\omega^{1/2}$ for a Plane Parallel Electrode of HY80 Exposed to 3.5 wt% NaCl at 25°C, Cathodic Potential Range	25
10	Reduced Admittance Versus $\omega^{1/2}$ for a Plane Parallel Electrode of HY80 Exposed to 3.5 wt% NaCl at 25°C, Anodic Potential Range	27
11	Reduced Admittance Versus ω for a Plane Parallel Electrode of HY80 Exposed to 3.5 wt% NaCl at 25°C	28
12	Schematic of Impedance Measurement Systems for Stress Corrosion Crack and Corrosion Fatigue Tests	30
13	Facility for Measuring Impedance Spectra of Stress Corrosion Cracking or Corrosion Fatigue Test Specimens	31

14 Detail of Test Chamber..... 32

15 Detail of Test Specimen..... 33

16 Impedance Response of the Ti-6Al-4V Specimen Before and After the Appearance of a Macroscopic Crack in Aerated 3.5% NaCl Solution..... 36

17 The Effect of Load on the Impedance Response of a Mature Crack in Ti-6Al-4V in Aearated 3.5% NaCl Solution..... 39

18 CT Specimen Geometry for Determining the Electrochemical Mechanical Impedance for the Propagation of a Crack..... 44

19 Simplified Equivalent Circuit for a Stress Corrosion Crack..... 47

20 Complex Plane Plot of the Electrochemical/Mechanical Impedance for the Propagation of a Crack Through HY80 Steel in 3.5% NaCl Solution at 25°C Under Sinusoidal Loading Conditions..... 49

21 Electromechanical/Frequency Plot for an HY80 Specimen 51

22 Crack Growth Flow Chart 61

23 DC Transmission Line Model Calculation of the Potential, Crack Length, and Crack Velocity as a Function of Time for a Crack Grown at Constant Current in HY 80 Steel..... 66

24 DC Transmission Line Model Calculation of the Potential Versus Distance into the Crack as a Function of Time for for HY80 in 3.5% NaCl..... 67

25 DC Transmission Line Model Calculations of Interfacial Current, Metal Ion Concentration, and Crack Electrolyte pH as Function of Distance into Crack..... 68

26 DC Transmission Line Model Calculations of Velocity Versus Applied Potential, Velocity Versus Potential (Expanded), and Log (Velocity) Versus Applied Current..... 71

TABLES

1	Properties of HY80 Steel.....	14
2	Properties of Ti-6Al-4V.....	15
3	Parameter Array.....	62
4	Data Array.....	63
5	Physical and Electrochemical Parameters Used for Model Computations.....	65

ACKNOWLEDGMENTS

The authors would like to thank Dr. Larry Ablow for his contributions on modeling the diffusion within angular cracks, Mr. Andrew Werner and Mr. George Cartwright for their assistance with the design and operation of the experiments, and Ms. Mary Bartholomew, Mr. Lee Gerrans, Ms. Kitta Reeds, Ms. Caren Rickhoff, and Ms. Ruth Tanti for their efforts in preparing and editing this manuscript.

Section 1

INTRODUCTION

1.1 BACKGROUND

The load-bearing capacity of most alloys can be degraded by a corrosive anvironment. Two common forms of environment-aenaitive mechanical property degradation are stress corrosion cracking (SCC) and corrosion fatigue (CF). Both forms greatly influence the aafety, reliability, and economics of many components used in military and commercial power generation, transportation, and energy conversion systems. Therefore, substantial effort haa been made to understand environment-assisted crack growth, to identify and develop materials that have better environment resistance, and to formulata predictive models.[1-15]

These efforta have resulted in various quantitative models being propoaed for predicting SCC, CF, or other types of environment-assisted crack growth. Wei and Landes,[10] for examp'e, conaidered the crack growth rate in a CF aituation to consist of the sum of the crack growth rate in an inert environment and the rate in the environment of interest. The Wei and Landea theory has been ahown to explain adequately many features of the CF behavior of Ti and Ti-6Al-4V in NaCl solutions.[11] Furthermora, thia work emphasized the need for a better understanding of the processes that occur at the crack tip, particularly at threshold load levels for crack growth and at low losding frequencies (< 1 Hz).

For SCC alone, Logan[7] propoaed a model for cracking in aqueous environments based on a slip-dissolution mechaniam at the crack tip. This mechaniam, now widely accepted,[5-7] relates crack growth to the enhanced anodic diaaolution current at the crack tip resulting from the intermittent mechanical rupture of an environmentally created film at the crack tip.

Logan's model has bean modified to include a vsriety of rate-controlling processes that include repassivaton rate, microcraep, solution ranewal, snd critical charge concepts.[8] If the procasses occurring within the crack were better understood, it would be possible to datermine the sppropriate slip-dissolution model for any given material, environment, and load application.

Quantitative modaling of the cracking process is difficult becausa it involves complex interactions between the cracking material, the environment, and the applied load. Because specimen microstructure, surface chemistry, electrochemistry, and loading conditions are expected to influence cracking behavior, they should be accounted for in attempts to model crack growth. Clearly, simultaneous characterization of the mechanical and electrochemical state at the crack tip is required for development of a reliable, predictive crack growth model.

The mechanical state at the crack tip ia usually described in these models using classical fracture mechanics parameters such as the linear elastic stress intensity (K parameter)[16,17] or, more recently, tha elastic-plastic stress intensity (J parameter).[18,19] Unfortunately, the alectrochemical state of the crack tip is not so easily characterized because, until recently, no reliabla experimental method existed that could either provide measurements directly within the crack or convert measurements made external to the crack into crack tip parameters. Some attempts have been made to measure the local chemistries that develop at crack tips by using microanalyticsl chemical techniques on specimens that are actually cracking or on artifical crevices that had been constructed to simulate stress corrosion cracks. Howevar, most of the past crack growth models have used electrochemical data obtained on bulk specimens and have assumed that such data, for example, the free corrosion potential, are representative of values inside the crack, or these bulk values were extrapolated to crack tip values by means of some postulated model. However, crack growth rates predicted by such models can be several orders of magnituda different from those sctually observed.[20,21]

One possible method for evaluating the electrochemical state of material near a crack tip is the AC impedance technique. This technique, under development for the past several years,[22-26] has only recently been applied to the problem of environmentally assisted cracking. This approach shows promise for determining crack tip electrochemical parameters by applying the transmission line model to deconvolve the measured AC impedance spectra of growing cracks.

1.2 PROGRAM OBJECTIVES

The above background discussion highlights the need to characterize simultaneously the electrochemical and mechanical states in a growing stress corrosion or corrosion fatigue crack. Thus, the objective of this research program was to generate electrochemical and mechanical data for actively growing corrosion fatigue cracks and then use these data to develop a preliminary predictive model for SCC and CF.

To accomplish these objectives we used standard fracture mechanics methods and analyses to characterize the mechanical state of the crack in Ti-6Al-4V and HY-80 steel in 3.5% NaCl solution and the AC impedance technique to characterize the electrochemical state. The electrochemical and mechanical data were used to calibrate a transmission line model, and this model was then used to predict quantitatively the electrochemical and mechanical state at the tip of an actively growing crack.

This report describes the results of our efforts to meet these objectives. Section 2 describes the development of the transmission line model. Section 3 reviews the electrochemical and mechanical experimental techniques employed in this program and the results obtained. In Section 4 the transmission line model is presented along with the experimental data used to develop a predictive model for crack growth. Section 5 outlines the conclusions and recommendations for additional work.

Section 2

DEVELOPMENT OF THE DISCRETE TRANSMISSION LINE MODEL

In the diacrete transmission line model the stress corrosion or corrosion-fatigue crack is treated as a cracked electrode. The solid and electrolyte phases in the cracked electrode are represented by resistance elements parallel to the direction of the corrosion current flux, and the interfacial resistance is represented by an impedance distributed between the other two resistancea. The electrode may be treated as "one-dimensional" if the potential (E), current flux (I), and reactant concentrations (c) vary only with the depth within the crack and not with the lateral position along the crack. In thia case, the local values of E, I, and c may be replaced by their average values in a line perpendicular to the crack plane.

Ksenzheck and Stender[27] discussed the conditions that are applicable to transforming a three-dimenaional problem into a one-dimensional one. The mathematical model for the electrical representation shown in Figure 1 requires solutions to a set of differential equationa of the following form:

$$\frac{d^2 I_s}{dx^2} + \frac{d\ \ln(Z)}{dx}\ \frac{dI_a}{dx} - \frac{(r_s + r_e)I_s}{Z} = -\frac{r_e\ I}{Z} \qquad (1)$$

$$\frac{d^2 I_e}{dx^2} + \frac{d\ \ln(Z)}{dx}\ \frac{dI_e}{dx} - \frac{(r_a + r_e)I_e}{Z} = -\frac{r_a\ I}{Z} \qquad (2)$$

$$\frac{d^2 \Delta E}{dx^2} - \frac{(r_s + r_e)}{Z}\ \Delta E = 0 \qquad (3)$$

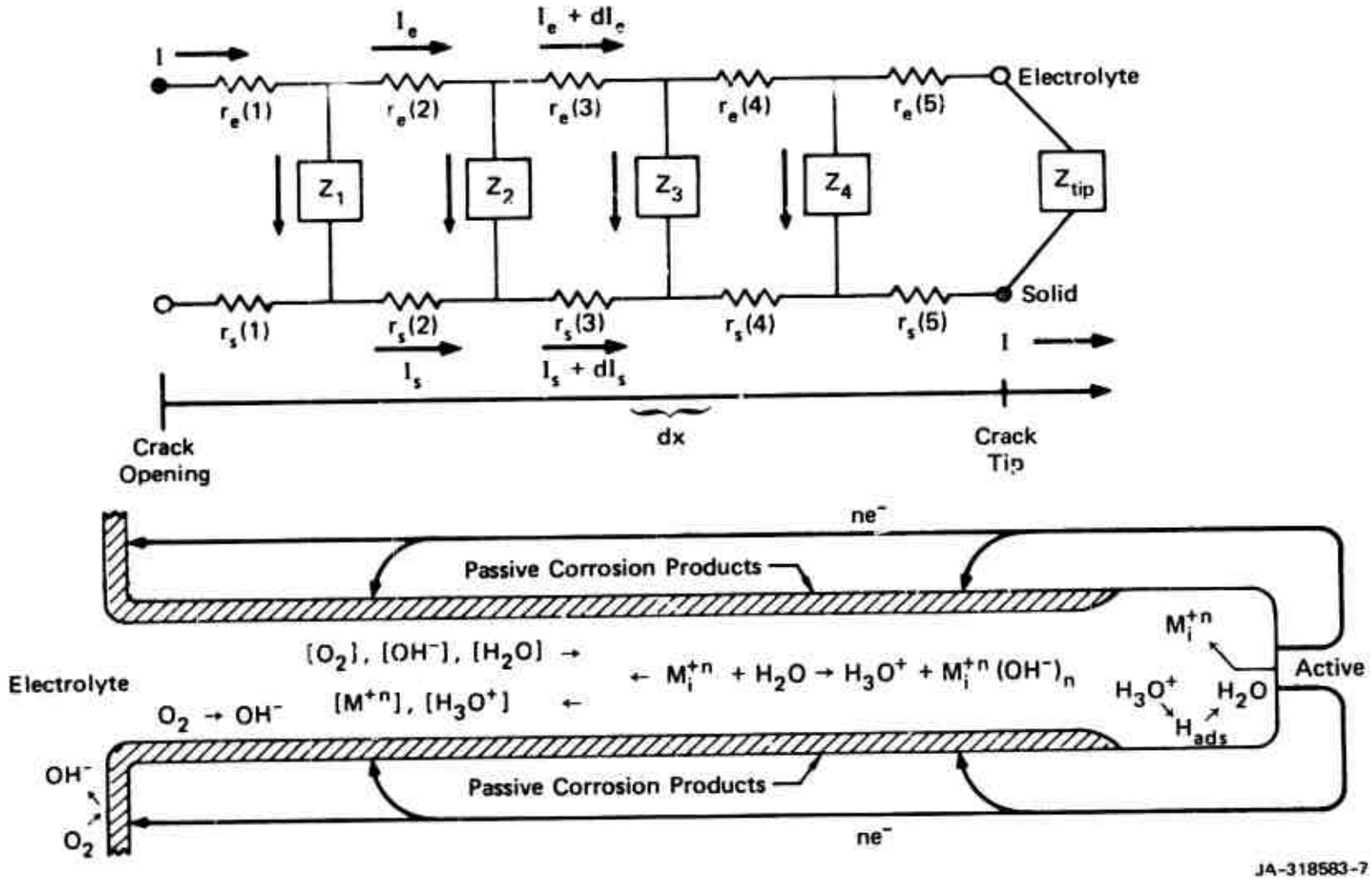

FIGURE 1 TRANSMISSION LINE MODEL FOR A CRACK IN AN AQUEOUS ENVIRONMENT

where subscripts e and s refer to the electrolyte and solid phases, Z is the interfacial impedance, x is distance into the crack, r is the resistance, $I = I_s + I_e$, and $\Delta E = E_a - E_e$.

For the simplest set of boundary conditions shown in Figure 1, corresponding to an electrolyte-filled right cylindrical crack in which r_s and r_e are independent of x and the solid and electrolyte phase current contacts are diametrically opposed, the transmission line impedance Z_{tl} is given by [28]

$$Z_{tl} = \frac{4r_s r_e + (r_s^2 + r_e^2)(e^{\gamma l} + e^{-\gamma l})}{(r_s + r_e)(e^{\gamma l} - e^{-\gamma l})} + \frac{r_s r_e l}{r_s + r_e} \qquad (4)$$

where l is the current crack length, and

$$\gamma = [(r_s + r_e)/Z_i]^{1/2} \qquad (5)$$

The interfacial impedance, Z_i, in equation (5) is equivalent to that at a plane-parallel electrode. That is, it contains the information that would be available if it were possible to determine the electrochemical kinetic properties of each infinitesimal element, dx, of the electrode thickness in the x direction.

The conventional[22-24] equivalent circuit for Z_i is shown in Figure 2. The components of this circuit contain the electrochemical kinetic parameters that are important in evaluating the behavior of a cracked electrode. Brief descriptions of these parameters follow.

Double-Layer Capacitance, C. The double-layer capacitance, C, is directly proportional to the area of the electrolyte/solid phase interface. Thus, given a knowledge of the double-layer capacitance per unit area, C', under the prevailing conditions of reactant concentration, temperature, and potential, one can determine C by deconvolving the measured transmission line impedance. This value of C can then be used to estimate the total wetted area per unit electrode thickness,[28]

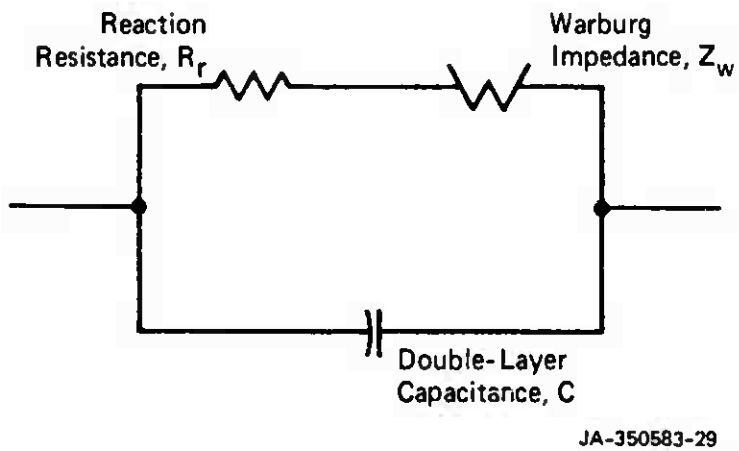

FIGURE 2 INTERFACIAL IMPEDANCE ELEMENT; RANDLES' EQUIVALENT CIRCUIT

which we define as A'. Values of C' may be available from the literature or can be measured directly for a plane-parallel electrode of known area.

Warburg Coefficient, σ. At moderate frequencies ($\gtrsim$ 1 Hz), the Warburg impedance, Z_w, can be expressed as [22,24,29]

$$Z_w = \sigma(1 - j)\omega^{1/2} \tag{6}$$

where

$$\sigma = \frac{RT}{n^2F^2cA''(2D)^{1/2}} \tag{7}$$

in which c is the reactant concentration and A" expresses the electrode electrolyte area per unit length that is actively engaged in reaction. The other parameters in equation (7) have their usual meanings. The relationship between A' and A" can be used to define an area efficiency that accounts for the presence of passive zones, which do not contribute to the cell current during crack growth.

Diffusion Layer Thickness, δ. At the limit of low frequency, an apparent resistive shunt to the Warburg impedance is observed.[29-32] This resistance defines the steady-state DC operating behavior, and its value may be used in conjunction with σ to calculate the effective diffusion layer thickness, δ. In the derivation of equation (6), semi-infinite linear diffusion was assumed. However, in the wide regions near the crack mouth, natural convection will limit the thickness of the diffusion layer, whereas in the narrower regions near the crack tip, the dimension of the diffusion layer is proportional to the crack opening. Thus, we can account for the steady-state DC behavior[22,30-35] in the model of the cracked electrode by introducing the Nernst diffusion layer thickness as a boundary condition.

Interfacial Reaction Resistance, R_r. The reaction resistance together with A" and δ can be used to obtain information regarding the

electrode kinetics[14,29,36] within the crscked electrode. The exchsnge current density, i_o, can be determined from the relstionship

$$R_r = RT/nFA'i_o \tag{8}$$

When used in conjunction with the Stern-Geary relationship,[37] R_r provides a measure of the instantaneous corrosion rate within the crack.

Electrolyte Resistsnce, r_e. The electrolyte resistance per unit length in the cracked electrode, r_e, gives a measure of the amount, composition, and distribution of electrolyte in the crack. The electrolyte resistance is controlled primarily by the crack width and to a smaller extent by the diffusion of reactsnt species from the bulk electrolyte and the diffusion of reaction products from the crack tip.

Solid Electrode Resistance, r_s. The solid phase resistance per unit length in the cracked electrode, r_s, provides a measure of the resistive component in the cracked electrode. Reduction of the impedance data to obtain the parameters of interest for cracked electrodes involves applying nonlinear regression analysis to sn impedance model or equivalent circuit. Broers and coworkers[38-40] demonstrated the applicability of the transmission line model for characterizing porous electrodes in molten carbonate fuel cells, and we believe that these methods can be applied to a growing SC or CF crack.

An additional impedance element, Z_{tip}, has been included in Figure 1 to account for the special electrochemical characteristics of the crack tip. For example, if the crack grows by a mechanism of film rupture and anodic dissolution at the crack tip, then Z_{tip} can be represented as s special case of the equivalent circuit in Figure 2, with R_r determined by the exchange current density for metal disaolution (possibly involving terms for precipitation of oxide and repasaivation). Under the conditions of a cyclic mechanical load, the area term A' in equation (8) must also be given as a periodic function about a mean value, A_o'. In the simpleat case, A' would be a linear function of the mechanical load or crack-opening displacement. Thus,

$$A_{tip} = A^{o}_{tip} \sin(\omega t + \phi) \tag{9}$$

where ω is the frequency of the load variation, and ϕ is the phase delay between load variation and film rupture.

Equation (9) suggests a second method of evaluating the electrochemistry of the crack tip environment, using the transmission line model. Under a steady electrical bias (a small DC voltage more positive than the free corrosion potential), a DC current can be made to flow from the specimen to a suitable counterelectrode. This current originates with the anodic dissolution at the crack tip and is given by

$$I(\omega t) = \eta / R_r \tag{10}$$

where $\eta = V_{applied} - V_{free\ corrosion}$.

Substituting equation (9) into equation (8) and then substituting the resulting expression for R_r into equation (10) yields

$$I(\omega t) = \frac{\eta n F A^{o}_{tip} \sin(\omega t + \phi) i_o}{RT} \tag{10a}$$

This expression for $I(\omega t)$ describes the crack tip current expected for cyclic load conditions.

This can be viewed as a sinusoidal current source originating at the crack tip. The current source is situated where the interfacial reaction resistance (R_r in Figure 2) is placed in Z_{tip} in Figure 1.

Alternatively, we can define an electrochemical/mechanical impedance,

$$Z_{em} = Z/I \tag{11}$$

which may be examined as a function of the frequency (and amplitude) of the mechanical load variation.

The advantage of an electrochemical/mechanical impedance study is that the perturbation is applied exactly at the point of interest (the crack tip). In the alternative method, a variable frequency electrical potential variation is applied to the mouth of a crack in a specimen cycled with a constant frequency mechanical load; however, this results in a perturbation that decreases in amplitude at the crack tip as the crack increases in length.

Section 3

EXPERIMENTAL METHODS AND RESULTS

3.1 TEST MATERIALS AND ENVIRONMENT

Two test materials were used in this program: a titanium alloy (Ti-6Al-4V) and a medium-strength low-alloy steel (HY 80). These materials were selected because of their possible application in submarine hull structures and for the range of electrochemical and corrosion-fatigue behavior these materials cover. The chemistry and mechanical properties of the Ti-6Al-4V and HY 80 are given in Tables 1 and 2, and the microstructures are shown in Figure 3. Note that the HY 80 has a bainitic microstructure typical of a quench and temper heat treatment, whereas the Ti-6Al-4V exhibits an alpha-beta structure typical of the mill-produced hot-rolled and annealed condition.

The test environment selected for this program was the standard 3.5% NaCl solution. This environment was created by dissolving the appropriate amount of reagent grade NaCl in deionized water. This solution was aerated and continuously refreshed into the test chamber at a rate of about 1 liter/hr.

3.2 ELECTROCHEMICAL/MECHANICAL EXPERIMENTS

To generate the electrochemical/mechanical data needed for the transmission line model, we performed three types of AC impedance-based experiments in this program: (1) planar (uncracked) electrode experiments to characterize the bulk electrochemical properties of the materials without any mechanical loading, (2) cracked electrode experiments to characterize the voltage/current response during active loading of a crack, and (3) cracked electrode electromechanical impedance experiments to characterize the voltage displacement response during active loading of a crack.

Table 1

PROPERTIES OF HY80 STEEL
(5.08-cm-thick plate, Mil-S-16216H, ASTM Grain Size 8)

Elemental Analysis			Mechanical Properties[a]	
Element	wt%	Heat Treatment	Parameter	Value
C	0.17	Austentized at	σ_{ys}	87.8 ksi
Mn	0.34	1010°C for 120	σ_{uts}	106 ksi
P	0.010	minutes and water	%E	23.7%
S	0.10	quenched;	%RA	66.7%
Si	0.23	Tempered at	CVN	95 ft-lb
Cr	1.56	682°C for 120		at -120°F
Ni	2.88	minutes and air		
Mo	0.24	cooled.		
Cu	0.17			
Ti	0.001			
V	0.001			

[a]Definitions:

σ_{ys} = 0.2% offset yield strength.

σ_{uts} = ultimate tensile strength.

%E = percent total tensile elongation to failure.

% RA = reduction in area of necked region at fracture.

CVN = charpy V-notch impact energy; CVN was determined under the following conditions: Type A, notch V, full size, longitudinal orientations.

Table 2

PROPERTIES OF Ti-6Al-4V
(AMS 4911, 40.6-cm-thick plate)

Elemental Analysis			Mechanical Properties[a]	
Element	wt%	Heat Treatment	Parameter	Value
C	0.03	Hot rolled and annealed	σ_{ys}	131 ksi
Al	6.25		σ_{uts}	143 ksi
Fe	0.07		%E	12.4
V	3.95		%RA	26.3
O_2	0.162			
N_2	0.015			
H_2	0.002			

[a]Definitions:

σ_{ys} = 0.2% offset yield strength.

σ_{uts} = ultimate tensile strength.

%E = percent total tensile elongation to failure.

%RA = present reduction in area of necked region at fracture.

CVN = charpy V-notch impact energy.

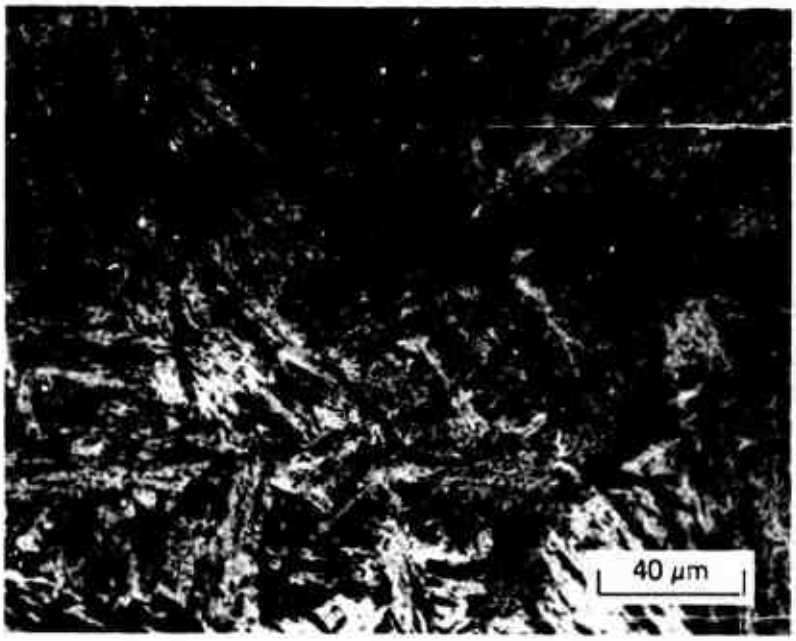

(a) HY80 (Looking onto plane of crack path)

(b) Ti-6Al-4V (Looking onto plane of crack path)

JP 4333 11

FIGURE 3 MICROSTRUCTURE OF ALLOYS TESTED

The methods used and the results obtained for each of these three experiments are discussed in the following subsections. However, before discussing these experiments, it is important first to review some of the advantages and limitations encountered when applying these electrochemical techniques.

To calculate accurately the many electrochemical parameters that can be obtained from AC measurements, it is necessary to obtain high-precision impedance measurements over a wide range of frequencies, particularly at very low frequencies. The unavailability of adequate instrumentation has been the principal limitation to the characterization of cracked or porous systems by AC techniques and is largely responsible for the only modest success of Broers and coworkers.[38-40] More recently, Mund et al.[41] analyzed the performance of hydrogen electrodes in alkaline fuel cells systems from AC impedance measurements applied to a transmission line model.

The current work of Hills and coworkers[42-44] provides good verification for the application of the transmission line model and the extension of equilibrium AC measurements for predicting the steady-state electrochemical parameters. In one set of experiments, the interfacial impedance components were calculated from the measured impedance of a packed bed of graphite spheres using the transmission line model, and the results were compared with the interfacial impedance measured directly for a single sphere.

Figure 4 shows the impedance data obtained for a packed-bed electrode superimposed on the least-squares best fit of data to equation (4). The tabulated values of the double-layer capacitance, Warburg coefficient, and exchange current density for the packed bed were calculated from this regression fit. These values were compared with the interfacial impedance parameters measured directly for a single graphite sphere isolated from the bed. The substantial agreement between the two sets of calculated impedance parameters is strong verification for the applicability of the transmission line model to characterizing porous or cracked electrodes.

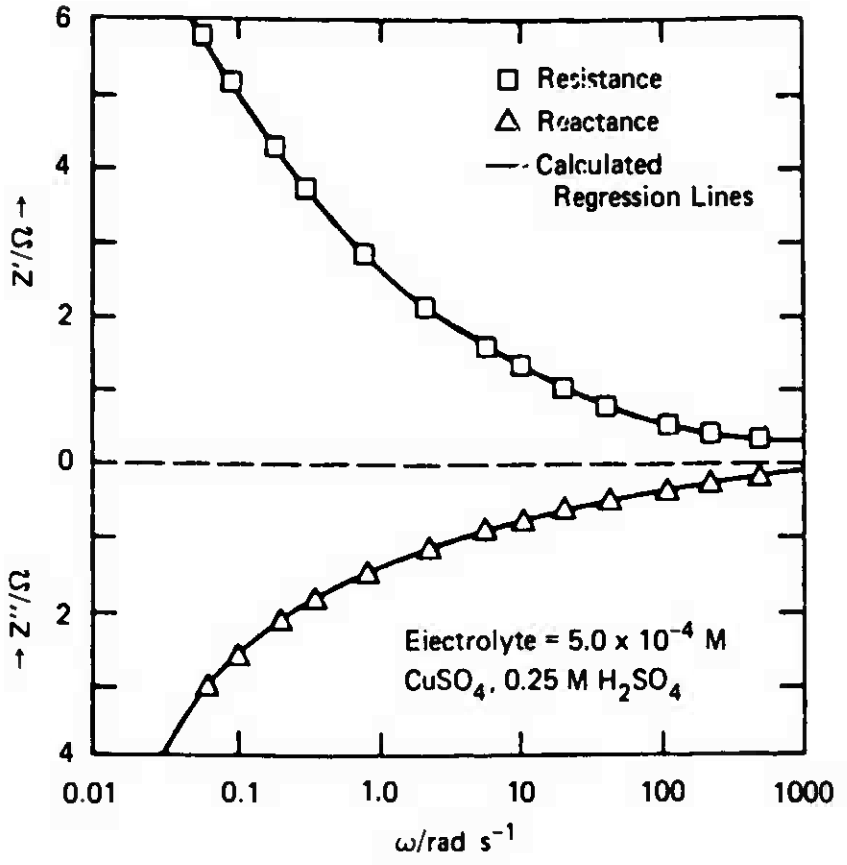

Derived Parameters	Packed Bed	Single Sphere	
C_d	154×10^{-6}	130×10^{-6}	F cm^{-2}
σ	120	120	$\Omega\ s^{-1/2}\ cm^{-2}$
i_o	6.3×10^{-3}	12.4×10^{-3}	cm^{-2}

JA-350522-17

FIGURE 4 MEASURED AND CALCULATED IMPEDANCE SPECTRA FOR A BED OF 600-μm GRAPHITE SPHERES

(From Reference 4)

This previous research clearly shows that many important operating parameters of porous and cracked electrodes are contained within the measured impedance dispersion. However, two factors are fundamental in the application of this method to the in situ determination of electrode characteristics. First, impedance measurements must be of sufficient precision (better than 0.1% for each impedance component),[22] and second, the measurements must be made over a frequency range wide enough (10^{-3} to 10^{4} Hz) to adequately resolve the impedance spectrum and to allow subsequent deconvolution to obtain the electrochemical parameters.

The requirements for a high-speed, high-precision, impedance measurement system capable of operating at very low frequencies have been presented in detail by Macdonald and McKubre.[22] In general, these requirements are in conflict. Maximum acquisition speed is available from noise or transform methods, but these methods are not very precise.[22] High precision is best achieved with a frequency-by-frequency measurement technique such as phase-sensitive detection, but the measurements are time consuming. Fortunately, this is not a serious hindrance when such equipment is automated and the experiments are computer-controlled. We used such automated, computer-controlled equipment in the experiments described in the following subsections.

3.2.1 Planar Electrode Experiments

Experiments were performed on planar uncracked electrodes of HY80 and Ti-6Al-4V exposed to aerated 3.5 wt% NaCl to obtain the electrochemical parameters needed for developing the DC, crack propagation model and to aid in interpretating the results of electromechanical impedance testing. The experimental setup for these tests is shown in Figure 5. Specimens were mounted with one planar surface exposed to the electrolyte.

Figure 6 presents the Tafel plot obtained for Ti-6Al-4V at very low sweep rates; the sweep was initiated at the cathodic limit of -500 mV versus the saturated calomel electrode (SCE). The apparently well-behaved Tafel law behavior evidenced by the region of linear

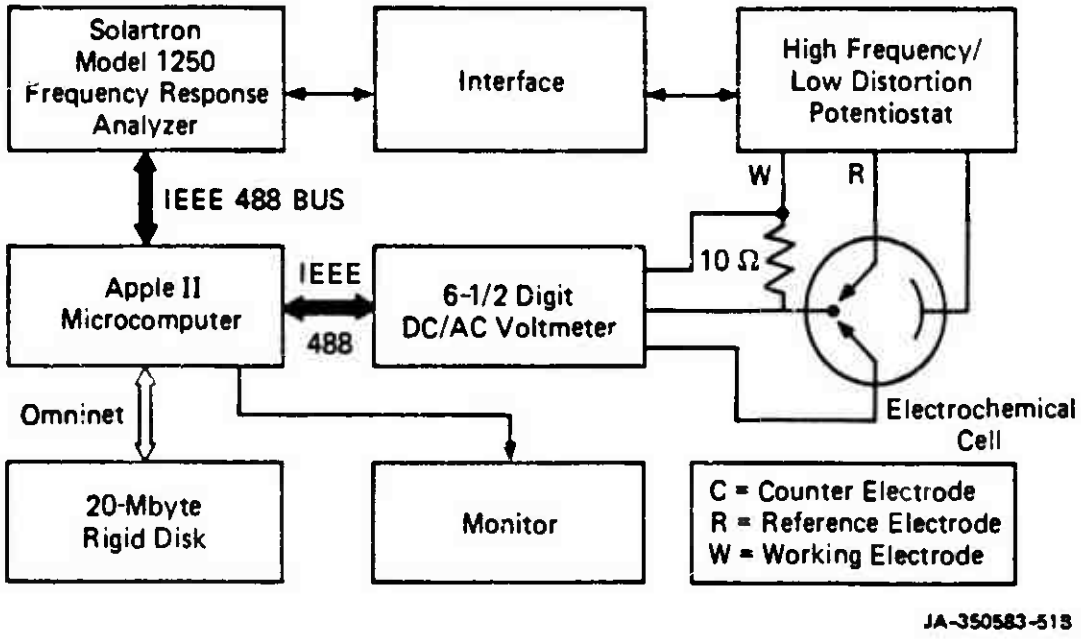

FIGURE 5 EXPERIMENTAL CONFIGURATION FOR AC AND DC TEST ON PLANE PARALLEL ELECTRODES

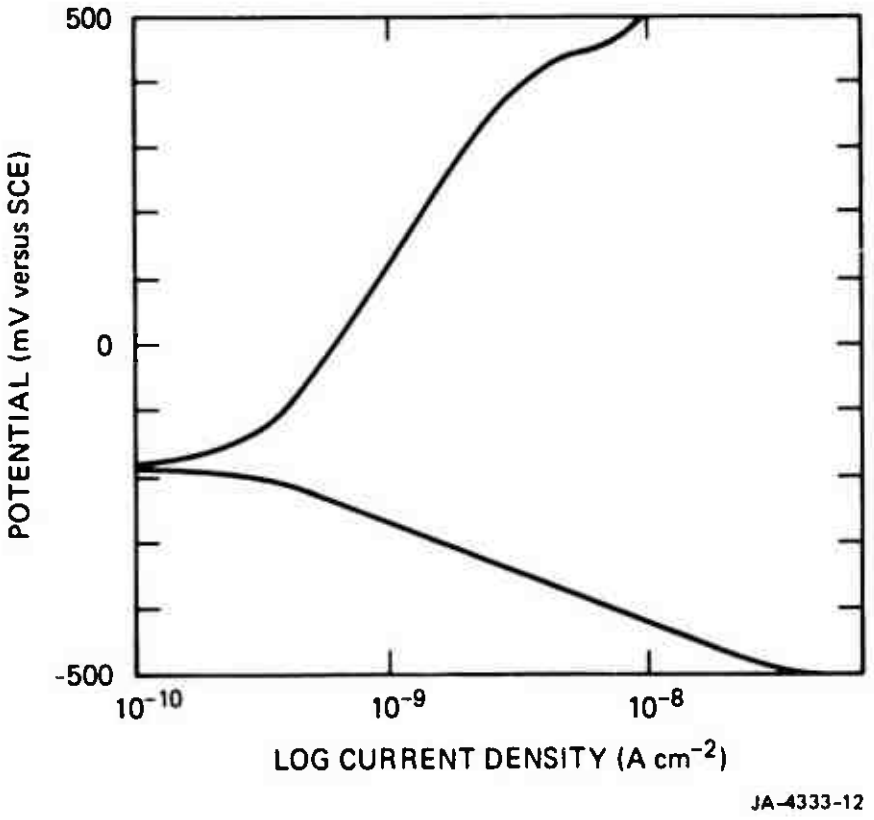

FIGURE 6 TAFEL PLOT FOR A PLANE PARALLEL ELECTRODE OF Ti-6Al-4V EXPOSED TO 3.5 wt% NaCl AND 25°C, VOLTAGE SWEEP RATE = 0.01 mV s^{-1}

relationship between voltage and the logarithm of current auggests charge-transfer kinetic rate control in both the anodic and cathodic regions.

The AC impedance behavior of this electrode, however, strongly indicates that the reaction kinetics of the Ti-6Al-4V electrode surface is dominated by the presence of a semiconducting oxide film such as TiO_2. Evidence of the dominance of semiconductor-electrochemical effects can be seen in the Mott-Schottky plot presented as Figure 7. The reciprocal of the measured capacitance squared is plotted versus potential at 25-mV steps from -200 to -1200 mV versus SCE. Regions of linearity in such a plot indicate the presence of a space-charge layer[45,46] (band bending within the oxide film). The type of frequency dispersion ahown in Figure 7 (that is, the lines at each frequency do not superimpose) is unusual and may be due to impedance effects within the electrolyte phase (the electrical double layer) or to heterogeneity within the oxide itself. The extrapolated intercept of this family of lines with the axis at $C \to \infty$ ($1/C^2 \to 0$) indicates the position of minimum band bending (the "flat-band" potential), which is a characteristic of each semiconducting oxide.[45,46] This intercept of ~ 1100 mV SCE is within 100 mV of that expected for pure TiO_2. This 100 mV offset is a result of the defect structure and doping of the Ti-6Al-4V film that forms in the chloride environment.

The HY80 specimena showed a more conventional bulk electrochemical response than the Ti-6Al-4V. The HY80 specimen did not show Mott-Schottky behavior, which is not surprising becauae the corrosion film that develops is poroua and without uniform composition through its thicknesa; that ia, the donor density variea through the film thickness. Figure 8 shows the impedance locus or Nyquist[47] reaponse of a plane parallel electrode of HY80 exposed to aerated 3.5 wt% NaCl, at the free corrosion potential. The depressed aemicircular form is that expected for a metal electrode actively corroding under mixed kinetic/mass transport control. Figure 9 presents data collected at the same electrode, covering a range of potentials more cathodic than the

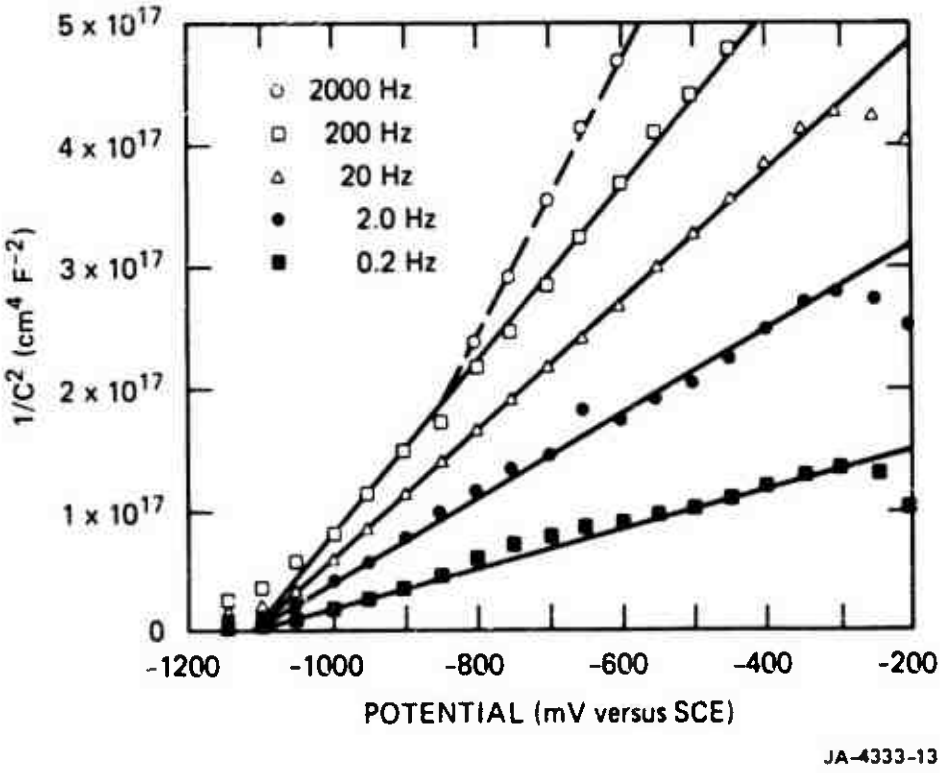

FIGURE 7 MOTT-SCHOTTKY PLOT FOR A PLANE PARALLEL ELECTRODE OF Ti-6Al-4V EXPOSED TO 3.5 wt% NaCl AT 25°C

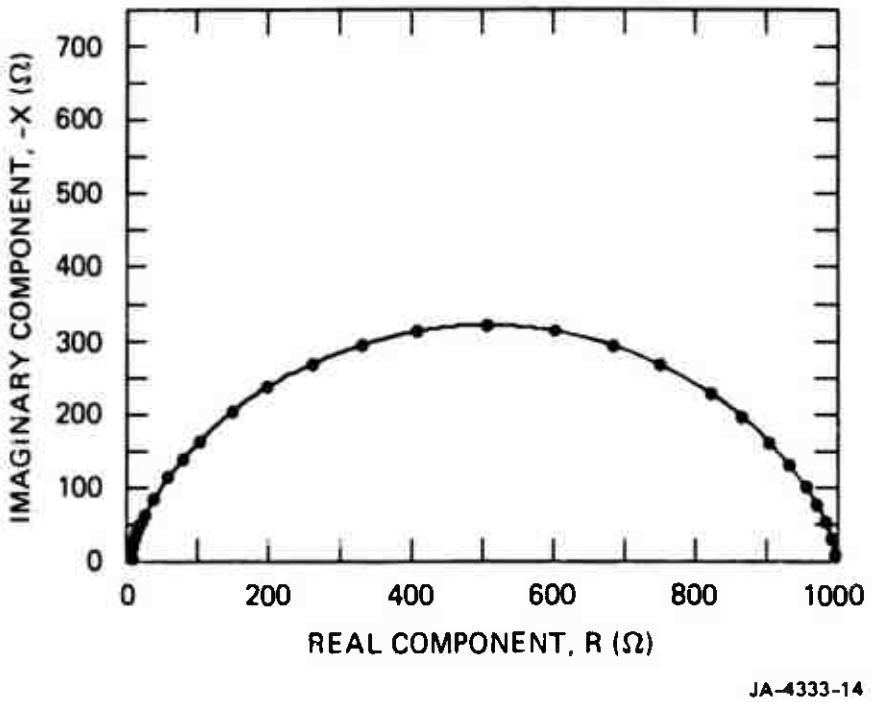

FIGURE 8 IMPEDANCE LOCUS PLOT FOR A PLANE PARALLEL ELECTRODE OF HY80 EXPOSED TO 3.5 wt% NaCl AT 25°C

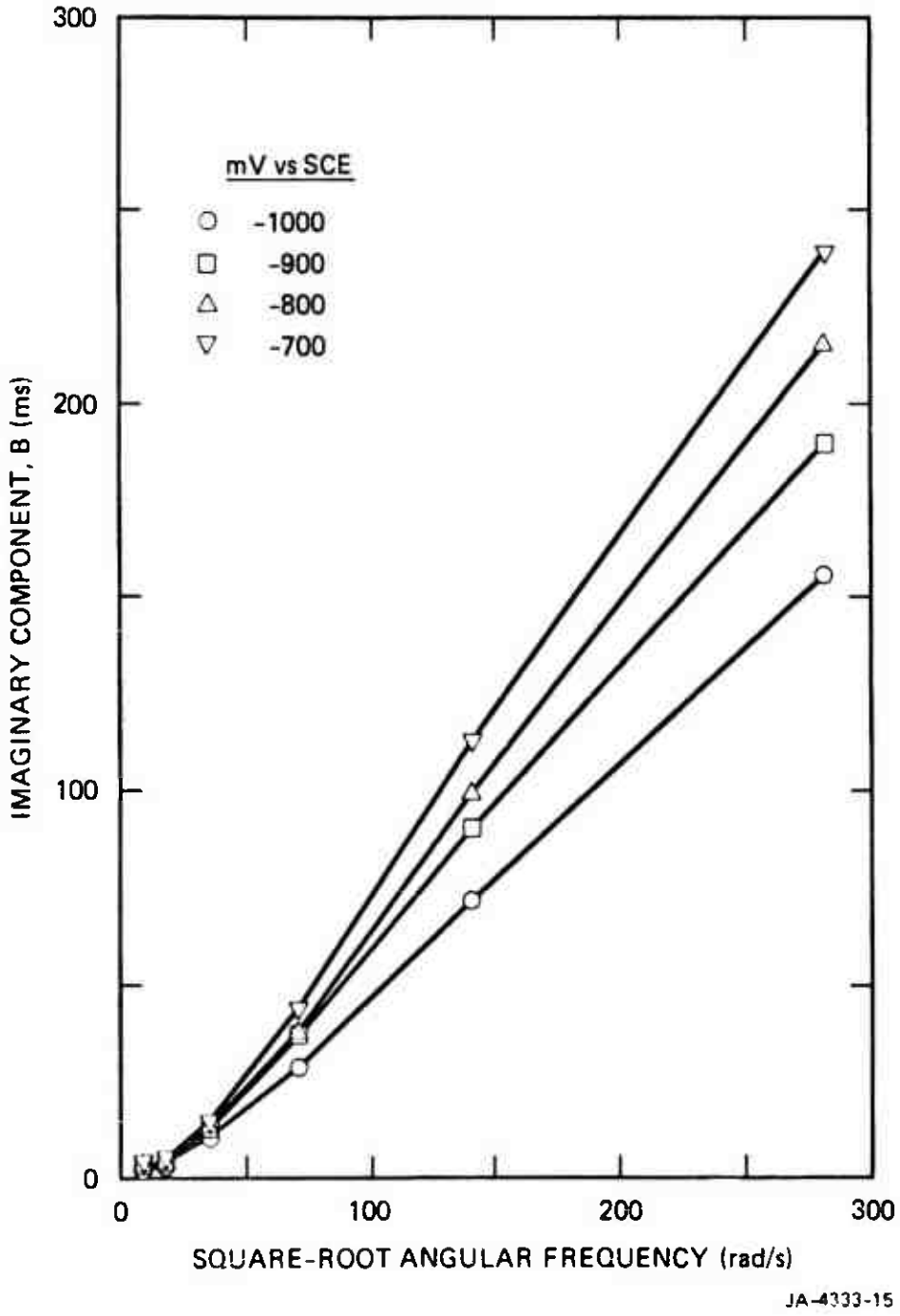

FIGURE 9 REDUCED AOMITTANCE VERSUS $\omega^{1/2}$ FOR A PLANE PARALLEL ELECTROOE OF HY80 EXPOSED TO 3.5 wt% NaCl AT 25°C, CATHODIC POTENTIAL RANGE

free corrosion potential of HY80 (~ -600 mV versus SCE in aerated 3.5 wt% NaCl). These data are plotted as the reduced admittance, B, versus the square root of the angular frequency, $\omega^{1/2}$,

$$B = -X/[(R - R_s)^2 + X^2] \qquad (12)$$

where $\omega^{1/2} = (2\pi f)^{1/2}$, X is the imaginsry component of the impedance, R is the real component of the impedance, R_s is the uncompensated series electrolyte resistance, and f is the frequency of the impedance measurement in Hz.

The family of straight linea in Figure 9 indicates thst, at potentials more negative than (cathodic to) the free corrosion potential, the impedance of an HY80 surface is dominated by diffusional effects within the electrolyte.[47] At potentiala higher than -700 mV, however, deviation from a linear B versus $\omega^{1/2}$ dependence occurs, as shown by the data at -550, -450, and -400 mV, plotted in Figure 10. These data are replotted in Figure 11 versus ω. The straight lines shown are regreasion fits to the data points; this linearity indicates that the imaginary part of the admittance is dominated by a capacitance of approximately 20 $\mu F\ cm^{-2}$.[47] The slope of $dB/d\omega$ is equal to the double-layer capacitance and can be seen in this potential range because of the absence of diffusional control effects.

At -300 mV versua SCE, the electrode admittance increasea greatly snd again displays linesrity versua $\omega^{1/2}$, as shown in Figure 10. Thia is the tranapaasive region for HY80, and the electrode impedance becomes dominated by the maaa transport of corrosion producta from the electrode surface.

In summary, the recults of planar electrode experiments on bulk Ti-6Al-4V and HY80 specimens ahowed that, over an extended potential range, the Ti-6Al-4V specimen behsved ss if it were covered by a dense semiconducting oxide layer. It exhibited the characteristic linear $1/C^2$

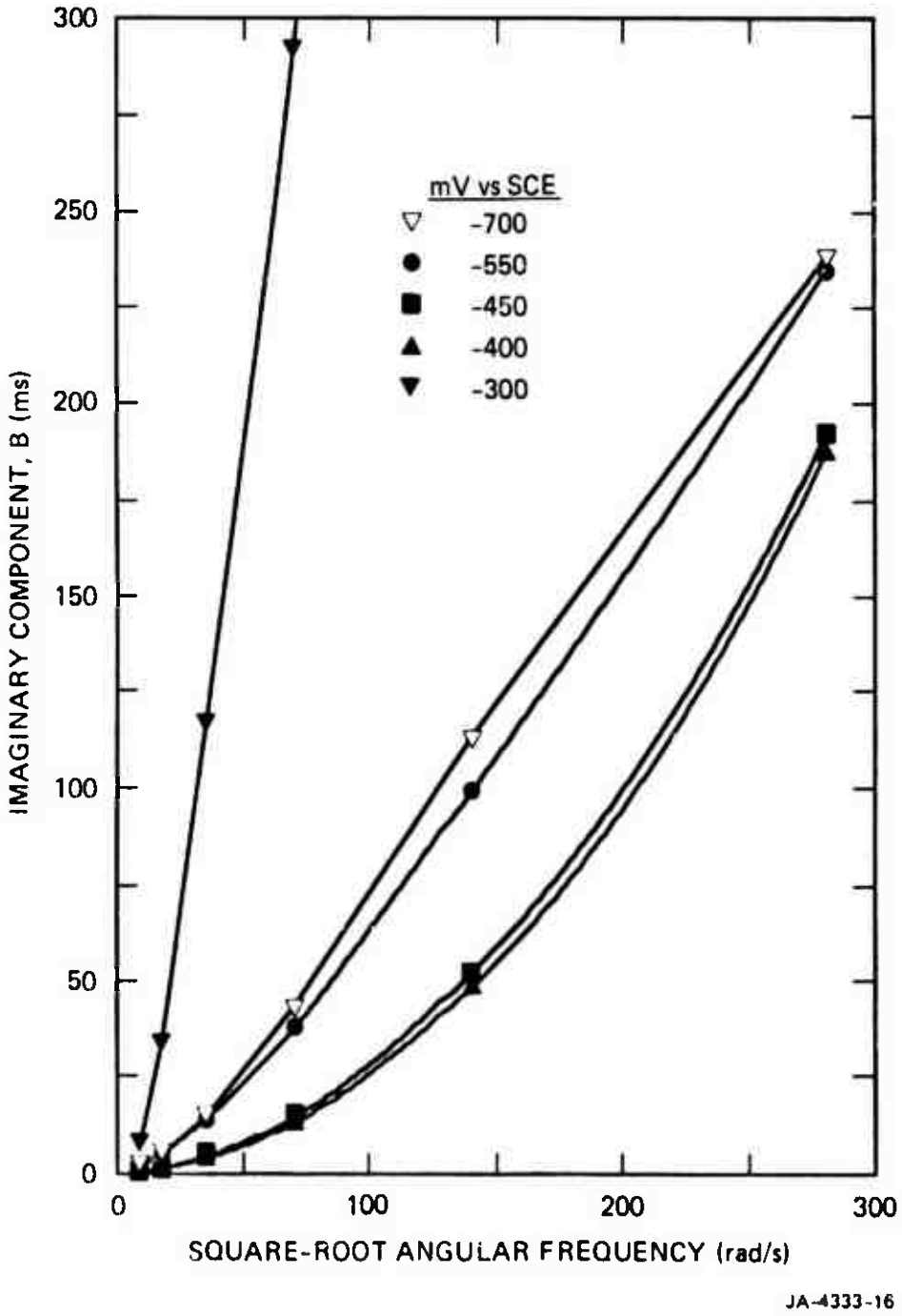

FIGURE 10 REDUCED ADMITTANCE VERSUS $\omega^{1/2}$ FOR A PLANE PARALLEL ELECTRODE OF HY80 EXPOSED TO 3.5 wt% NaCl AT 25°C, ANODIC POTENTIAL RANGE

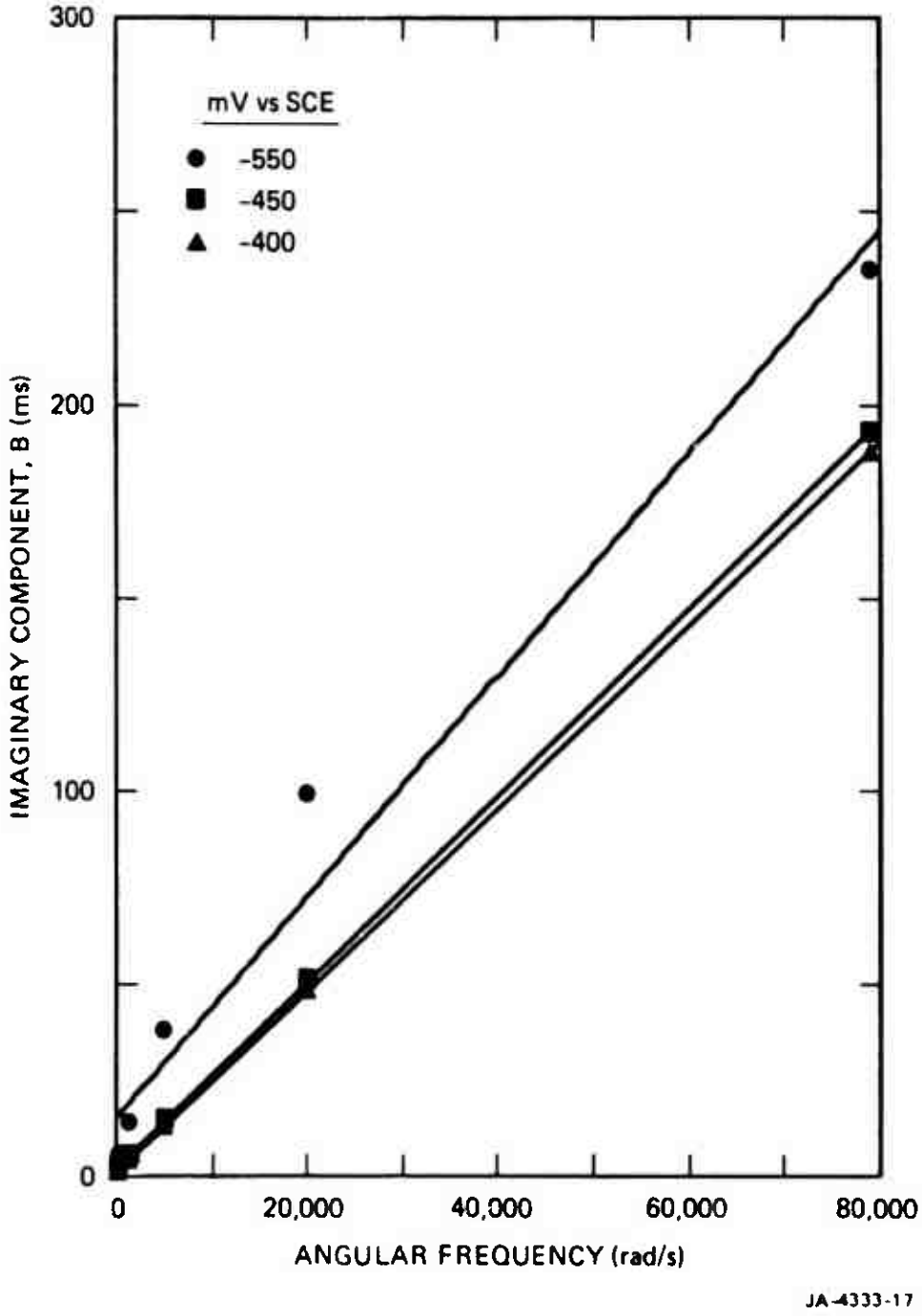

FIGURE 11 REDUCED ADMITTANCE VERSUS ω FOR A PLANE PARALLEL ELECTRODE OF HY80 EXPOSED TO 3.5 wt% NaCl AT 25°C

versus voltage behavior. On the other hand, the dependence of the impedance response on voltage for HY80 was more complex although more typical of a corroding electrode. At potentials less than and equal to the free corrosion potential, the electrode impedance response was dominated by diffusion, presumably of reactant (dissolved O_2) to the electrode. At potentials up to 200 mV more positive than the free corrosion potential, in the potential range where a pseudo-passive film is expected to form, the impedance appears to be dominated by an essentially voltage-independent capacitance, almost certainly due to the electrical double layer in the electrolyte. At still more positive potentials, in the transpassive range, the electrode impedance appears to be dominated by the diffusion of reaction products from the electrode surface.

3.2.2 Mechanically Loaded Cracked Electrode Experiments

We developed an experimental facility designed to obtain data on crack electrochemistry during CF and SCC of various materials in aqueous solutions at room temperature and pressure. Figure 12 diagrams the experiment arranged for impedance measurement of specimens under mechanical load conditions. Photographs of the setup are shown in Figure 13 (electronics), Figure 14 (test chamber), and Figure 15 (test specimen).

As detailed in Figure 12, impedance measurements were obtained using a Solartron Model 1250 frequency response analyzer (FRA) operated under microcomputer control. The Model 1250 is an automated, digitally demodulated, stepped frequency, impedance meter capable of 0.01% precision for each impedance component in the frequency range 10^{-4} to 6×10^4 Hz. This instrument and the preceding series of frequency response analyzers (Solartron Model 1172 and 1174) have been used extensively in recent years to meaaure impedances in electrochemical systems.[48-52]

The FRA was operated under the control of an Apple II-Plus microcomputer equipped with 64 kbyte of internal random access memory (RAM),

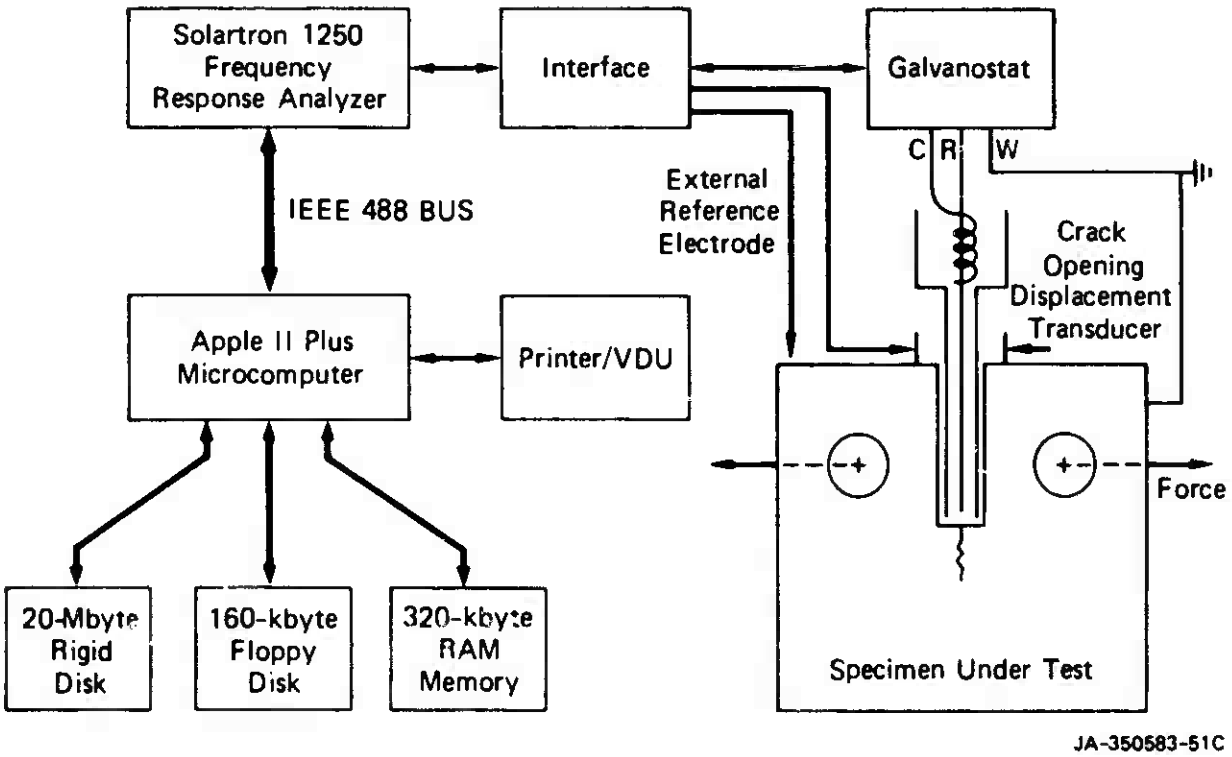

FIGURE 12 SCHEMATIC OF IMPEDANCE MEASUREMENT SYSTEM FOR STRESS CORROSION CRACK AND CORROSION FATIGUE TESTS

JP-4333-4

FIGURE 13 FACILITY FOR MEASURING IMPEDANCE SPECTRA OF STRESS CORROSION CRACKING OR CORROSION FATIGUE TEST SPECIMENS

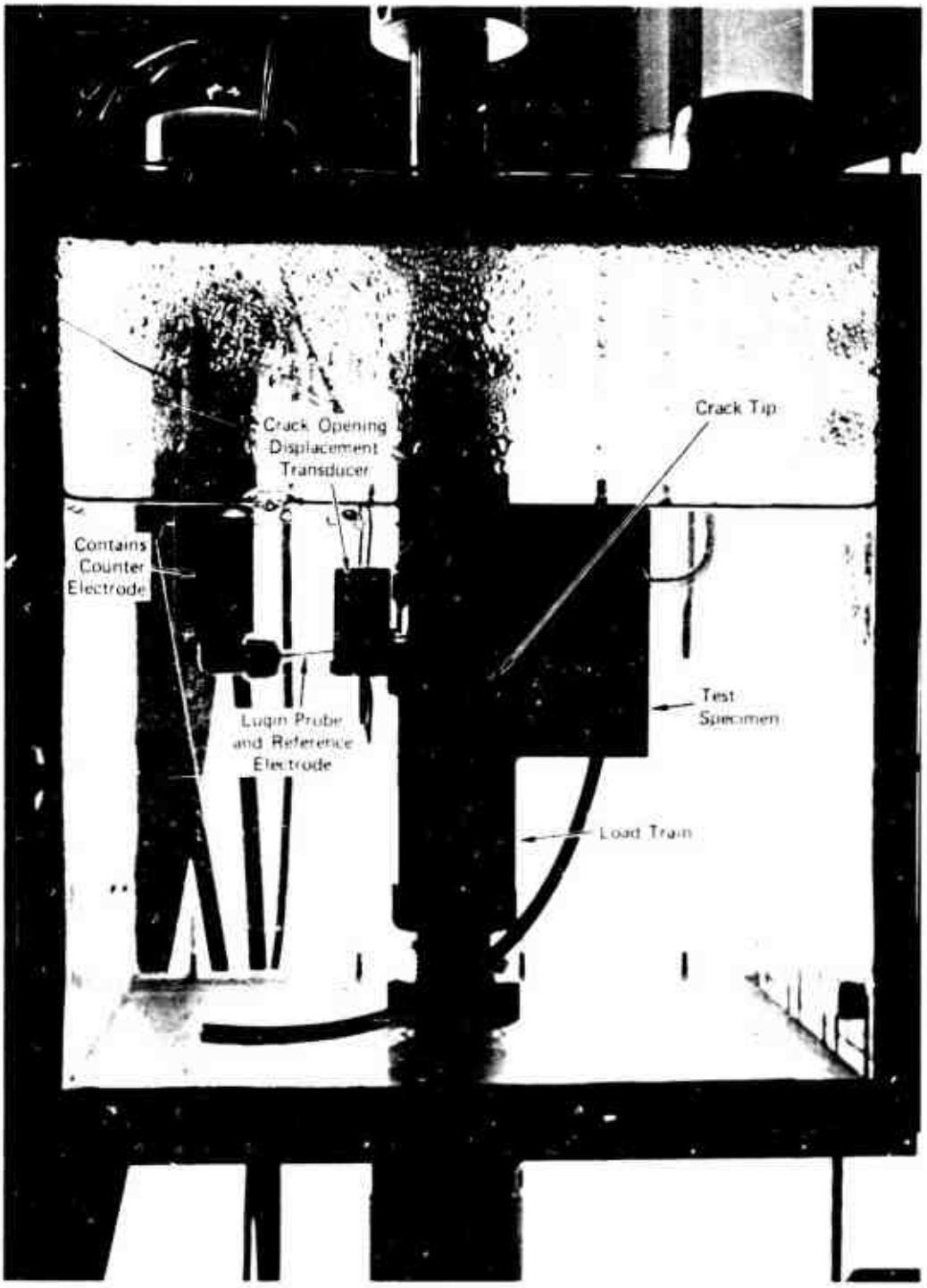

FIGURE 13 DETAIL OF TEST CHAMBER

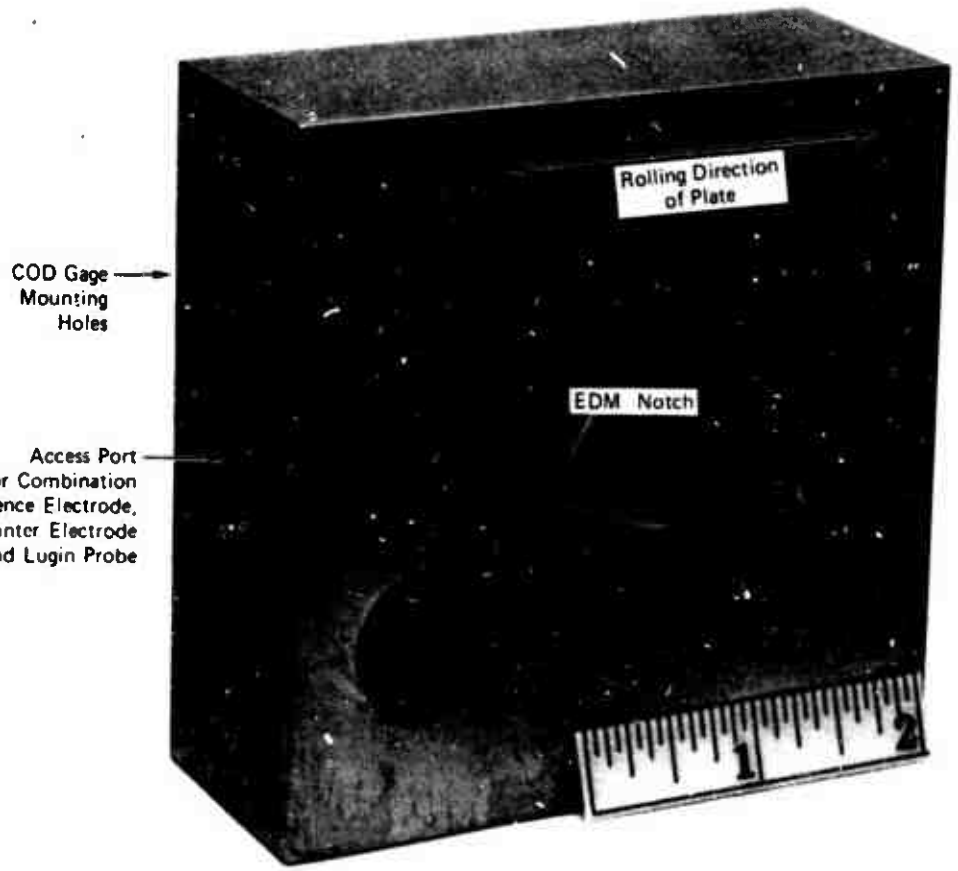

JP-4333-6A

FIGURE 15 DETAIL OF TEST SPECIMEN

320 kbyte of external RAM (Axlon "Ramdisk 320"), and a 20-mbyte rigid disk (Corvus Model 20 MB/M). The control program was written at SRI in Basic and 6502 Machine languages and is included as Appendix A.

Some experiments were performed under potentiostatic control, using a Princeton Applied Research Model 173/276 potentiostat; however, most of the experiments were performed under pseudo-galvanostatic control. In the latter mode, a resistance several orders of magnitude larger than the cell impedance is placed in series with the counter electrode, and a large AC voltage is applied. To a good approximation, the current is determined by the AC voltage divided by the series resistance, independent of cell impedance.

For experiments in which the load is cycled, the periods of the mechanical and electrical cycles must be synchroninzed by integrating the impedance data over one complete cycle of the mechanical load. Thus, the results represent an average over a full cycle of crack-opening displacement. If these cycles are not synchronized, the data may contain a large amount of systematic error and will inevitably show considerable scatter. For example, if the impedance measurements are integrated over a time that is shorter than the mechanical load cycle, multiple determinations (at different electrical perturbation frequencies) may be made during a single mechanical cycle. These determinations will cover the range from maximum to minimum crack opening and will appear as scatter in the data set.

Because it is necessary to integrate over at least one cycle at the electrical perturbation, some error will be introduced at low frequencies when the impedance data are integrated over more than one (but not an integer number of) mechanical cycle. This error is inevitable and results in some scatter in our data at very low frequencies (< 0.01 Hz).

An environmental chamber was constructed that attached to a servo-hydraulic mechanical testing machine. This chamber and the associated attachments allow us to circulate aerated or deaerated 3.5% NaCl solution (or other electrolytes) at controlled temperatures past our fatigue precracked compact tension specimens. The crack growth can be

measured by optical methods or by the compliance method, by means of a water-immersible LVDT mounted on the specimen. A special composite reference/counter electrode incorporates a silver/silver chloride electrode in a 0.25-inch-diameter Lugin probe, positioned about 0.1 inch from the start of the fatigue precrack. The fatigue precrack is at the bottom of a 2.00-inch-deep notch (1.50 inches wide by 0.010 inch thick), and the tip of the 0.25-inch-diameter Lugin probe is centered at the bottom of this notch to minimize "edge effects" on the electrochemical measurements. The counter electrode is located in a chamber to which the Lugin probe is attached. This arrangement allows us to polarize only the area at the Lugin probe tip and thus measure the response of this area.

The cracked electrochemical AC impedance measurements were obtained on Ti-6Al-4V in aerated 3.5% NaCl solutions. These tests were performed under load control with ΔK varying from 10-30 ksi $\sqrt{in.}$ with R values of 0 to 0.2. No experiments of this type were performed on HY-80.

Figures 16 and 17 show impedance data for the growth of a crack in Ti-6Al-4V. The data designated as "no crack" in Figure 16 show the impedance response in the range $10^{-3} < f < 10^{4}$ Hz for a specimen subjected to a 5-Hz cyclic load, but showing no superficial indication of having cracked. In the Nyquist domain this data set appears as a semicircle whose center is located above the real axis. The low-frequency intercept on the real axis is very close to 2000 Ω. The high-frequency region is shown in an amplified form in Figure 16(b). A second semicircular region is observed with a high-frequency intercept on the real axis at 52.8 Ω. The high-frequency intercept corresponds to the series resistance due to the electrolyte path between the tip of the reference electrode and the base of the notch in the specimen.

In the Bode plot [Figure 16(c)], these data exhibit a single minimum in the phase occurring at approximately 0.15 Hz. The magnitude information shows two limiting plateaus (corresponding to the intercepts with the real axis in the Nyquist plot) separated by linear regions of slope -1/2, -1, and -1/4 with increasing frequency.

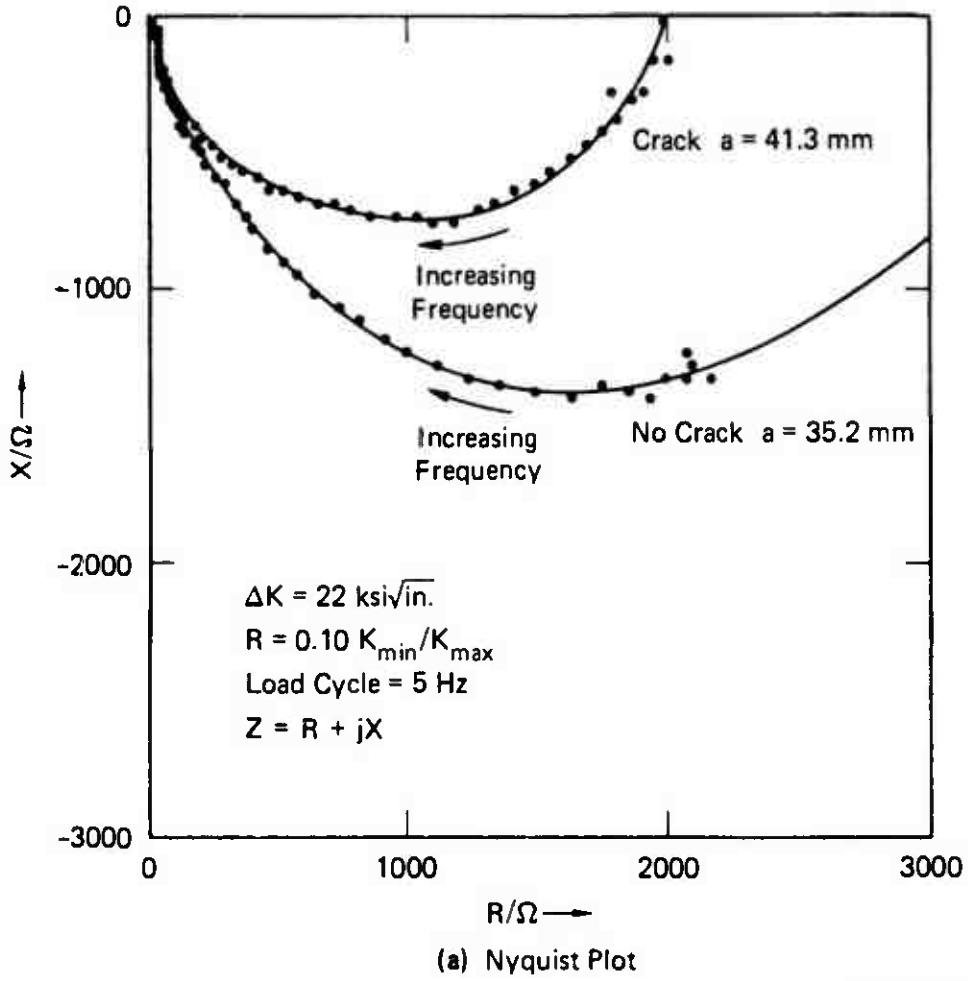

FIGURE 16 IMPEDANCE RESPONSE OF THE Ti-6Al-4V SPECIMEN BEFORE AND AFTER THE APPEARANCE OF A MACROSCOPIC CRACK IN AERATED 3.5% NaCl SOLUTION

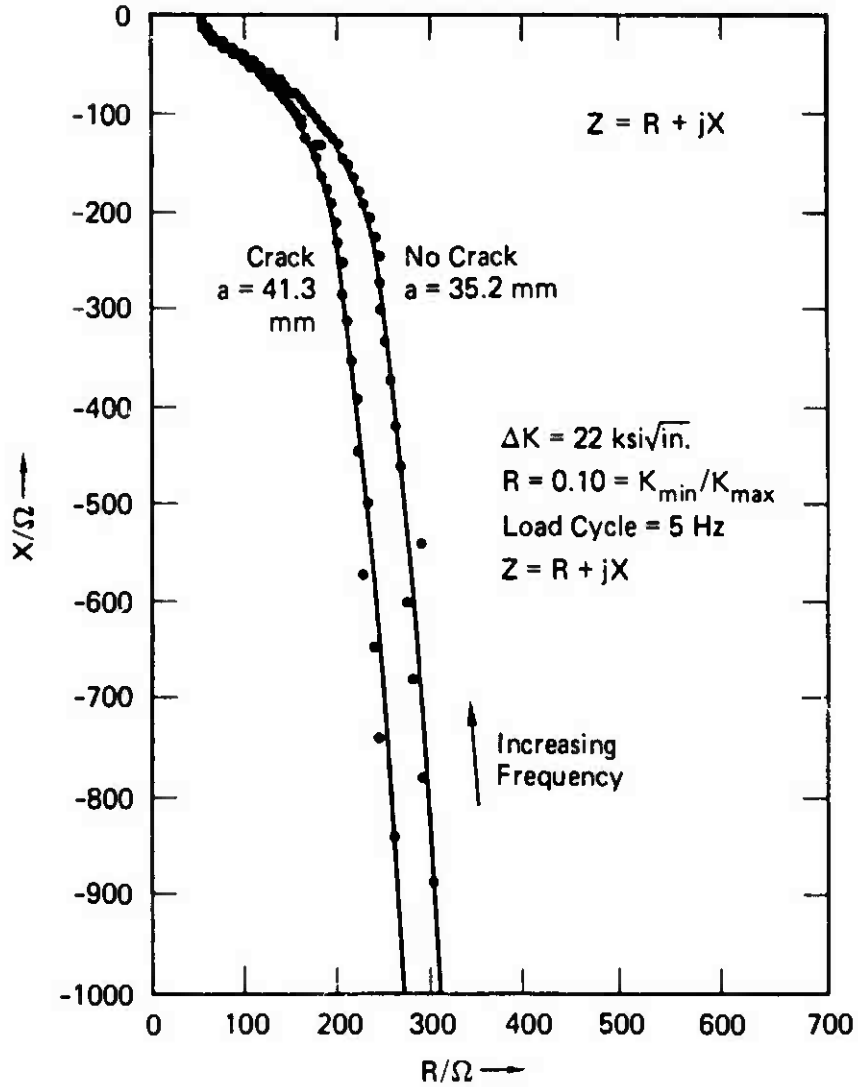

(b) Expanded Nyquist Plot

JA-4333-10A

FIGURE 16 IMPEDANCE RESPONSE OF THE Ti-6Al-4V SPECIMEN BEFORE AND AFTER THE APPEARANCE OF A MACROSCOPIC CRACK IN AERATED 3.5% NaCl SOLUTION (Continued)

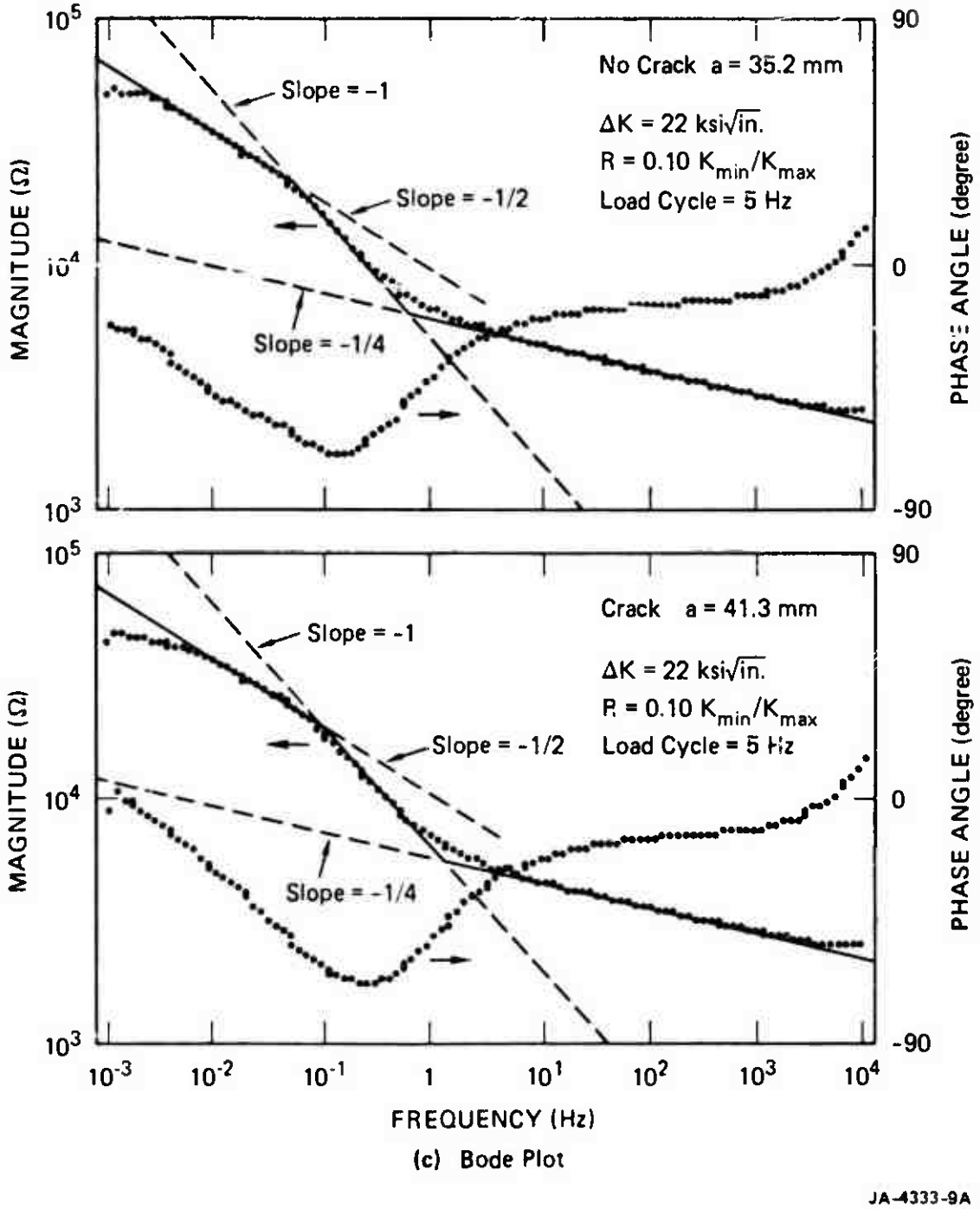

(c) Bode Plot

JA-4333-9A

FIGURE 16 IMPEDANCE RESPONSE OF THE Ti-6Al-4V SPECIMEN BEFORE AND AFTER THE APPEARANCE OF A MACROSCOPIC CRACK IN AERATED 3.5% NaCl SOLUTION (Concluded)

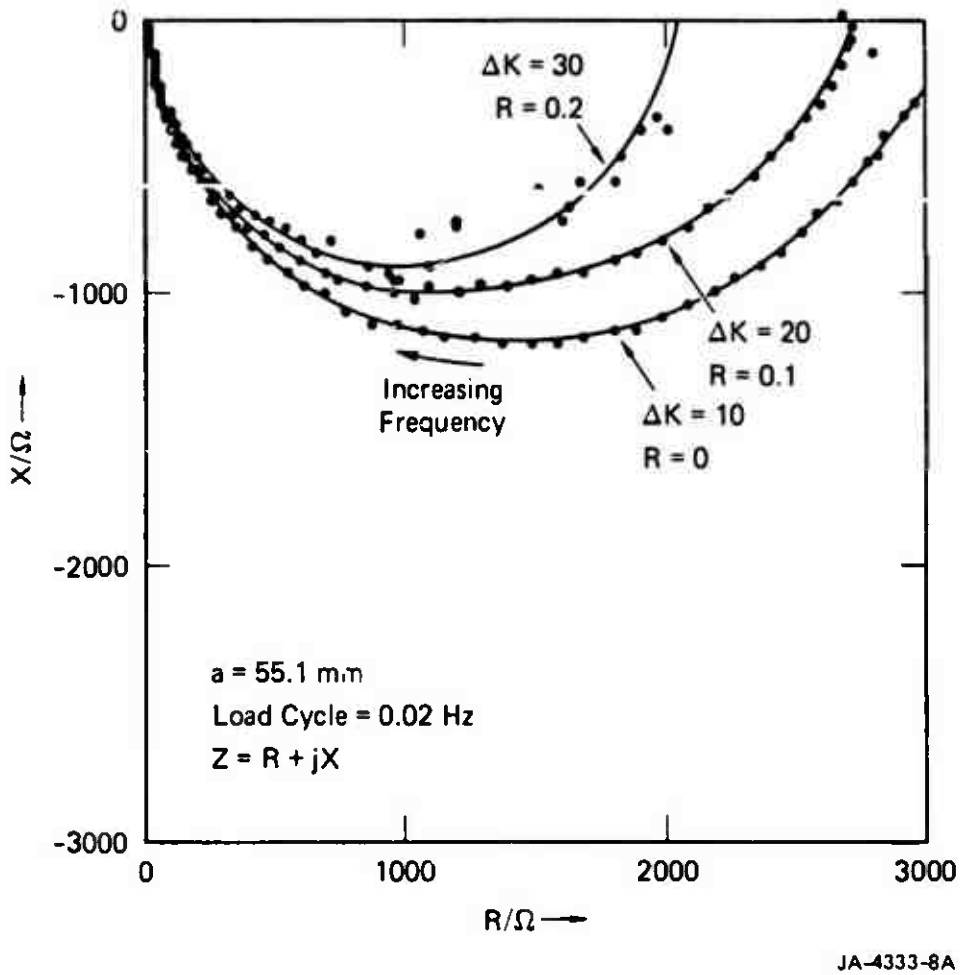

FIGURE 17 THE EFFECT OF LOAD ON THE IMPEDANCE RESPONSE OF A MATURE CRACK IN Ti-6Al-4V IN AERATED 3.5% NaCl SOLUTION

Examining these linear regions in order of decreasing frequency, we see that the region at slope -1/4 corresponds to the high-frequency semicircle in the Nyquist plot, shown in Figure 16(b). This region is present for unstressed specimens before cyclic loading and appears to be completely unchanged during the entire growth of the crack. We speculate that this region is associated with diffusion in the plane of the machined notch and perpendicular to the axis of the reference electrode. Although the region of slope -1/4 has significant extent in the Bode plot, the impedances involved are very small and have little significance in a linear (e.g., Nyquist) plot of the data. We will not consider this zone further in this report.

At intermediate frequencies, all data sets obtained show a region with a slope of -1. This region corresponds to a f^{-1} dependence and is the form expected for the equivalent circuit in Figure 2, at intermediate and high frequencies, when diffusion of metal ions from the electrode surface are not rate limiting. A region of slope -1 in a Bode plot corresponds tc a semicircle with its center located on the real axis in the Nyquist representation. The beginnings of a semicircle of great magnitude (on the scale shown) can be seen in Figure 16(b); the parameters of this aemicircle are determined by the interfacial reaction resistance, R_r, and the double-layer capacitance, C (aee Section 2).

Impedance data obtained from unatreased specimens before the application of a cyclic load display a f^{-1} dependence (Bode slope = -1) down to limitingly low frequencies. Only under cyclic loading conditions does a region of slope -1/2 appear, and this region becomes increasingly significant as a crack grows. Thus, we associate the region of slope -1/2 in a Bode plot with the presence of a crack.

Figures 16(a), (b), and (c) each show two curves: one labeled "crack" and the other labeled "no crack" on the baais of visual inspection of the aides of the compact tension specimen. Because both show a region of $f^{-1/2}$ dependence, the curve designated as "no crack" in Figure 16(c) must have at least a veatigial rupture, asaociated with cyclic loading of the oxide film at the crack tip. The curve labeled

"crack" was obtained when a crack of about 3 mm was observed at the side of the specimen.

A region of apparent $f^{-1/2}$ dependence (slope -1/2) for the impedance within the crack is predicted by equations (4) and (5). The transmission line impedance, Z_{tl}, contains terms in $e^{\gamma l}$, which can be expanded as a Taylor series:

$$e^{\gamma l} = 1 + \gamma l + (\gamma l)^2/2! + (\gamma l)^3/3! + \ldots \quad (13)$$

For $\gamma l << 1$, the third and subsequent terms in this series can be neglected. Substituting equation (13) into equation (4), we obtain an expression of the form

$$Z_{tl} = a + b/\gamma + \text{additional terms} \quad (14)$$

where a and b are undetermined constants and the higher order terms have decreasing significance.

Because γ is a function of $Z_i^{-1/2}$ [aee equation (5)], the impedance of Z_i placed in a transmission line will have a major component that has the square root of the frequency power dependence of the interfacial impedance itself. Thus, for Z_i containing parallel resistance (R_p) and capacitive (C_p) elements only,

$$1/Z_i = 1/R_p + j2\pi fC_p \quad (15)$$

and γ will be a function of $f^{1/2}$; from equation (14), Z_{tl} will be a function of $f^{-1/2}$, which is the form observed.

The preceding discussion is important becauae an $f^{-1/2}$ dependence is often attributed to diffusional proceases at a plane-parallel electrode.[22-24] By mathematically fitting the measured impedance data to the form predicted by equation (4), we can clearly see that the observed responae is due to a capacitive element contained within a

transmission line, rather than to diffusion; the coefficients obtained do not correspond to any known diffusional process.

The capacitance under consideration is simply that of the electrical double layer on the sides of the growing crack. A resistance appears in parallel with this capacitance and is associated with faradaic processes on the crack wall. At present, we are unable to determine whether this faradaic process is anodic (metal dissolution) or cathodic (reprecipitation of metal or hydrogen evolution). To resolve this and other important issues, we constructed a discrete (finite element) transmission line model for the growing crack based on the electromechanical parameters calculated from impedance measurements, as discussed in Section 4.

The two data sets presented in Figure 16 are not greatly different in form; the major changes observed are in the characteristic frequency and the intercept with the real axis at limiting low frequencies. The characteristic frequency (f_o = frequency of minimum phase) moves from 0.14 to 0.32 Hz between the first and second data sets, and the limiting low-frequency intercept decreases from 3915 to 1995 Ω. This decrease is believed to be an effect of crack opening. For the data set labeled "no crack," the vestigial crack, although short, is very tight and the impedance is large. Under the same load conditions, the crack-opening displacement increases as the crack grows, and the impedance becomes less. In fact, a plot of limiting resistance versus crack length shows a minimum at about 1-cm crack length, the resistance then increasing as the crack lengthens, indicating that effects of crack length becnme more important than the average crack-opening displacement.

The effects of crack-opening displacement were examined by varying the cyclic load conditions. Specimens were cycled at a mean load, plus and minus the cyclic load perturbation. Figure 17 shows the effects of varying both the mean and the perturbation stress levels for a mature crack (= 2 cm long) cycled at 0.02 Hz. For these data (and for all impedance dsts presented in this report), each impedance determination represents an sverage taken over one complete period of the cyclic load

and thus reflects some weighted average of crack opening displacements. Figure 17 clearly shows the effect of crack opening (proportional to load) on the limiting low-frequency resistance. From a superficial examination, it appears that the effects of the load perturbation level are more significant than those of mean load. However, we have not attempted to separate the effects of mean and perturbation stress levels quantitatively.

In summary, the results of electrochemical experiments on a cracked Ti-6Al-4V specimen under cyclic load conditions in 3.5% NaCl suggest that the AC impedance appears to be due to faradaic processes at the crack tip and a transmission line impedance associated with the crack walls. We also observed that, at least qualitatively, crack length and crack opening displacement appear to affect the measured impedance.

3.2.3 Electrochemical/Mechanical Impedance Experiments

It is also possible to define an impedance in terms of the electrochemical response of a fractured specimen to a mechanical input that causes crack propagation. One case in which this analysis can be applied usefully is for the electrochemically assisted (stress corrosion) cracking of metals submerged in an electrolyte and subjected to a cyclic mechanical load or stress. With some simplification, crack growth due to cyclical film rupture at the growing crack tip, followed by metal dissolution, can be considered as described below.

Figure 18 shows schematically the case of a crack growing in to a metal, under constant current control and cyclic load conditions. The loading conditions can be controlled to achieve a sinusoidal variation in the specimen load:

$$p = \bar{p} + \tilde{p} \sin(\omega t) \qquad (16)$$

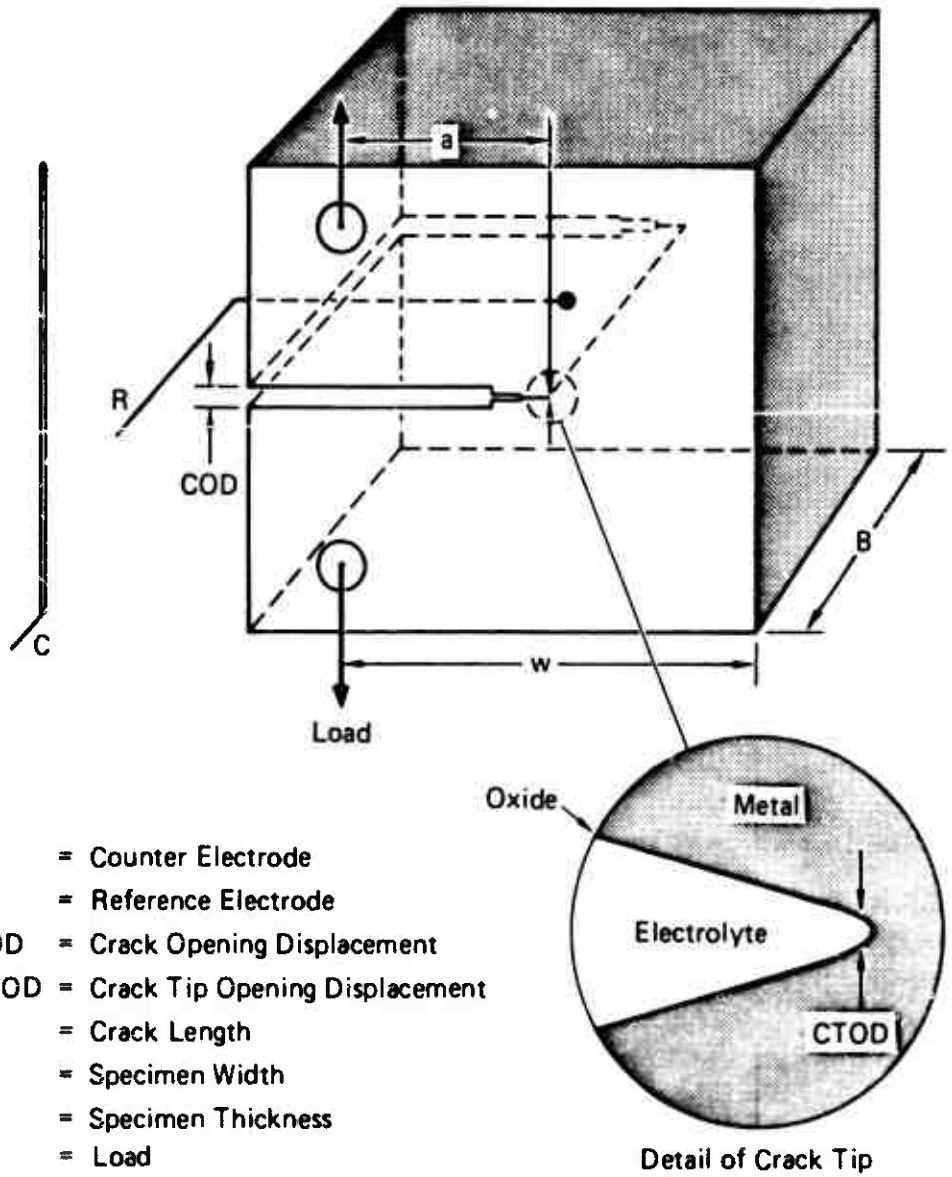

C = Counter Electrode
R = Reference Electrode
COD = Crack Opening Displacement
CTOD = Crack Tip Opening Displacement
a = Crack Length
w = Specimen Width
B = Specimen Thickness
p = Load

FIGURE 18 CT SPECIMEN GEOMETRY FOR DETERMINING THE ELECTROCHEMICAL MECHANICAL IMPEDANCE FOR THE PROPAGATION OF A CRACK

where $\bar{p}$ is the mean specimen load and $\tilde{p}$ the amplitude of the superimposed sinusoidal perturbation. To a first approximation, the area exposed at the crack tip can be considered to be proportional to the crack tip opening displacement.

$$A = \gamma B(CTOD) \tag{17}$$

$$CTOD = K^2/2E\sigma_{ys} \tag{18}$$

$$A = \gamma B\ K^2/2E\sigma_{ys} \tag{19}$$

where

γ = a proportionally constant determined by the mechanical properties of the oxide film and metal at the crack tip

B = specimen thickness

CTOD = crack tip opening displacement

E = Elastic modulus of the specimen

σ_{ys} = yield strength of the specimen

K = stress intensity factor = $p/B\ f(a/w)$[53]

where

$$f(a/w) = w^{-1/2}(1-a/w)^{-3/2}\ (2 + a/w)\ [0.886 + 4.64\ (a/w) - 13.32\ (a/w)^2 + 14.72\ (a/w)^3 - 5.6\ (a/w)^4] \tag{20}$$

where

p = applied load

a = crack length

w = specimen width

and (a/w) is determined from[54]

$$(a/w) = 1.0012 - 49.6U + 23.057U^2 - 323.91U^3 + 1789.3U^4 - 3513.2U^5 \quad (21)$$

where

$$U = [(BE[COD]/p)^{1/2} + 1]^{-1}$$

COD = crack opening displacement measured at a distance 0.345 w from the load line towards the front face of the specimen.

The value for COD is determined from

$$COD = p\ g(a/w) \quad (22)$$

where

$$g(a/w) = (1/EB)\left(1 + \frac{0.345}{a/w}\right)\left(\frac{1 + a/w}{1 - a/w}\right)[1.6396 + 11.02(a/w - 6.449(a/w)^2 - 31.14(a/w)^3 + 47.251(a/w)^4 - 18.343(a/w)^5] \quad (23)$$

Combining equations (22) and (16), we obtain

$$COD = [\bar{p} + \tilde{p}\sin(\omega t)]\ g(a/w) \quad (24)$$

Figure 19 shows the approximate* equivalent circuit for the inside of the crack, with the impedance of the oxide-passivated walls appearing in parallel with the impedance element due to dissolution of exposed metal at the crack tip. The variation in applied load described by equation (16) results in a sinusoidal perturbation of the exposed crack tip area such that

---

*Because of the potential distribution along the crack, this equivalent circuit should more properly be represented as a nonuniform, finite transmission line for the oxide wall impedance, with the crack tip as a terminating impedance. Such a case is shown in Figure 1.

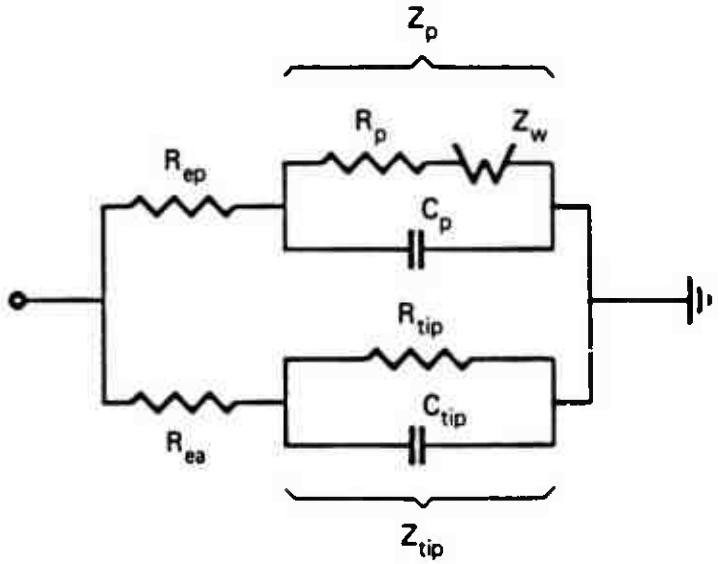

R_{ep} = Electrolyte Resistance to Crack Walls
R_p = Charge Transfer Resistance at Passive Walls
C_p = Double Layer Capacitance at Passive Oxide
Z_w = Diffusional Impedance at Passive Walls
Z_p = Interfacial Impedance at Passive Walls
R_{ea} = Electrolyte Resistance to Crack Tip
R_{tip} = Charge Transfer Resistance at Exposed Metal
C_{tip} = Double Layer Capacitance of Exposed Metal
Z_{tip} = Interfacial Impedance at Crack Tip

JA-4333-19

FIGURE 19 SIMPLIFIED EQUIVALENT CIRCUIT FOR A STRESS CORROSION CRACK

$$C_{tip} = C^{o}_{tip} \quad A \approx \frac{C^{o}_{tip}\,\gamma}{2E\sigma_{ys}B}\,[\bar{p} + \tilde{p}\,\sin(\omega t)]^{2}[f(s/w)]^{2} \qquad (25)$$

$$R_{tip} = R^{o}_{tip}/A \approx \frac{2R^{o}_{tip}\,E\sigma_{ys}B}{\gamma[\bar{p} + \tilde{p}\,\sin(\omega t)]^{2}[f(a/w)]^{2}} \qquad (26)$$

Without going through the algebra, for the equivalent circuit shown in Figure 19, we can obtain an expression for the electrochemical/mechanical impedance (Z_{em}) for this system, defined as the ratio of the AC voltage that appears at the reference electrode, to the COD due to the sinusoidal load variation under DC galvanostatic conditions:

$$Z_{em} = \frac{\tilde{V}_{Ref}}{\tilde{d}} = \bar{V}_{tip}\,(R_{ep} + Z_{p})\,\left(\frac{1}{R^{o}_{tip}} + j\omega C^{o}_{tip}\right)\frac{\gamma B}{a} \qquad (27)$$

Under optimal conditions, Z_{em}, measured over a range of frequencies, can be used to deconvolve the equivalent circuit parameters in a manner analogous to that of electrochemical impedance analysis. The advantage of this method, in the example given, is that measurements can be made under dynamic load conditions and that the perturbation is imposed at the point of principal interest, near the crack tip.

In this experiment we galvanostatically imposed a 0.5 mA current between the counter electrode and the crack tip. The potential was measured with the Ag/AgCl reference electrode located at the crack tip. The mechanical frequency [ω in equation (24)] was varied from 20 mHz to 10 Hz.

Figure 20 presents the real versus imaginary components of the electrochemical/mechanical impedance response measured for an HY80 steel specimen of geometry shown in Figures 15 and 18, immersed in 3.5 wt% NaCl. Because of the form of equation (24), these plots are somewhat more complex than a conventional Nyquist plot. Nevertheless, these data are amenable to standard methods of electrical analysis. We observe that the processes at the growing crack tip dominate at low frequencies,

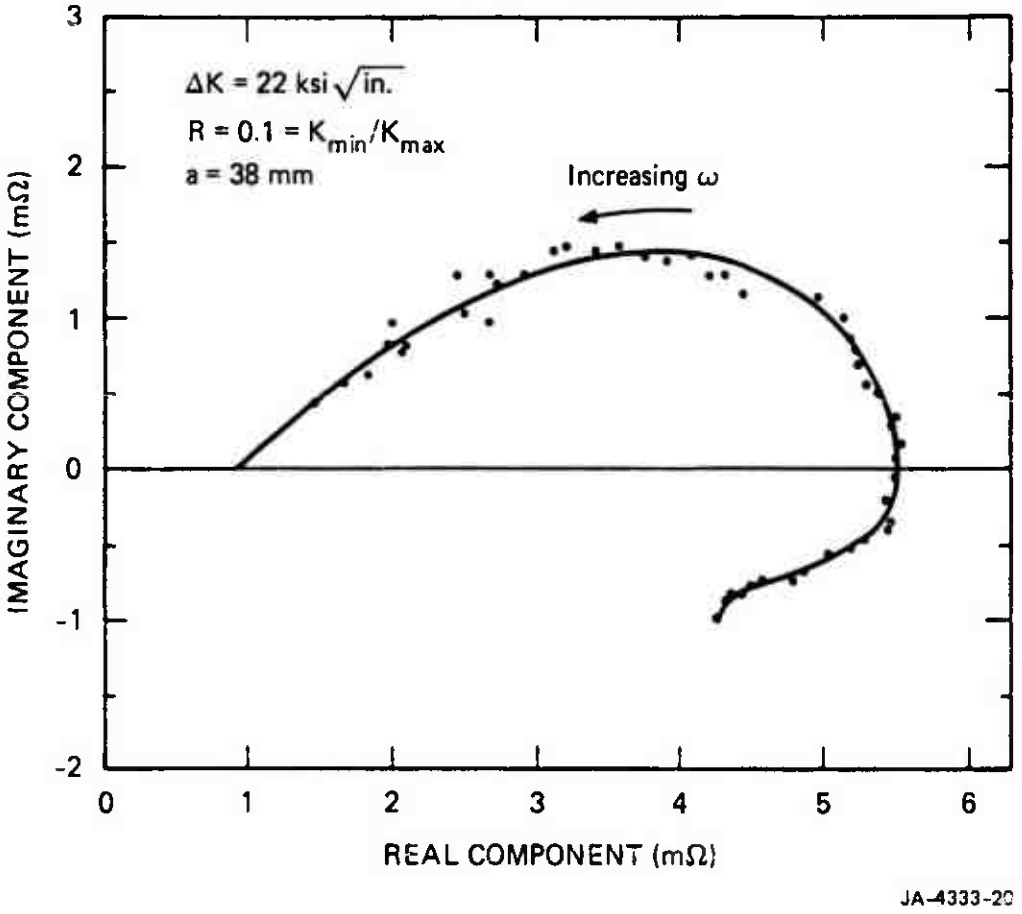

FIGURE 20 COMPLEX PLANE PLOT OF THE ELECTROCHEMICAL/MECHANICAL IMPEDANCE FOR THE PROPAGATION OF A CRACK THROUGH HY80 STEEL IN 3.5% NaCl SOLUTION AT 25°C UNDER SINUSOIDAL LOADING CONDITIONS

and the properties of greatest interest, R_{tip} and C_{tip}, can be deconvolved at limitingly low frequencies.

Figure 21 shows the logarithm of the electrochemical/mechanical admittance ($Y_{em} = 1/Z_{em}$) plotted versus log frequency, for a typical data set, as a function of the number of mechanical load cycles experienced by the specimen during crack growth. These data show some evolution in the crack tip parameters (the low-frequency, decending portion of the curves), but considerably more changes appear in the crack wall impedance, reflecting the effect of increased crack wall area with increasing crack length. Also, note that the crack grew about 5.7 mm during this portion of the test.

To summarize the experimental results of the electrochemical/ mechanical impedance data, we found that this technique was sensitive to crack wall area at frequencies above about 1 Hz and more sensitive to the crack tip at mechanical frequencies below 0.1 Hz. To understand the detaila of these data and the electrochemical impedance, a more detailed electrochemical/mechanical model needs to be constructed. This model together with the impedance data can then be used to measure the relevant electrochemical and mechanical parameters that occur in a growing SCC or CF crack. As described in the next section, this approach was implemented by modeling the cracking process as a discrete transmittion line.

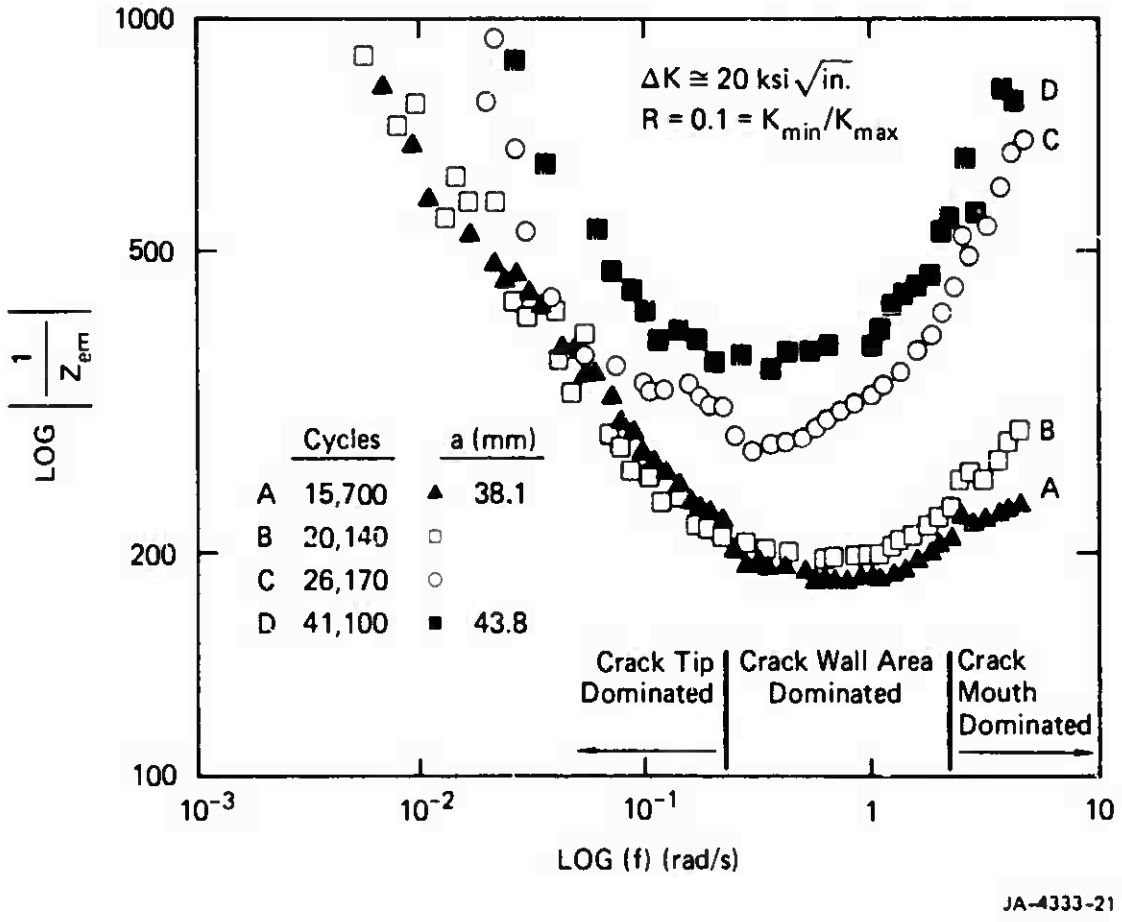

FIGURE 21 LOG ($|1/Z_{em}|$) VERSUS LOG (FREQUENCY) FOR AN HY80 SPECIMEN EXPOSED TO 3.5 wt% NaCl AT 25°C

Section 4

APPLICATIONS OF THE DISCRETE TRANSMISSION LINE MODEL TO CRACK GROWTH PREDICTION

4.1 OVERVIEW

In developing a quantitative model intended to predict the combined effects of electrochemical corrosion and mechanical stress on crack growth, the first concern is to calculate the chemical, electrochemical, and mechanical parameters at the crack tip, from the prevailing conditions external to the specimen. The problem of computing the mechanical stress and strains in the elastic/plastic zone surrounding the crack tip, from the externally measured load and crack opening displacement, has been addressed by numerous authors[18,19,55-59] and is not the subject of this report.

Instead, we are concerned with the manner in which the DC potential, the anodic and cathodic currents, the solution pH and conductivity, and the concentrations of metal oxide and metal ions vary with distance and time within the interpenetrating electrolyte volume of a crack growing in a metal, submerged in a bulk volume of electrolyte.

In general, two distinct types of models can be used to obtain the required distributions. A system of first- and second-order nonlinear differential equations can be used to describe the processes of diffusion and interfacial reaction and the static potential distribution. Inevitably, this system of equations cannot be solved analytically, and numerical methods and mathematical approximations must be used to obtain a solution.

An alternative approach has been developed by McKubre for studying porous stripping electrodes[28,31,42-44] in which the transmission line equivalent circuit, described in Section 2, is considered to consist of a large, but finite number of discrete elements. This type of model

also requires a numerical solution, but offers the advantage of modeling most of the important physical and chemical processes by taken into account the full degree of nonlinearity of electrochemical systems. Of particular significance is that many of the electrochemical parameters necessary to solve the discrete transmission line can be obtained by making low-frequency AC measurements close to the potential of zero current and solving analytically for the continuous transmission line impedance.

The basic features of the discrete transmission line model, applied to a stressed crack, can be seen in Figure 1. Briefly, we consider the resistivities of the solid (metal) and electrolyte phases to be interconnected by the impedance of the metal/electrolyte interface where charge carriers change from electrons to ions. In the discrete model the electrical equivalent circuit is assumed to consist of N discrete zones, each of length a/N, associated with the crack walls, plus an additional zone representing the tip. In general, the interfacial impedance of an arbitrary section of crack wall will depend on the local potential difference between the metal and electrolyte phases, the nature and concentration of dissolved species (principally metal and hydrogen ions and oxygen), and the presence and character of an interfacial oxide film.

The selection of the tip impedance determines the nature of the electrochemically assisted cracking. We are concerned here only with mechanisms of crack growth by anodic dissolution following film rupture. With appropriate modification, the model may nevertheless be used to test mechanisms of crack growth involving de-alloying or hydrogen embrittlement.

Because of the geometry and possible concentration gradients within the crack, the electrolyte resistance at each element of the transmission line is not constant with time or distance. Generally, the metal phase resistance is much less than that of the electrolyte and can be considered to be constant.

The current that flows into the crack (or the potential at the crack surface near the crack tip) was imposed, in our experiments, by a potentiostat with respect to an external counter electrode. Under open circuit conditions this current (or potential) is imposed by the reaction of redox species on the exposed surface of the specimen.

4.2 ASSUMPTIONS

We consider electrochemical and chemical reactions occurring at the crack tip (t) on the crack walls (w), and in the crack electrolyte volume (v). The important reactions are taken to be as follows:

Site(s)	Reaction	Reaction No.
t, w	$M \rightleftharpoons M^{a+} + ae^-$	(5.1)
v	$M^{a+} + a/2\ H_2O \rightleftharpoons MO_{a/2} + aH^+$	(5.2)
w, t	$a/2\ H_2 \rightleftharpoons aH^+ + ae^-$	(5.3)
w, t	$M + a/2\ H_2O \rightleftharpoons MO_{a/2} + aH^+ + ae^-$	(5.4)

All reactions are considered to be reversible. Reaction (5.1) accounts for metal dissolution, which in conjunction with the chemical reaction (5.2) accounts for oxide formation by dissolution/precipitation. Reaction (5.3) is simple electrolysis, and reaction (5.4) accounts for the direct electrochemical reaction between metal and surface metal oxide film.

The following concepts and assumptions have been applied to simplify the model.

- Only metal dissolution (reaction 5.1) and the crack tip is influenced by the crack opening displacement.
- There is no oxygen within the crack volume and thus reaction (5.3) is the only source of net cathodic current.

- The crack is considered to be a wedge and the area of metal exposed at the crack tip is determined by the tangent of the crack opening angle, Θ.

$$\mathrm{Tan}(\Theta) = \mathrm{COD}/a \tag{28}$$

where COD = crack opening displacement, a = crack length.

- In the electrochemical reactions all symmetry factors (α) are considered to be equal to 1/2.
- The chemical reaction (5.2) rapidly achieves equilibrium.
- At the steady state the activities of H_2O and H_2 are invariant.
- The activity of the metal oxide phase is equal to the monolayer surface coverage, $\emptyset$, with a maximum of 1.
- At all points the crack is so thin that there exists no limitation due to diffusion perpendicular to the walls.
- The presence of an (NaCl) ensures that the electrolyte phase resistivity does not change significantly with metal or hydrogen ion concentrations.

4.3 EQUATIONS

Anodic dissolution at the crack tip is considered to proceed via the Butler-Volmer equation, with the area exposed, A_t, being proportional to D.

$$A_t = \gamma \mathrm{COD}/a \tag{29}$$

where γ is a constant, and

$$\mathrm{COD} = \bar{D} + |d| \sin(\omega t) \tag{30}$$

These equations (29 and 30) were used as a simplified version of Equations (19) and (24) to reduce the model run time. Equations (19) and (24) will be incorporated in the future. Equation (30) considers the effect of sinusoidal COD loading of the compact tension on the dynamics of crack growth, and a model is being developed to calculate the electromechanical impedance under dynamic conditions that also includes modeling of the γ factor in equation (29). In this section we consider only steady-state conditions, and we define an effective opening displacement, $\overline{D}$, which is a function of COD, d and the sinusoidal loading rate.

The current associated with metal dissolution at the crack tip, due to an applied overvoltage, under steady-state conditions can be expressed as

$$I_{M/M^{a+}} = i^{o}_{M/M}\, a+ \,(\gamma\overline{D}/a)\,\{\exp[\,\frac{aF}{\alpha RT}\,(\Delta V_N - V^{o}_{M/M^{a+}} - V_{cp}]$$

$$- \exp\,[\,\frac{-aF}{\alpha RT}\,(\Delta V_N - V^{o}_{M/M}\, a+ - V_{cp})]\} \qquad (31)$$

where ΔV_n is the interfacial overvoltage in element N, F is Faraday's constant, T is temperature in Kelvin, V^{o} is the equilibrium potential, i^{o} is the exchange current density, subscript M/M^{a+} refers to the metal dissolution reaction (5.1), and V_{cp} is the local concentration overvoltsge determined by

$$V_{cp}(N) = -\,(nF/RT)\,\ln[H^{+}] \qquad (32)$$

The standard state for i^{o} and V_{cp} is taken to be 1 molar.

Crack growth is determined at discrete, equal time steps. Within each time interval reactions (5.1), (5.3), and (5.4) are evaluated on the crack walls in each segment of the transmission line, according to the local conditions of concentration and potential.

At the end of each time interval, reaction (5.2) in each segment is considered to be at an equilibrium determined by

$$K = \frac{[MO_{a/2}][H^+]^a}{[M^{a+}][H_2O]^{a/2}} \tag{33}$$

where the activity of water, $[H_2O]$, is considered to be unity, and the activity of the oxide film, $[MO_{a/2}]$, is taken to be equal to the fractional area coverage with a maximum of 1.0 (at one monolayer coverage).

The extent of crack growth in esch time interval, t, is calculated from the volume of metal dissolved at the crack tip in a rectangular parallelipiped whose width is the width (B) of the crack opening angle and γ and whose depth is the increased crack length, Δa. Thus,

$$\Delta L = \frac{\left(I^{tip}_{M/M^{a+}}\right)(t)}{nF\ \overline{MW}\ \overline{\rho}\ \gamma\ \theta\ B} \tag{34}$$

where $\overline{MW}$ and $\overline{\rho}$ are the average molecular weight and density of the dissolved metal, respectively, and the other symbols have been previously defined.

The concentrations within each segment of the transmission line are modified by the combined effects of (1) chemical and electrochemical reactions, (2) the diluting effect as the volume is increased with crack growth (in flow of bulk electrolyte from outside the crack), and (3) diffusion. The effecta of diffusion along the crack length are accounted for at the same discrete time intervals as crack growth. A comprehensive model for transverse diffusion is presented in Appendix B. Briefly, we consider the propagation of concentration profiles between nearest neighbors that initially have uniform, but different concentrations. Adjacent zones have different cross-sectional areas and different volumes in the wedge-shaped crack profile. Different approximations are uaed for long and short times.

The final consideration is of the thickness of the "passivating" metal oxide film. This film has an important role in localizing the

metal dissolution process at the crack tip. We consider the metal oxide to conduct both electrons and ions. The electronic conductive properties are accounted for by the solid-state reaction between metal and metal oxide [reaction (5.4)]. The primary role we envisage for the metal oxide, however, is as a diffusion barrier. At greater than monolayer coverages, we consider that the direct metal dissolution reaction on the crack walls is impeded by the diffusion of metal ions across the metal oxide membrane. The passive current density, i_p, is therefore given by

$$i_p = nFD \frac{C_S - C_N}{y_N} \tag{35}$$

where D is the diffusion coefficient, C_S is the saturation solubility of metal ions in the metal oxide phase,* C_N is the concentration of metal ions at the crack electrolyte/metal oxide interface, and y_N is the oxide film thickness. We simplified the calculation by assuming that metal salt will precipitate when the activity of metal ions reaches unity within the oxide phase. We can therefore define the maximum passive current density (for $C_S = 1$ and $C_N = 0$) as

$$i_p^0 = -nFD/y_N \tag{36}$$

and the passive dissolution current in each segment is given by

$$I_N = i_p^0 (1 - C_N)/y_N \tag{37}$$

---

*Note that we have not specified whether or not the film is porous. In the event that it is, the values of C_S and D would change, but the principle of a diffusion barrier remains the same.

4.4 IMPLEMENTATION

The model described in this section has been implemented as a computer program written in BASIC for the Apple II microcomputer. A listing is provided as Appendix C, and a schematic flow chart is given in Figure 22. Briefly, the program allows for the initialization of the physical and electrochemical parameters used to define crack-growth conditions. These parameters are stored in the array ZM(26) and have the meanings shown in Table 3.

The transmission line is considered to consist of N segments, where $N < 200$. Data are saved in the array ZN(9,200) for the metal and electrolyte phase voltages and resistances, the interfacial currents for the electrochemical reactions $M \rightleftarrows M^{a+}$, $H_2 \rightleftarrows 2\ H^+$, and $M \rightleftarrows MO_{a/2}$, and for the hydrogen and metal ion concentrations in the crack electrolyte, and the oxide monolayer thickness, in each segment. The allocation of these variables is shown in Table 4.

Before the application of stress or potential, a vestigial crack is considered to exist, filled with electrolyte at the bulk pH, with the walls covered in a monolayer of oxide, and the metal ion concentration in chemical equilibrium. The data array is initialized with these concentrations at the outset of computation. The program then guesses an initial value of the applied potential that will result in the net DC current. The resistances, potentials, and currents are then calculated in each mesh of the transmission line, progressively, from the reference electrode to the crack tip. If the sum of the calculated interfacial currents is not equal to the net DC current that enters the crack (within the specified tolerance), then the initial value of applied potential is adjusted and the computation loop reiterated.

Following a successful solution of the current and potential profiles, the changes in concentration resulting from chemical and electrochemical reactions, the crack advancement, and effects of diffusion are evaluated, and the resultant profiles are output to printer and/or disk.

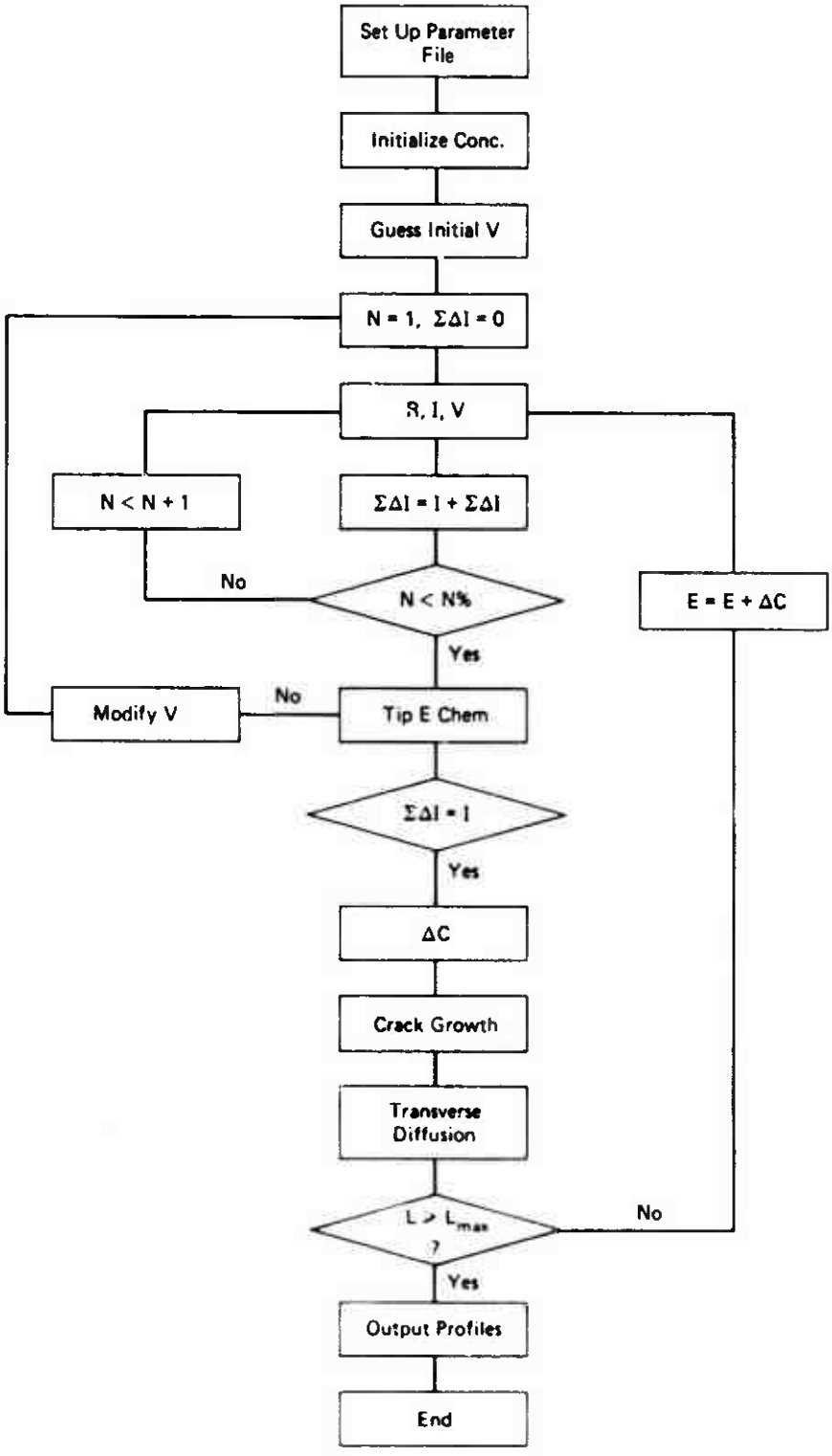

FIGURE 22 CRACK GROWTH FLOW CHART

Table 3

PARAMETER ARRAY

Array Element ZM(x)	Parameter	Units
x = 1	DC current	A
2	Specimen width	cm
3	Specimen height	cm
4	Specimen length	cm
5	Crack opening angle	radians
6	Bulk electrolyte pH	---
7	Electrolyte resistivity	Ω cm
8	Metal resistivity	Ω cm
9	Mechanical stress factor, γ	cm
10	Number of electrons/ion	--
11	Computation interval	s
12	Number of elements	--
13	Computation tolerance	mV
14	Maximum number of iterations	--
15	Exchange current density, M/M^{a+}	A cm^{-2}
16	Equilibrium potential, M/M^{a+}	V
17	Exchange current density, $M/MO_{a/2}$	A cm^{-2}
18	Equilibrium potential, $M/MO_{a/2}$	V
19	Exchange current density, H/H^{+}	A cm^{-2}
20	Equilibrium potential, H/H^{+}	V
21	Chemical equilibrium constant	--
22	Charge per monolayer of oxide	C cm^{-2}
23	Charge per volume of oxide	C cm^{-3}
24	Metal ion diffusion coefficient	cm^2 s^{-1}
25	Passive current density	A cm^{-2}
26	Mechanical loading frequency	Hz

Table 4

DATA ARRAY

Array Element ZM(x)	Parameter	Units
M = 0	Solid phase voltage, $V_{s,N}$	V
1	Electrolyte phsse voltage, $V_{e,N}$	V
2	Solid phase resistance, $R_{s,N}$	Ω cm^{-1}
3	Electrolyte phase resistance, $R_{e,N}$	Ω cm^{-1}
4	Interfacial current, M/M^{a+}	A
5	Interfacial current, H/H^{+}	A
6	Interfscial current, $M/MO_{a/2}$	A
7	Hydrogen ion concentration, $[H^{+}]$	mole dm^{-3}
8	Metsl ion concentration, $[M^{a+}]$	mole dm^{-3}
9	Metal oxide thickness, X_N	monolayers

This procedure is repeated at the interval specified until the crack achieves its desired length.

4.5 RESULTS

A series of computations was performed in a preliminary attempt to verify the model predictions, using estimated physical and electrochemical parametera for HY80 steel in 3.5 wt% NaCl. The parameters used are summarized in Table 5. Figures 23 through 26 show the results of computations that conform closely to the initial crack velocities measured experimentally for the compact tension specimens. We measured the crack velocity to be about 2.3×10^{-7} m s^{-1} and the model predicts an initial velocity of 6×10^{-7} m s^{-1} (see Figure 21).

For the first computation (parameters C1 in Table 5), a crack was grown from $a = a^{o} + 0.05$ cm to $a = a^{o} + 0.76$ cm where $a^{o} = 3.6$ cm at a constant crack current of +1 mA. This computation used a COD cycling at 1 Hz, which corresponds to a ΔK of ~20 ksi $\sqrt{in.}$; this ΔK value did not change appreciably as the crack grew over this small distance. Figure 23 ahows the time dependence of the crack velocity, crack length, and potential at the orifice. The crack propagates initially at an essentially constant rate of 0.6 μm s^{-1}, but after about 10 days, the crack decelerates rapidly; at 30 days the crack velocity is essentially zero. Under constant current conditions the potential at the orifice increaaes monotonically with time, as the active zone at the crack tip becomes further removed. Because the crack velocity decreases rapidly after the crack has grown approximately 0.5 cm, one is inclined to attribute this decrease to a decreasing ΔK or correspondingly a significantly lower crack tip ruptured area that decreases as the crack length increaaes. This is not the caae becauae the stress intensity and area exposed at the tip have changed very gradually and only by a small amount over the total range of crack lengths calculated. It nevertheless appears that the model is predicting a ΔK threshold value near 20 ksi $\sqrt{in.}$ This decrease in crack growth rate seems to be due to precipitation of oxide along the crack length.

Table 5

PHYSICAL AND ELECTROCHEMICAL PARAMETERS
USED FOR MODEL COMPUTATIONS

Parameter Number	Description	Computation Number C1	Computation Number C2	Units
1	Applied DC current	10^{-3}	$0 \rightarrow 10^{-2}$	A
5	Crack opening angle	0.003	0.003	rad
6	Bulk electrolyte pH	6.0	6.0	—
7	Electrolyte resistivity	20.0	20.0	Ω cm
8	Metal resistivity	10^{-5}	10^{-5}	Ω cm
9	Mechanical stress factor	7×10^{-4}	7×10^{-4}	cm
15	Exchange current, M/M^{a+}	10^{-2}	10^{-2}	A cm^{-2}
16	Equilibrium potential, M/M^{a+}	-200	-200	mV
17	Exchange current, $M/MO_{a/2}$	10^{-4}	10^{-4}	A cm^{-2}
18	Equilibrium potential, $M/MO_{a/2}$	-100	-100	mV
19	Exchange current, M/M^{+}	10^{-4}	10^{-4}	A cm^{-2}
20	Equilibrium potential, M/M^{+}	0	0	mV
21	Chemical equilibrium constant	10^{-6}	10^{-6}, 10^{-3}	—
24	Diffusion coefficient, M^{a+}	2×10^{-5}	2×10^{-5}	cm^2 s^{-1}
25	Passive current density	10^{-6}	10^{-6}	A cm^{-2}
26	Mechanical loading frequency	1	1	Hz

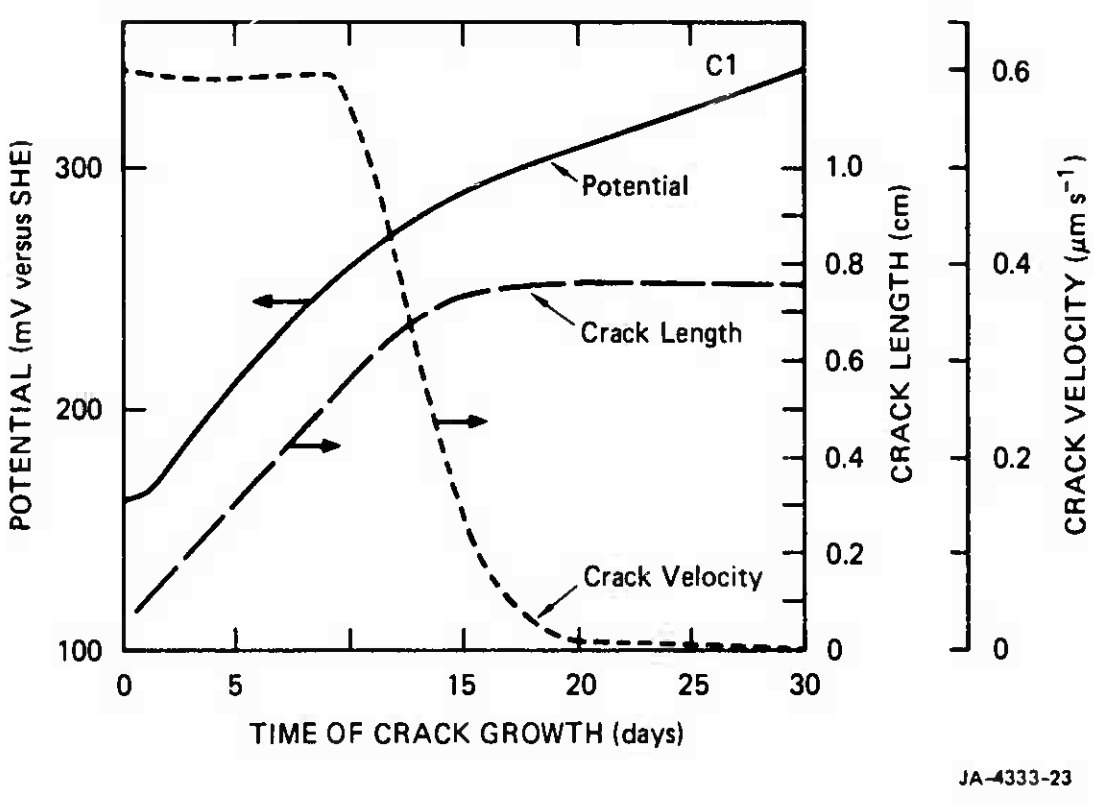

FIGURE 23 DC TRANSMISSION LINE MODEL CALCULATION OF THE POTENTIAL, CRACK LENGTH, AND CRACK VELOCITY AS A FUNCTION OF TIME FOR A CRACK GROWN AT CONSTANT CURRENT IN HY80 STEEL

Initial conditions C1 in Table 5.

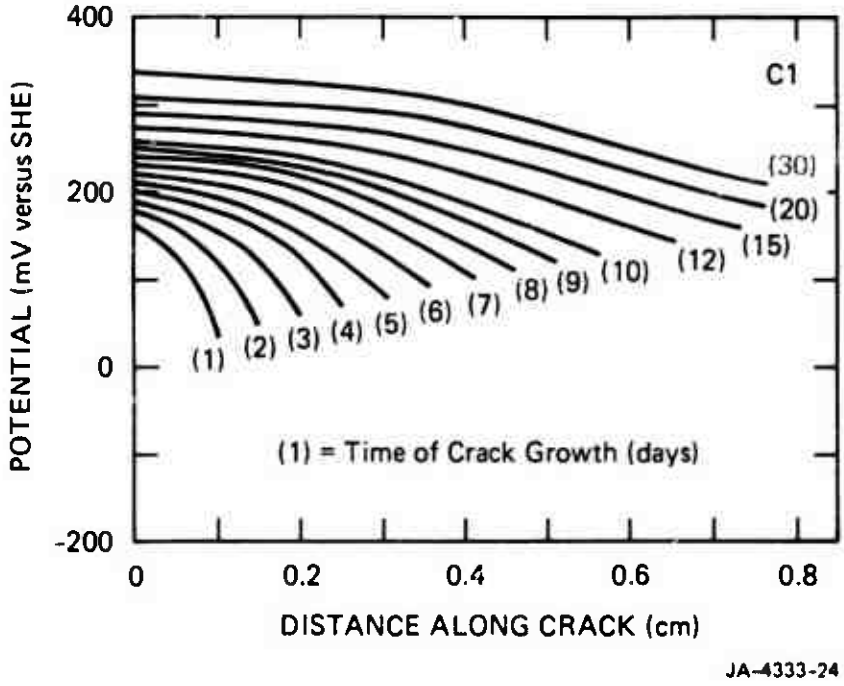

FIGURE 24 DC TRANSMISSION LINE MODEL CALCULATION OF THE POTENTIAL VERSUS DISTANCE INTO THE CRACK AS A FUNCTION OF TIME FOR HY80 IN 3.5% NaCl

Initial conditions C1 in Table 5.

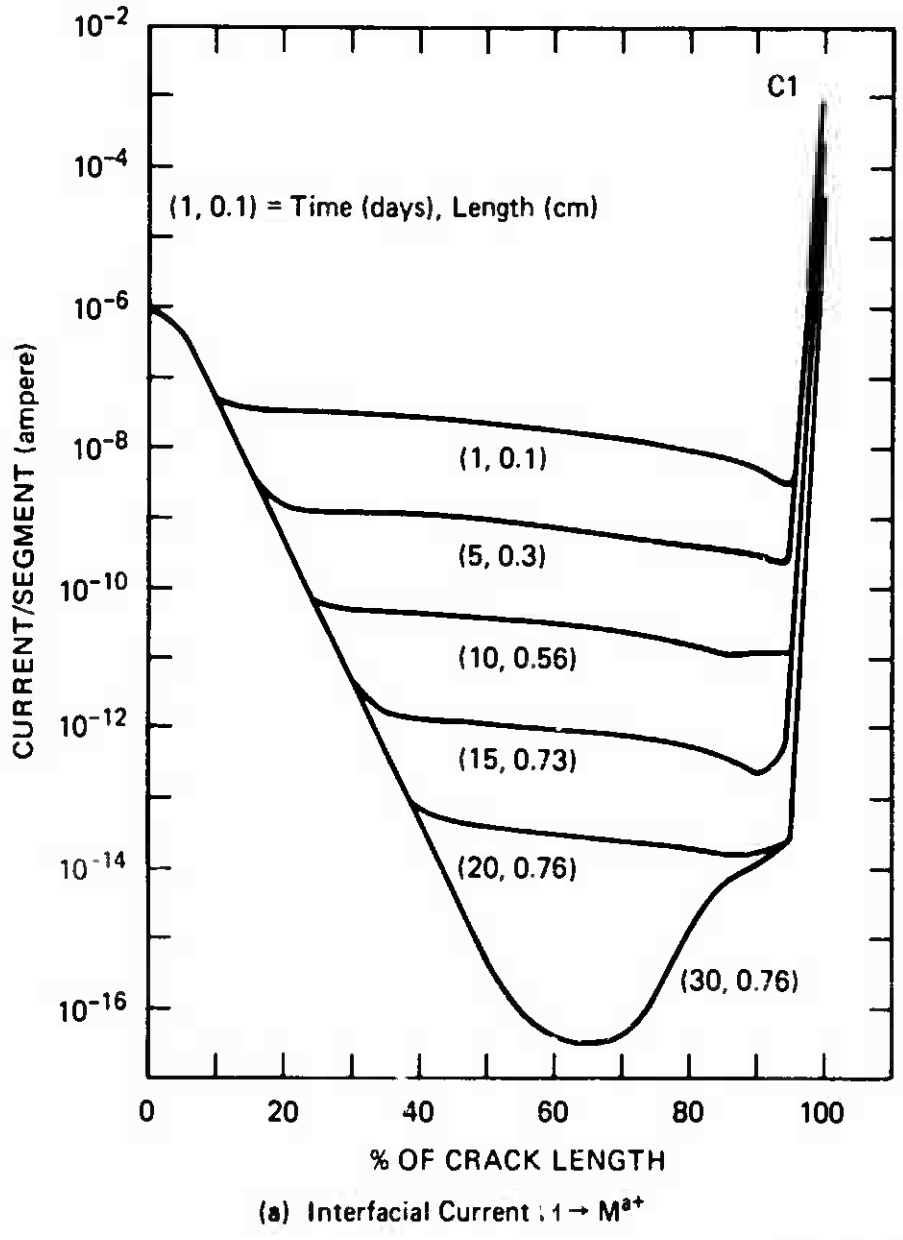

FIGURE 25 OC TRANSMISSION LINE MOOEL CALCULATIONS OF INTERFACIAL CURRENT, METAL ION CONCENTRATION, ANO CRACK ELECTROLYTE pH AS A FUNCTION OF OISTANCE INTO CRACK

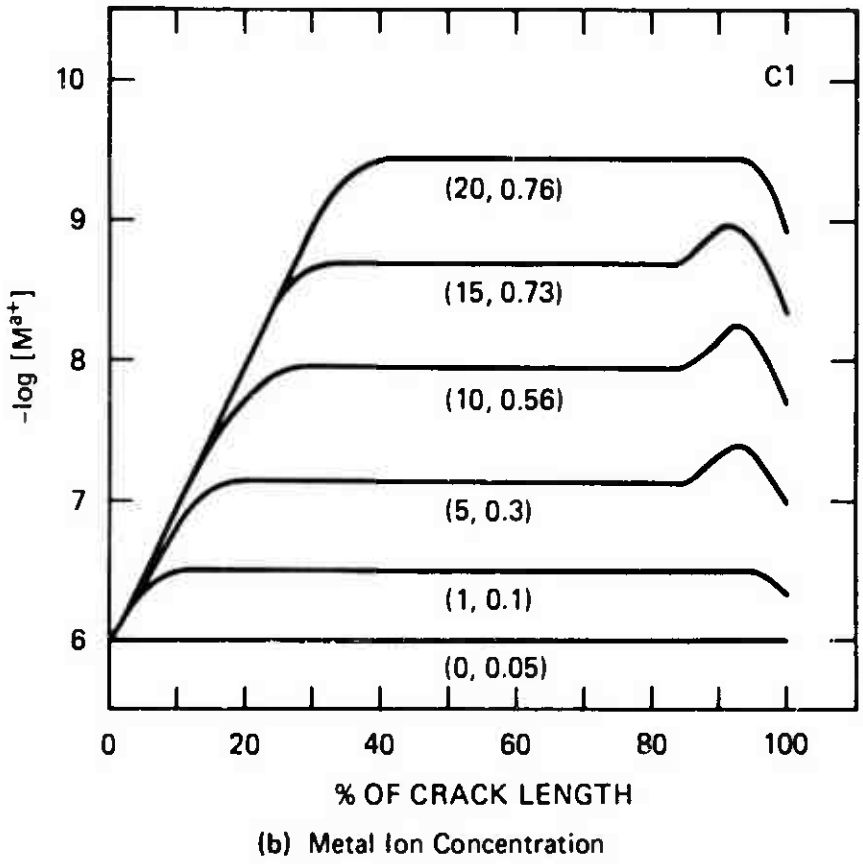

(b) Metal Ion Concentration

JA-4333-26

FIGURE 25 DC TRANSMISSION LINE MODEL CALCULATIONS OF INTERFACIAL CURRENT, METAL ION CONCENTRATION, AND CRACK ELECTROLYTE pH AS A FUNCTION OF DISTANCE INTO CRACK (Continued)

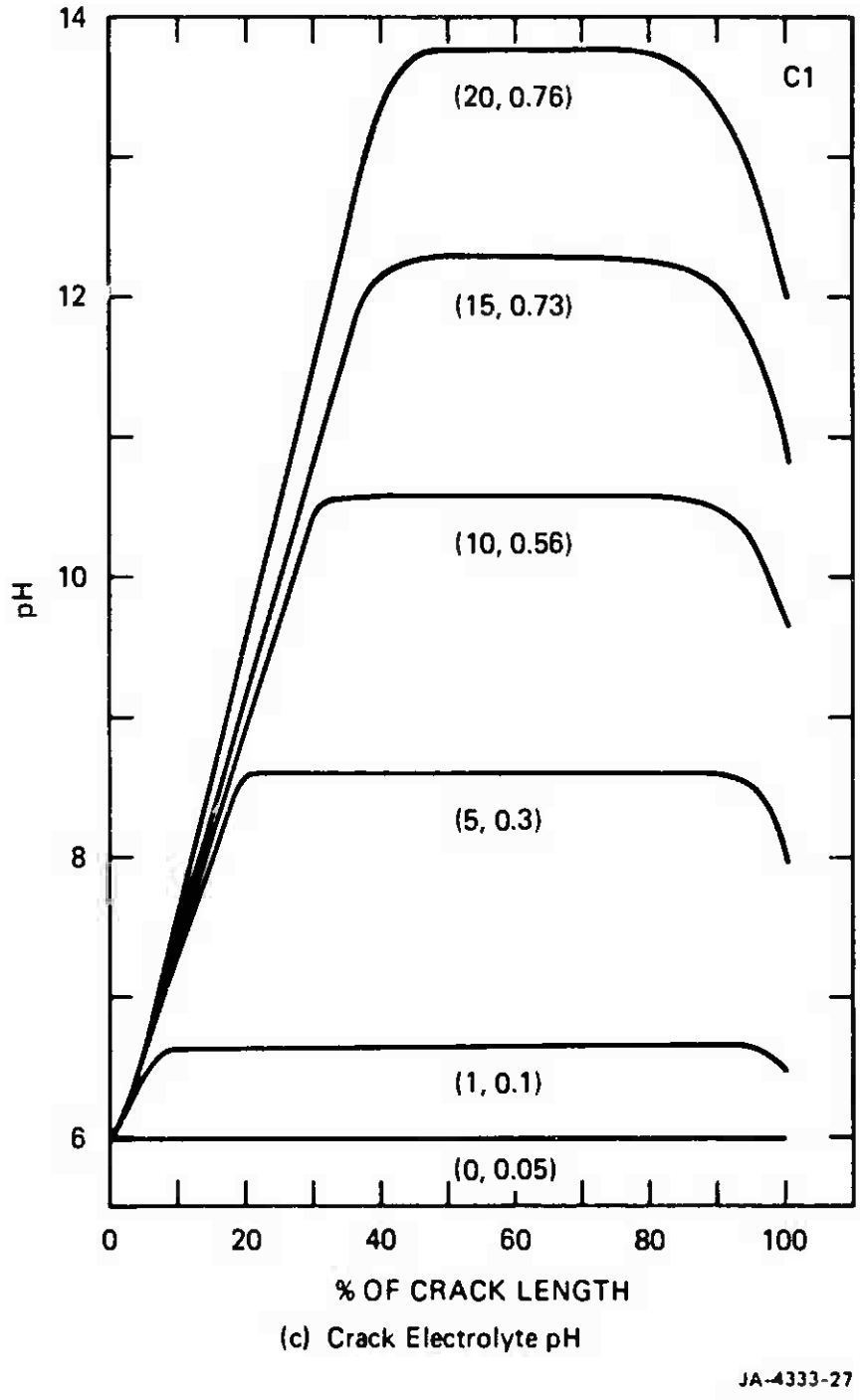

FIGURE 25 DC TRANSMISSION LINE MODEL CALCULATIONS OF INTERFACIAL CURRENT, METAL ION CONCENTRATION, AND CRACK ELECTROLYTE pH AS A FUNCTION OF DISTANCE INTO CRACK (Concluded)

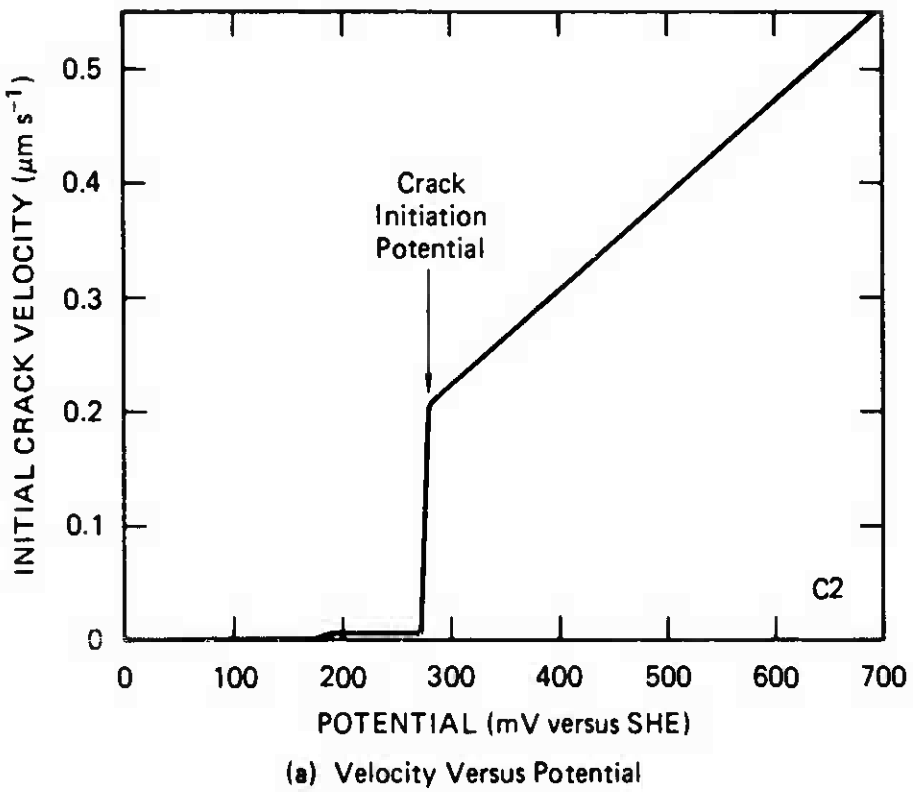

FIGURE 26 DC TRANSMISSION LINE MODEL CALCULATIONS OF VELOCITY VERSUS APPLIED POTENTIAL, VELOCITY VERSUS POTENTIAL (EXPANDED), AND LOG (VELOCITY) VERSUS APPLIED CURRENT

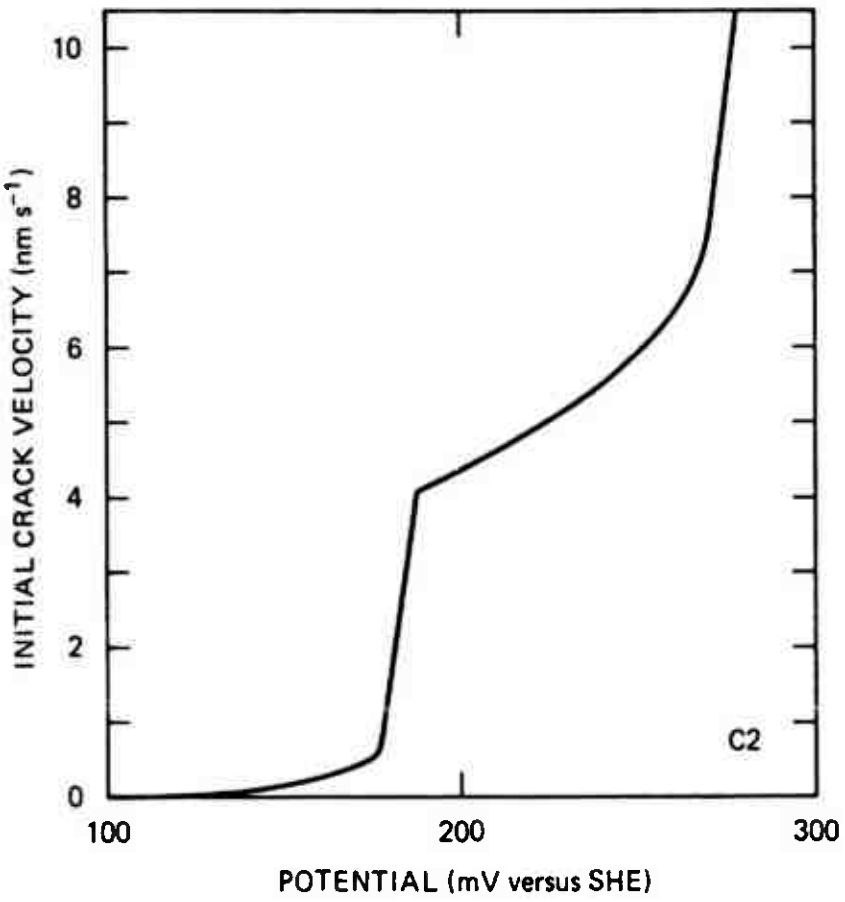

(b) Velocity Versus Potential (Expanded Scale)

JA-4333-29

FIGURE 26 DC TRANSMISSION LINE MODEL CALCULATIONS OF VELOCITY VERSUS APPLIED POTENTIAL, VELOCITY VERSUS POTENTIAL (EXPANDED), AND LOG (VELOCITY) VERSUS APPLIED CURRENT (Continued)

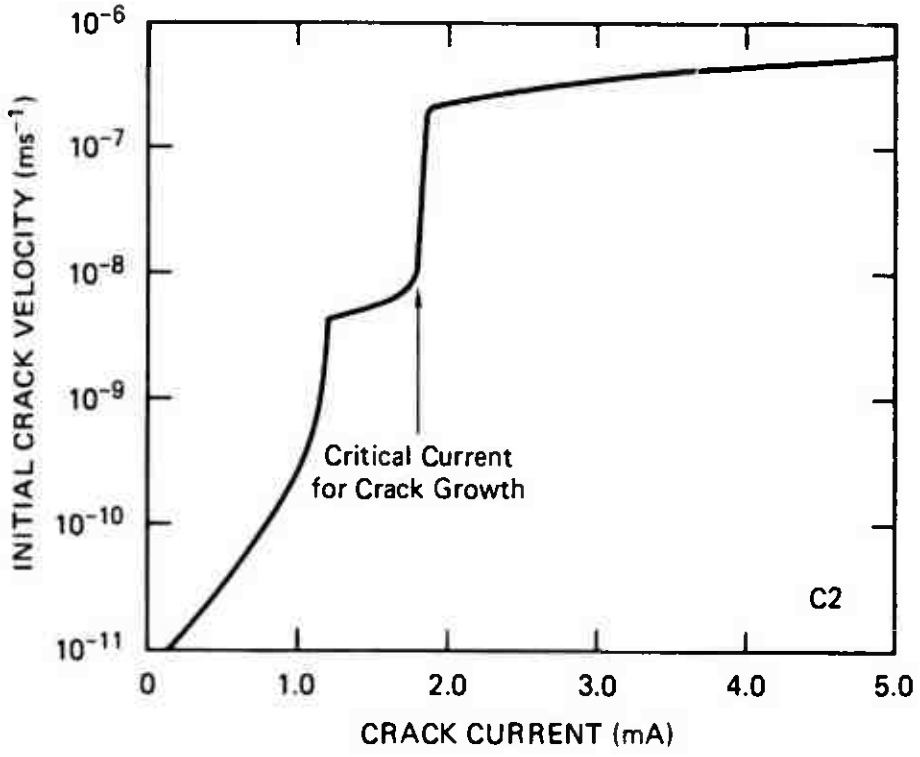

(c) Log (Velocity) Versus Current

JA-4333-30

FIGURE 26 DC TRANSMISSION LINE MODEL CALCULATIONS OF VELOCITY VERSUS APPLIED POTENTIAL, VELOCITY VERSUS POTENTIAL (EXPANDED), AND LOG (VELOCITY) VERSUS APPLIED CURRENT (Concluded)

Figure 24 presents profiles of the potential difference between the solid and electrolyte phases (the potential driving force for electrochemical reaction) as a function of distance and time. For this example the equilibrium potential for metal dissolution is taken to be -200 mV versus the standard hydrogen electrode (SHE); thus, the baseline of this plot represents the approximate potential of zero dissolution current. As expected, the potential decreases between the crack orifice and the crack tip due to the finite conductivity of the electrolyte, the existence of electrochemical reactions at the crack walls, and the presence of reaction products in the crack electrolyte volume. Somewhat unexpectedly, for the conditions chosen, this potential drop is not a large fraction of the total overvoltage driving metal dissolution, and the potential drop decreases (as a percentage) with increasing crack length.

This observation is surprising in view of the results of previous calculations.[8,9] Nevertheless, it is necessary that a significant fraction of the externally imposed potential be reflected at the growing crack tip to account for the observation of a critical potential for crack growth.[60]

The origins of the deceleration in crack growth rate observed after 10 days for computation C1 can be seen clearly in Figures 25(a) through (c). These figures show a normalized crack length, with the time of growth and actual length given in parentheses. Figure 25(a) presents the component of the total interfacial current due to metal dissolution via reaction (5.1), as a function of time and length. The ordinate is plotted logarithmically to accommodate the large range of interfacial currents. Independent of time and length, the majority of the dissolution current flows from the region of film rupture at the crack tip. Despite the presence of a passivating oxide film, some metal dissolution also occurs on the walls of the crack. To a first approximation, however, the crack can be considered as active at the tip, partially active at the orifice, and passive (with respect to metal dissolution) in the central segments.

Figure 25(b) shows the concentration of metal ions (plotted as -log[metal ion]) within the crack volume. For the example calculated the concentration is constant before the imposition of an external current, at a value determined by the chemical equilibrium between metal ions, hydrogen ions, and the aurface metal oxide. As the crack grows, metal ions become depleted in the central aegments due to the formation of metal oxide. Metal ions are produced by dissolution at the crack tip, but the effect of this concentration does not propagate deeply along the crack length.

Because reaction (5.2) is assumed to be at equilibrium, the depletion of metal ions in the central segments requires that the hydrogen ion concentration also be low. Thus, Figure 25(c) shows a trend toward alkalinity in the crack volume, with local acidification at the crack tip.

A second series of calculations was performed to determine the effect of crack current (or external potential) on the initial crack velocity. The parameters used are listed as "C2" in Table 5, and the results are summarized in Figures 26(a) through (c). Figure 26(a) shows the steady state crack velocity for a vestigial crack 0.1 cm long, plotted versus the potential of the electrolyte at the crack orifice for $K = 10^{-6}$. This plot exhibits a discontinuity at about 275 mV versus SHE. Below this potential the crack grows very slowly, whereas at higher potentials crack velocity increases roughly linearly with potential. One can interpret this discontinuity as a crack initiation potential although a closer inspection of the velocity versus potential profile near 200 mV [see Figure 26(b)] reveals two abrupt steps in velocity, one at 180 mV and the other at 275 mV. Figure 26(c) shows the same data plotted as the logarithm of crack velocity versus the current that flows into the crack, which allows us to determine the critical current for crack growth of ~ 18 mA for the conditions selected.

The results obtained for a chemical rate constant of 10^{-3} are not plotted but show that, with larger values of the chemical rate constant, the discontinuities in velocity, shown in Figure 26, disappear, and the

crack growth rate becomes a simple monotonic function of potential (or current). A second major effect of the chemical rate constant is that large values of the chemical rate constant result in general acidification of the crack electrolyte.

Section 5

CONCLUSIONS

From the results of this program, we draw the following conclusions regarding the use of AC impedance techniques and transmission line modeling to obtain electrochemical/mechanical properties states distributed within actively growing environmentally assisted cracks:

- The AC impedance response of the uncracked Ti-6Al-4V was found to behave as if the titanium alloy were covered with a dense TiO_2 semiconducting oxide layer. The HY80 exhibited more complex behavior although more typical of a corroding electrode. At transpassive and cathodic potentials the electrode impedance behavior was dominated by diffusional behavior, whereas in the potential range where a pseudo-passive film is expected to form, the impedance response was dominated by the double-layer capacitance in the electrolyte.

- The AC impedance response measured on cracked Ti-6Al-4V specimens under corrosion-fatigue conditions was found to depend on environmentally induced crack growth, total crack length, and change in stress intensity (ΔK). The electromechanical impedance of HY80 steel undergoing corrosion fatigue was modeled as a simplified equivalent circuit. The electromechanical impedance HY80 was also measured. This electromechanical impedance technique was sensitive to crack wall area at frequencies above 1 Hz and more sensitive to the crack tip at mechanical frequencies below 0.1 Hz.

- A DC transmission line model of growing corrosion-fatigue cracks constructed from HY80 undergoing corrosion fatigue was used to predict crack growth rates and potential and chemistry distributions within the crack. The predicted crack growth rates were in reasonable agreement with the experimentally measured values. The model also predicted a reasonable ΔK threshold for crack growth. At present, the model treats the crack tip region rather simply, but several models exist that could be incorporated rather easily in the future.

The results of this program have shown that a technique combining AC impedance, electrochemical/mechanical impedance, and transmission line

modeling offers the potential to determine both the mechanical and electrochemical processes that occur within streaa corrosion and corrosion-fatigue cracks. At present, it is one of the few techniques with this capability. The results did not conclusively show that the combination of AC impedance, electromechanical impedance, and transmission line modeling can be uaed quantitatively to predict crack growth ratea because the transmission line model was not used to reproduce the electromechanical impedance. We recommend additional effort to use the transmission line model in conjunction with the electromechanical/electrochemical impedance to obtain the critical mechanical and chemical parameters at the crack tip. It is clear that, with more modeling and experimental work on a wider variety of materiala, load cyclea, and aqueous environments, the electrochemical/mechanical technique developed in this program can become an important research tool.

REFERENCES

1. A. J. Forty and D. Van Rooyen, Eds., Proceedings of Conference on Fundamental Aspects of Stress Corrosion Cracking (NACE, Houston, Texas, 1969).

2. O. F. Devery, A. J. McEvily, and R. W. Staehle, Eds., Corrosion Fatigue: Chemistry, Mechanics and Microstructure (NACE, Houston, Texas, 1979).

3. Z. A. Foroulis, Ed., Proceedings of Conference on Environment-Sensitive Fracture of Engineering Materials (The Metallurgical Society of AIME, Warrendale, Pennsylvania, 1979).

4. J. C. Scully, Ed., The Theory of Stress Corrosion Cracking in Alloys, (NATO, Brussels, 1971).

5. A. J. McEvily and A. P. Bond, J. Electrochem Soc., 112, 131 (1965).

6. F. P. Ford, Metal Science, 326 (July 1978).

7. H. L. Logan, J. Res. Nat. Bur. Stand., 48, 99 (1952).

8. P. Doig and P.E.J. Flewitt, Proc. Roy. Soc., 357, 439 (1977).

9. P. Doig and P.E.J. Flewitt, Met. Trans., 124, 923 (1981).

10. R. P. Wei and J. D. Landes, Mater. Res. Stand., 9, 25 (1969).

11. P. B. Dawson and R. M. Pelloux, Met. Trans., 54, 723 (1974).

12. D. Schlain, "Corrosion Properties of Titanium and Its Alloys," Bureau of Mines Bulletin No. 619, U.S. Department of the Interior (1964).

13. J. D. Jackson and W. K. Boyd, "Corrosion of Titanium," DMIC Memorandum 218 (Battelle Memorial Institute, Columbus, Ohio, 1966).

14. Werkst. Korros., 30, 846 (1979).

15. J. F. Newman, Corrosion Science, 21, 487 (1981).

16. R. D. Caligiuri, L. E. Eiselstein, and M. J. Fox, "Low Temperature Sensitization of Weld Heat-Affected Zones in Type 304 Stainless Steel," lecture presented at Proceedings of International Atomic Energy Agency Specialists Meeting on Subcritical Crack Growth, held at Freiburg, Germany (May 1981).

17. F. P. Ford, "A Mechanism of Environmentally Controlled Crack Growth of Structural Steels in High Temperature in High Temperature Water," lecture presented at Proceedings of International Atomic Energy Agency Specialists Meeting on Subcritical Crack Growth," held at Freiburg, Germany (May 1981).

18. H. Riedel and J. R. Rice, Fracture Mechanics, P. C. Paris, Ed. (ASTM STP 700 1980), p. 112.

19. H. Riedel, J. Mech. Phys. Solids, 29, 35 (1981).

20. T. P. Hoar and F. P. Ford, Corrosion Science, 13, 729 (1973).

21. F. P. Ford, "Understanding Micromechanisms of Fracture," lecture presented at Gordon Conference, New Hampshire (1981).

22. D. D. Macdonald and M.C.H. McKubre, "Impedance Measurement in Electrochemical Systems," Chapter 2 in Modern Aspects of Electrochemistry, J. O'M Bockris, Ed., Vol. 16 (Plenum, New York, 1982).

23. D. D. Macdonald and M.C.H. McKubre, "Electrochemical Impedance Techniques in Corrosion Science," in Electrochemical Corrosion Testing, ASTM STP 727, Florian Mansfeld and Ugo Bertocci, Eds. (ASTM, 1981), pp. 110-169.

24. M. Sluyters-Rehback and J. H. Sluytera, in Electroanalytical Chemistry, Vol. 4, A. J. Bard, Ed. (Marcel Dekker, New York, 1970), pp. 1-128.

25. L. E. Eiselstein, R. D. Caligiuri, S. S. Wing, and B. C. Syrett, "Accelerated Corrosion of Copper-Nickel Alloys in Sulfide-Polluted Seawater: Mechanism No. 2," lecture presented at Corrosion 82, Houston, Texaa (1982).

26. M.C.H. McKubre and D. D. Macdonald, "The Rotating Cylinder-Collector Electrode (RCCE)," J. Electrochem. Soc., 127, 632 (1980).

27. O. S. Ksenzheck and V. V. Stender, Dokl. Akad. Nauk SSR, 106, 487 (1956); 107, 280 (1956).

28. M.C.H. McKubre, "Equilibrium and Steady State Studies of Continuou. Flow-Through Electrode Syatema," report to The Univeraity, Southampton Univeraity, Southampton, England (1978).

29. J. McHardy, J. M. Baris, and P. Stonehart, J. Appl. Electrochem, 6, 371 (1976).

30. J. O'M Bockris and A.J.N. Reddy, Modern Electrochemiatry (Plenum Press, New York, 1973).

31. M.C.H. McKubre, Ph.D. thesis, Victoria Univeraity, Wellington, New Zealand (1976).

32. J. H. Sluyters, thesis, Utrecht, The Netherlands (1959).

33. A. B. Yzermans, thesis, Utrecht, The Netherlanda (1965).

34. P. Drosaback and J. Schultz, Electrochim. Acta, 9, 1391 (1969); 11, 669 (1966).

35. J. R. Macdonald, J. Electroanal. Chem., 32, 317 (1971).

36. D. D. Macdonald, Transient Techniques in Electrochemiatry (Plenum Press, New York, 1977).

37. M. Stern and A. L. Geary, J. Electrochem. Soc., 104 (1), (1957).

38. G.H.J. Broers and M. Schenke, in International Symposium Brennstoffelmente, K. Schwabe and E. Winkler, Eds. (Akademic-Verlag, Berlin, 1968), p. 299.

39. G.H.J. Broers and M. Schenke, in Hydrocarbon Fuel Cell Technology, B. S. Baker, Ed. (Academic Presa, New York, 1965), p. 225.

40. G.H.J. Broera, in Fuel Cella (American Institute of Chemical Engineers, New York, 1963), p. 90.

41. K. Mund, G. Richter, and F. von Sturm, J. Electrochem. Soc., 124, 1 (1977).

42. M.C.H. McKubre and G. J. Hilla, "The Use of AC Impedance Meaauremenla to Characterize the Steady-State Propertiea of Continuous Flow-Through Electrodes" (to be published).

43. G. J. Hills and M.C.H. McKubre, SRI International (unpublished work).

44. M.C.H. McKubre and G. J. Hills, FORTAN IV programs written at The University, Southampton University, Southampton, England.

45. M. J. Madou and M.C.H. McKubre, J. Electrochem. Soc. 130, 5 (1983).

46. M. J. Madou, "A Semiconductor Electrochemiatry Approach to the Study of Oxide Films on Nickels, Iron and Cadmium Electrodes," SRI Annual Report on Project 5703 (1984).

47. D. D. Macdonald and M.C.H. McKubre, Chapter 2 in Modern Aspects of Electrochemistry, No. 14, O.M. Bockris, B. E. Conway, and R. E. White, Eds. (Plenum Press, New York, 1962).

48. G. Gabrielli and M. Keddam, Electrochim. Acta, 19, 355 (1974).

49. R. D. Armstrong, M. P. Bell, and A. A. Metcalfe, J. Electroanal. Chem., 84, 6 (1977); K. L. Bladen, J. Appl. Electrochem., 7, 345 (1977); A. A. Metcalfe, J. Electroanal. Chem., 88, 187 (1978).

50. D. Lelevre and V. Plichon, Electrochim. Acta, 23, 725 (1978).

51. P. Casson, N. A. Hampson, and M. J. Willars, J. Electroanal. Chem., 97, 21 (1979).

52. R. D. Armstrong, M. F. Bell, and A. A. Metcalfe, J. Electroanal. Chem., 77, 287 (1977).

53. E399, Volume 10, "1982 Annual Book of ASTM Standards," ASTM, p. 611.

54. A. Saxena and S. J. Hudak, Int. J. Fract., 14, p. 453 (1978).

55. M. L. Williams, J. Appl. Mech., 24, 109-114 (1957).

56. J. R. Rice and M. A. Johnson, in Elastic Beh: ior of Solids, M. F. Kanninen et al.

57. J. W. Hutchinson, J. Mech. Phys. Solids, 16, 13-31 (1968).

58. J. R. Rice and G. F. Rosengren, J. Mech. Phys. Solids, 16, 1-12 (1968).

59. R. M. McMeeking, J. Mech. Phys. Solids, 25, 357-381 (1977).

60. Private communication, D. D. Macdonald, SRI International (January 1986).

Appendix A

IMPEDANCE DATA MANAGEMENT AND CONTROL PROGRAM

```
1  REM  "OMSS.MAIN 15/JUN/1983
3  REM BY M.C.H.MCKUBRE
10  HIMEM: 36300: LOMEM: 24577
90 ZN% = 120: IF NP% <  > 0 THEN 1000
100  DIM ZM(12B),ZN(5,ZN%),ZZ(9),ZT(32),ZO$(B)
110  PRINT  CHR$ (4);"BLOAO B.FRA"
140 ZM(1) = 1:ZM(2) = 1:ZM(11) = 100:ZM(12) = 1:ZM(13) = 1:ZM(21) = 1:ZM(22) = 1:ZM(23) = 1:ZM(24) = 1:
    ZM(25) = 1:ZM(34) = 65535:ZM(35) = 1:ZM(3B) = ZN%:ZM(39) = 1.1:ZM(44) = I:ZM(45) = 0201:ZM(49) = 2
    00
150 ZM(51) = 1:ZM(53) = 1:ZM(55) = 1:ZM(56) = ZN%:ZM(57) = 1:ZM(B4) = 2:ZM(B5) = 2:ZM(B6) = 2:ZM(121) =
    2:ZM(122) = 1:ZM(123) = 1
160 X =  FRE (0):SB% = 6:OB% = 1:VB% = 23
170  IF S% < 4 OR S% > 6 THEN S% = 5:O% = 1:V% = 0
200  GOSUB 20000
300  DATA  "FR","AM","B1","WF","MO",%SY","LE","SR","SL","AC","AS","AV","AE","AP","QA","QB","QW","SQ","S
    G","RG"
320  DATA "IS","IC","MS","MC","HA","AU","RA","OE","OC","IP","SA","S1","RE","MA","MI","GO","GO","GS","GR
    ","NH","NS","SS","HS","SC","SO","CO"
340  DATA  "VE","AA","PO","XI","XH","XL","XO","YI","YH","YL","YO","SP","PL","SM","ST","PG","VA","UP","O
    N","FD","FO","FC","LL"
360  DATA "BK","$L","$E","$C","$F","$B","$O","$1","$Q","$P","EP","JP","CP","TM","TT","OP","FN"
380  DATA "AF","BF","RF","TF","UA","UB","UR","UT","US","LA","LB","LR","LT","LG","SV","PP","PS","OS","OT
    ","RR","RH"
400  DATA "NR","NA","PN","ER","A1","AR","TS"
1000  TEXT : POKE 34,0: HOME : PRINT
1100  PRINT : PRINT "PROGRAM OPTIONS ARE:"
1120  PRINT : PRINT "  1...SET UP SOLARTRON"
1140  PRINT : PRINT "  2...HELP"
1160  PRINT : PRINT "  3...TAKE MEASUREMENTS"
1180  PRINT : PRINT "  4...CHAIN BODE PLOT"
1200  PRINT : PRINT "  5...CHAIN NYQUIST PLOT"
1220  PRINT : PRINT "  6...SAVE DATA ON DISK"
1230  PRINT : PRINT "  7...RETRIEVE DATA FROM DISK"
1240  PRINT : PRINT "  B...SET TIME"
1245  PRINT : PRINT "  9...CHAIN ANALYSIS PROGRAM"
1250  PRINT : PRINT "  0...EXIT PROGRAM"
1260 ZZ(3) = 0: VTAB (23):ZZ(4) = 0:ZZ(5) = 9: GOSUB 10100
1280  IF ZE%(0) = 1 THEN 1000
1300  ON ZZ(3) GO'O 1500,2500,3000,4000,5000,6000,7000,B000,9700
1320  HOME : VTAB 9: PRINT "EXIT PROGRAM": PRINT : PRINT "TYPE GOTO 1000 TO RESUME": END
1500  GOSUB 15000: GOTO 1000
1900 ZM(12B) = 1:M$ = "T1F2": GOSUB 29000:ZZ(4) = ZZ(3):M$ = "T1F0": GOSUB 29000: PRINT : PRINT "RS = "
```

```
    ;ZZ(4): PRINT : INPUT "USE THIS VALUE (Y/N) ? ";M$: IF M$ <  > "Y" THEN 15000
1920 ZM(51) = ZZ(4): GOTO 1500: REM  RP
2000  NOME : PRINT "INITIALISE"
2020  GOSUB 20000:M$ = ":'TT2'": GOSUB 21000
2040  GOSUB 29000: REM  KEITHLEY
2060  GOTO 15000
2500  NOME : VTAB 5: PRINT "  HELP:": PRINT "  ----": VTAB 10: PRINT "   THERE IS NO HELP AVAILABLE HER
    E.": PRINT "LIFE IS LIKE THAT. IT CAN SOMETIMES BE": PRINT "HARD AND CRUEL.": PRINT "   IF YOU DON
    'T KNOW WHAT YOU ARE DOING"
2510  PRINT "IT IS POSSIBLE THAT YOU SHOULD NOT": PRINT "BE DOING IT.": PRINT "   PLEASE DO NOT HESITAT
    E TO NOT": PRINT "CALL ME,": VTAB 19: HTAB 9: PRINT "MIKE"
2520  VTAB 23: GET ZO$(0): PRINT ZO$(0): GOTO 1000
3000  NOME : VTAB 3: PRINT "NAME AND LOCATION OF SAVE DATA FILE"
3010  GOSUB 11500: PRINT : PRINT "FILE NAME WILL BE PRECEDED BY DMSS(0)-": PRINT : INPUT "ENTER FILE NA
    ME = DMSS(0)-";ZO$(0)
3015 X =  FRE (0):ZF$ = ZO$(0):ZZ(8) = 77:ZO$(0) = "DMSS(P)-" + ZF$: GOSUB 11400:ZF$ = "DMSS(0)-" + ZF$
     + "$":ZZ(8) = 78
3020  PRINT : PRINT "STARTING FILE # ";:ZZ(3) = ZF%:ZZ(4) = 0:ZZ(5) = 100:ZZ(6) = 1: GOSUB 10100: IF ZE
    %(0) = 1 THEN 3020
3030 ZF% = ZZ(3):ZM(3) = ZM(118)
3040 X =  FRE (0): POKE 34,0: HOME : POKE 34,3: VTAB 1: PRINT "MEASUREMENT MODE # ";ZM(127): VTAB 2: PRINT
    ZF$;ZF%: VTAB 3: PRINT "SCALE FACTOR ";ZM(53)
3050 ZM(47) = 0: HOME : VTAB 5: PRINT "STATUS PAGE": PRINT "------ ----": VTAB 8: PRINT "TOTAL # OF POI
    NTS ";ZM%: VTAB 10: PRINT "TIMED SWEEP";: HTAB 19: PRINT "ON": IF ZM(125) = 0 THEN  VTAB 10: HTAB
    19: PRINT "OFF"
3060  VTAB 12: PRINT "DC VOLTAGE SWEEP";: HTAB 19: PRINT "ON": IF ZM(120) = 0 THEN  VTAB 12: HTAB 19: PRINT
    "OFF"
3070  VTAB 14: PRINT "FREQUENCY SWEEP";: HTAB 19: PRINT "ON": IF ZM(34) = ZM(35) THEN  VTAB 14: HTAB 19
    : PRINT "OFF"
3080  VTAB 16: PRINT "HARMONIC SWEEP";: HTAB 19: PRINT "ON": IF ZM(122) = ZM(123) THEN  VTAB 16: HTAB 1
    9: PRINT "OFF"
3090  VTAB 18: PRINT "INPUT FRONT/REAR";: HTAB 19: PRINT "FRONT": IF ZM(50) > 0 THEN  VTAB 18: HTAB 19:
     PRINT "REAR ": IF ZM(50) > 1 THEN  VTAB 18: HTAB 19: PRINT "BOTH"
3100  VTAB 2: HTAB 28: PRINT "START # ";ZM(124): VTAB 3: HTAB 29: PRINT "STOP # ";ZM(125)
3110  IF ZM(126) > 0 THEN  GOSUB 18200: IF ZZ(3) + ZZ(4) / 60 < ZM(124) THEN  FOR II = 1 TO 4444: NEXT
    II: GOSUB 18000: GOTO 3110
3120 FP% = 1: IF ZM(50) = 2 THEN FP% = 2
3130 ZM(56) =  INT ((ZM% / (FP% * ZM(55) * ZM(57)))
3140 ZM(39) = (ZM(34) / ZM(35)) ^ (1 / ZM(56))
3145 ZM(0,0) = ZM%: GOSUB 18200:ZM(1,0) = ZZ(3) + ZZ(4) / 60:ZM(2,0) = ZM(127):ZM(3,0) = ZM(53):ZM(4,0)
     = 1250
3150  VTAB 23: PRINT ZM(39),ZM(57),ZM(56)
3160  VTAB 5: CALL  - 958: PRINT
3170 J = 0: IF ZM(121) = 1 THEN ZM(3) = ZM(118): REM  INITIAL DC
3175  GOSUB 3900: REM SET DISPLAY
3180 II = 3: GOSUB 17000
3190  FOR JZM = 1 TO 441 * ZM(117): NEXT JZM
3200 ZM(1) = ZM(35): REM  F MIN.
3210 II = 1: GOSUB 17000
3220 ZM(29) = 0: IF ZM(1) >  = ZM(49) THEN ZM(29) = 1: REM COUPLING
3230 II = 29: GOSUB 17100
3240 ZM(25) = ZM(122): REM  INITIAL HARMONIC
```

```
3250 II = 25: GOSUB 17000
3260 FR% = 0:ZM(30) = 0: IF ZM(50) = 1 THEM ZM(30) = 1:FR% = 1: REM REAR
3270 II = 30: GOSUB I7I00:ZM(45) = 0100: IF ZM(127) = 2 THEM ZM(45) = 0200
32B0  IF ZM(I27) = 0 THEM ZM(45) = 020I
3290 J = J + 1: IF J = ZM% AMO ZM(12B) = I THEN 3620
3295  IF J > ZN% THEM 35B0: REM   FULL
3300 II = 45: GOSUB 17000: GOSUB IB000:II = 32: GOSUB 16900: REM   MEASURE
3310 M$ = ":'OP2,I'":II = 4: GOSUB 24000: IF ZZ(4) <  > 0 THEN 3300
3320  FOR ZS = 1 TO 3:ZM(ZS - I,J) = ZZ(ZS): NEXT ZS
3330  IF ZM(127) > 3 THEM II = 45:ZM(45) = 0200: GOSUB 17000: GOSUB 1B000:M$ = ":'OP2,I'":II = 4: GOSUB
      24000: REM  CH02
3340  IF ZM(127) < 3 THEM ZM(3,J) = 1:ZM(4,J) = 0
3350  IF ZM(127) = 3 THEM ZM(3,J) = ZM(1,J):ZM(4,J) = ZM(2,J):ZM(I,J) = ZZ(2):ZN(2,J) = ZZ(3)
3360  IF ZM(127) = 4 THEM ZM(3,J) = ZZ(2) - ZM(1,J):ZM(4,J) = ZZ(3) - ZM(2,J)
3370  IF ZM(I27) = 3 THEM ZM(3,J) = ZN(1,J):ZN(4,J) = ZM(2,J):ZM(1,J) = ZZ(2):ZM(2,J) = ZZ(3)
33B0  IF ZM(127) = 5 THEM  GOSUB 3B00: GOTO 3420
3390  GOSUB 9500:ZM(3,J) = I / ZM(51):ZM(4,J) = 6.2B232 * ZM(0,J) * ZM(52): GOSUB 9500:ZM(1,J) = ZM(I,J
      ) / ZM(53):ZM(2,J) = ZM(2,J) / ZM(53): REM SCALE
3400  GOSUB 99B0:ZM(3,J) = ZM(3): REM MAG.&PHASE
3420 II = 1:M$ = ":'?ER'": GOSUB 24000: VTAB 21: HTAB 12: PRINT ZZ(II)
3430 ZZ(3) = 7:ZZ(4) = ZM(122):ZZ(5) = ZM(11B):ZZ(6) = ZM(35): GOSUB 3990
3432 ZZ(3) = B:ZZ(4) = ZM(123):ZZ(5) = ZM(119):ZZ(6) = ZM(34): GOSUB 3990
3434 ZZ(3) = 9:ZZ(4) = 1:ZZ(5) = ZM(120):ZZ(6) = ZM(39): GOSUB 3990
3436 ZZ(3) = 10:ZZ(4) = ZM(25):ZZ(5) = ZM(3):ZZ(6) = ZM(1): GOSUB 3990
3440  VTAB 12: HTAB 9: PRINT J - I;"/";ZN%; TAB( 25);J;"/";ZM%
3450  FOR 11 = 0 TO 5: VTAB (13 + 11): HTAB 6: CALL  - B6B: PRINT ZM(1I,J - 1); TAB( 24);ZM(II,J): NEXT
      11
3460  INVERSE : VTAB 20: HTAB 12:ZO$(0) = "FRONT": IF ZM(30) = 1 THEN ZO$(0) = " REAR"
3462  PRINT ZO$(0);: HTAB 2B:ZO$(0) = "OC": IF ZM(29) = 1 THEN ZO$(0) = "AC"
3464  PRINT ZO$(0);: HTAB 36:ZO$(0) = "OFF": IF ZM(14) = 1 THEN ZO$(0) = "ON "
3466  PRINT ZO$(0): NORMAL
34B0  VTAB 4: CALL  - B6B: IF ZM(47) = 999 THEN  PRINT "TERMINATE"
3490  IF ZM(50) = 2 AND FR% = 0 THEN ZM(30) = 1:FR% = 1: GOTO 3270: REM  REAR
3500  IF ZM(25) < ZM(123) THEN ZM(25) = ZM(25) + 1: GOTO 3250: REM LOOP H
3510  IF ZM(1) >  = ZM(34) THEN 3540
3520 ZM(1) = ZM(1) * ZM(39): IF ZM(1) > ZM(34) THEN ZM(1) = ZM(34)
3530  GOTO 3210
3540  IF  SGN (ZM(120)) =  SGN (ZM(119) - ZM(3)) THEN ZM(3) = ZM(3) + ZM(120): GOTO 31B0
3550  REM OC LIMIT REACHED
3560  IF ZM(121) = 1 THEN 31B0
3570  GOTO 3210
35B0  REM FULL
3590  GOSUB 18000
3600 ZM(124) = ZM(124) + ZM(126): REM INC.TIME
3610 X =  FRE (0):ZF% = ZF% + 1:ZO$(0) = ZF$ +  STR$ (ZF%):ZZ(B) = 7B: GOSUB 11400: REM   SAVE DATA
3612  IF (ZZ(3) + ZZ(4) / 100) > ZM(125) OR ZM(47) = 999 THEN 1000: REM  TERMINATE
3616  IF ZM(121) = 2 THEN ZM(3) = ZM(3) + ZM(120): IF  SGN (ZM(12)) =  SGN (ZM(119) - ZM(3)) THEN 1000:
      REM OC LIMIT
3618  GOTO 3040: REM CLOSE LOOP
3620 ZM(1) = 60:II = 1: GOSUB 17000:ZM(0,ZM%) = 60: FOR A = 1 TO 441: NEXT A:M$ = "T1F1": GOSUB 29200:Z
     M(2,ZM%) = ZZ(3):M$ = "T1F0": GOSUB 29200:ZM(3,ZM%) = ZZ(3)
```

```
3630 ZM(18) = 0:II = 18: GOSUB 17000: FOR II = 1 TO 441: NEXT II:M$ = "TIF1": GOSUB 29200:ZM(4,ZM%) = Z
     Z(3):M$ = "T(F0": GOSUB 29200:ZM(5,ZM%) = ZZ(3)
3640 II = 20: GOSUB 16900: GOTO 3420
3800  REM CH1=I,CH2=V
3820 ZM(3,J) = ZM(25):ZM(4,J) = ZZ(2):ZM(5,J) = ZZ(3)
3840 ZZ(2) = 1 / ZM(51):ZZ(3) = 6.28232 * ZM(0,J) * ZM(52):ZZ(4) = ZM(I,J) * ZZ(2) - ZM(2,J) * ZZ(3):ZM
     (2,J) = ZM(I,J) * ZZ(3) + ZM(2,J) * ZZ(2):ZM(I,J) = ZZ(4): REM  I=E/R
3860 ZM(1,J) = ZM(I,J) * ZM(53):ZM(2,J) = ZM(2,J) * ZM(53):ZM(4,J) = ZM(4,J) * ZM(53):ZM(5,J) = ZM(5,J)
     * ZM(53): REM SCALE MULTIPLIER
3880  RETURN
3900  REM  DISPLAY
3920  REM
3930  VTAB 6: CALL  - 958: HTAB 8: PRINT "H    DCV    FREQUENCY": PRINT "INIT.": PRINT "FINAL": PRINT "
     STEP": PRINT "CURR.": FOR II = 0 TO 5: VTAB (13 + II): PRINT "#";II: NEXT II
3940  VTAB 20: PRINT "INPUT FROM      : COUPLING   :COMP "
3960  VTAB 21: PRINT "LAST ERROR: ": RETURN
3990  VTAB ZZ(3): HTAB 7: CALL  - 868: PRINT ZZ(4); TAB( I1);ZZ(5); TAB( I8);ZZ(6): RETURN
4000 ZD$(0) = "BODE": GOSUB 19900
4020 NP% = 1: CALL 520"DMSS.BODE"
5000 ZD$(0) = "NYQUIST": GOSUB 19900
5020 NP% = 1: CALL 520"DMSS.NYQUIST"
6000  REM SAVE DATA TO DISK
6010  GOSUB 11500: PRINT : PRINT "FILE NAME WILL BE PRECEDED BY DMSS(D)-": PRINT : INPUT "ENTER FILE NA
     ME = DMSS(D)-";ZD$(0):ZD$(0) = "DMSS(D)-" + ZD$(0)
6020 ZZ(8) = 78: GOSUB 11420: GOTO 1000
6500 ZD$(0) = ZD$(0) +  STR$ ( INT (ZZ(3) + 0.5)): RETURN
7000  REM  RETRIEVE DATA FROM DISK
7040 X =  FRE (0): GOSUB 11500: PRINT : PRINT "CURRENT FILE NAME = ";ZF$;"$";ZF%: PRINT : INPUT "   NEW
     FILE NAME = DMSS(D)-";ZD$(0):ZD$(0) = "DMSS(D)-" + ZD$(0): IF ZD$(0) <  > "DMSS(D)-" THEN ZF$ = Z
     D$(0)
7060 X =  FRE (0): INPUT "   NEW FILE  $   = ";ZF%:ZD$(0) = ZF$ + "$" +  STR$ (ZF%)
7080 ZZ(8) = 78: GOSUB 11300: GOTO 1000
8000  HOME : REM SET TIME
8020  GOSUB 18200: VTAB 8: PRINT "NEW TIME:": HTAB 9: INPUT "HOURS ";JZN: IF JZN > 99 OR JZN < 0 THEN 8
     020
8040  VTAB 11: HTAB 7: INPUT "MINUTES ";ZM(83): IF ZM(83) > 59 OR ZM(83) < 0 THEN 8040
8060 II = 83: GOSUB 17200: GOTO 1000
9000  REM DISPLAY COUNTER ROUTINE
9010  HTAB 30: PRINT "$ ";JZN;"   ": RETURN
9240  PR# 3: PRINT "@(:": PRINT "'";ZD$(0);"I'": PRINT "@?;@H:": PR# 0: INPUT ZD$(0): IN# 0: RETURN
9500  REM COMPLEXDIVISION
9520 ZZ(5) = ZM(3,J) * ZM(3,J) + ZM(4,J) * ZM(4,J)
9540 ZZ(6) = (ZM(1,J) * ZM(3,J) + ZM(2,J) * ZM(4,J)) / ZZ(5)
9560 ZZ(4) = (ZM(2,J) * ZM(3,J) - ZM(I,J) * ZM(4,J)) / ZZ(5)
9580 ZM(I,J) = ZZ(6):ZM(2,J) = ZZ(4): RETURN
9700 ZD$(0) = "ANALYSIS": GOSUB 19900
9720  CALL 520"DMSS.ANALYSIS"
9970  REM MAG. & PHASE
9980 ZM(3,J) =  SQR (ZM(1,J) * ZM(1,J) + ZM(2,J) * ZM(2,J))
9985 ZM(4,J) =  ATN (ZM(2,J) / ZM(1,J)) * 180 / 3.141592654)
9990 ZM(5,J) =  LOG (ZM(3,J)) /  LOG (10): RETURN
9999  PRINT  CHR$ (13); CHR$ (4);"SAVEDMSS.MAIN": END
```

```
10000  REM   Y/N SUBR
10010 ZE%(0) = 0: PRINT "YES ";: GET ZD$(0):ZZ(3) =  PEEK (36) - 4: IF ZD$(0) = "Y" OR ZD$(0) =  CHR$ (
    13) THEN ZZ(3) = 2: PRINT "": RETURN
10020  IF ZD$(0) = "N" THEN  POKE 36,ZZ(3): PRINT "NO ":ZZ(3) = 1: RETURN
10030 ZE%(0) = 1: GOSUB 10050: RETURN
10050  REM  ERROR SUBR
10060  PRINT  CHR$ (7):ZE%(0) = 1: RETURN
10100  REM    I/P SUBR
10110  CALL  - B6B
10120 ZE%(0) = 0: PRINT ZZ(3): INPUT "  ";ZD$(0): IF ZD$(0) = "" THEN ZZ(7) = ZZ(3): GOTO 10170
10130  FOR I = I TO  LEN (ZD$(0)):ZQ$ =  MID$ (ZD$(0),I,I)
10140  IF ZQ$ = "+" OR ZQ$ = "-" OR ZQ$ = " " OR ZQ$ = "." OR ZQ$ = "E" THEN 10160
10150  IF ZQ$ < "0" OR ZQ$ > "9" THEN 10050
10160  NEXT I:ZZ(7) =  VAL (ZD$(0))
10170  IF ZZ(7) < ZZ(4) OR ZZ(7) > ZZ(5) THEN 10050
10180 ZZ(3) = ZZ(7): IF ZZ(6) = I THEN ZZ(3) =  INT (ZZ(7))
10190  FOR I = 0 TO 200: NEXT I: RETURN
11300  REM  : LOAD ARRAY
11320  POKE 9B,90: POKE 99,ZZ(8): CALL 38152
11330  PRINT  CHR$ (4);"BLOAD"ZD$(0);",A"; PEEK (38394) +  PEEK (38395) * 256
11340  RETURN
11400  REM : SAVE ARRAY
11420  POKE 98,90: POKE 99,ZZ(B): CALL 38104
11430  PRINT  CHR$ (4);"BSAVE"ZD$(0)",A" PEEK (38394) +  PEEK (38395) * 256",L" PEEK (38396) +  PEEK (3
    8397) * 256"
11440  RETURN
11500  REM ASK SLOT,DRIVE AND VOLUME
11510  VTAB 6: CALL  - 95B: PRINT "POINTERS CURRENTLY SET AT :": VTAB 8: PRINT "    SLOT #";SZ: PRINT "
       DRIVE #";DZ: PRINT "  VOLUME #";VZ
11520  VTAB 12: PRINT "CHANGE POINTERS (Y/N) ? ";: GET ZD$(0): IF ZD$(0) = "N" THEN 11550
11530  PRINT : PRINT :ZZ(3) = SZ:ZZ(4) = 4:ZZ(5) = 6:ZZ(6) = 0: PRINT "    SLOT ";: GOSUB 10120: IF ZE%
    (0) = I THEN 11530
11532 SZ =  INT (ZZ(3) + 0.5)
11535  PRINT :ZZ(3) = DZ:ZZ(4) = 1:ZZ(5) = 2:ZZ(6) = 0: PRINT "   DRIVE ";: GOSUB 10120: IF ZE%(0) = I THEN
    11535
11537 DZ =  INT (ZZ(3) + 0.5): IF SZ <  > 6 THEN VZ = 0: GOTO 11550: REM FLOPPY
11540  PRINT :ZZ(3) = VZ:ZZ(4) = 1:ZZ(5) = 67:ZZ(6) = 0: PRINT "  VOLUME ";: GOSUB 10120: IF ZE%(0) = 1
     THEN 11540
11542 VZ =  INT (ZZ(3) + 0.5)
11550  PRINT : PRINT "PRESS ANY KEY TO CATALOG ": GET ZD$(0): PRINT : PRINT  CHR$ (4);"CATALOG,S"SZ",D"
    DZ",V"VZ
11560  PRINT : PRINT "ANOTHER CATALOG  Y/N ?  ";: GOSUB 10000: IF ZE%(0) = 1 THEN 11560
11570  IF ZZ(3) = 2 THEN 11500
11580  RETURN
15000  TEXT : POKE 34,0: HOME : VTAB 5: PRINT "SET-UP OPTIONS ARE:"
15020  PRINT : PRINT "  1...RETURN TO MAIN MENU"
15040  PRINT : PRINT "  2...CREATE/MODIFY SET-UP FILE"
15060  PRINT : PRINT "  3...RETRIEVE SET-UP FILE FROM DISK"
15080  PRINT : PRINT "  4...SAVE SET-UP FILE TO DISK"
15100  PRINT : PRINT "  5...EXECUTE SET-UP FILE"
15120  PRINT : PRINT "  6...RESET (INITIALIZE) SOLARTRON"
15140  PRINT : PRINT "  7...RESET (INITIALIZE) KEITHLEY"
```

```
15200 ZZ(3) = 1: VTAB (23):ZZ(4) = 1:ZZ(5) = 7: GOSUB 10100: IF ZE%(0) = 1 THEN 15000
15220  ON ZZ(3) GOTO 1000,15300,16600,16640,16700,2000,1900
15300  HOME : VTAB 5: PRINT "SET-UP WHICH SUBSYSTEM:"
15320  PRINT : PRINT "  1...GENERATOR"
15340  PRINT : PRINT "  2...ANALYSER"
15360  PRINT : PRINT "  3...SWEEP(S)"
15380  PRINT : PRINT "  4...IMPEDANCE STANDARD"
15400  PRINT : PRINT "  5...MEASUREMENT CONFIGURATION"
15460  PRINT : PRINT "  0...RETURN TO SET-UP OPTIONS"
15480 ZZ(3) = 0: VTAB (23):ZZ(4) = 0:ZZ(5) = 5: GOSUB 10100: IF ZE%(0) = 1 THEN 15300
15500  ON ZZ(3) GOTO 15600,15800,16000,16300,16500
15520  GOTO 15000
15600  HOME : VTAB 3: PRINT "GENERATOR"
15610  VTAB 6: PRINT "FREQUENCY ";:ZZ(3) = ZM(1):ZZ(4) = 1E - 5:ZZ(5) = 65535:ZZ(6) = 0: GOSUB 10100: IF
    ZE%(0) = 1 THEN 15610
15620 ZM(1) = ZZ(3)
15630  VTAB 9: PRINT "AMPLITUDE ";:ZZ(3) = ZM(2):ZZ(4) = 0:ZZ(5) = 10.23:ZZ(6) = 0: GOSUB 10100: IF ZE%
    (0) = 1 THEN 15630
15640 ZM(2) = ZZ(3)
15650  VTAB 12: PRINT "D.C. BIAS ";:ZZ(3) = ZM(3):ZZ(4) =  - 10.23:ZZ(5) = 10.23:ZZ(6) = 0: GOSUB 10100
    : IF ZE%(0) = 1 THEN 15650
15660 ZM(3) = ZZ(3)
15666  IF ZM(2) +  ABS (ZM(3)) > 14 THEN  VTAB 8: PRINT "COMBINED VOLTAGE TOO LARGE": GOTO 15630
15670  VTAB 15: PRINT "WAVEFORM (SIN=0,SQR=1) ";:ZZ(3) = ZM(4):ZZ(4) = 0:ZZ(5) = 1:ZZ(6) = 1: GOSUB 101
    00: IF ZE%(0) = 1 THEN 15670
15680 ZM(5) = ZZ(3)
15690  VTAB 18: PRINT "AMPLITUDE COMP. (OFF=0,ON=1) ";:ZZ(3) = ZM(14):ZZ(4) = 0:ZZ(5) = 1:ZZ(6) = 1: GOSUB
    10100: IF ZE%(0) = 1 THEN 15690
15700 ZM(14) = ZZ(3)
15710  IF ZM(14) = 0 THEN 15300
15720  HOME : VTAB 5: PRINT "AMPLITUDE OMPRESSION ON"
15730  VTAB 8: PRINT "SOURCE CHANNEL ";:ZZ(3) = ZM(11):ZZ(4) = 1:ZZ(5) = 2:ZZ(6) = 1: GOSUB 10100: IF Z
    E%(0) = 1 THEN 15730
15740 ZM(11) =  INT (100 * ZZ(3) + 0.5)
15750  VTAB 12: PRINT "VOLTAGE LEVEL ";:ZZ(3) = ZM(12):ZZ(4) = 1E - 4:ZZ(5) = 300:ZZ(6) = 0: GOSUB 1010
    0: IF ZE%(0) = 1 THEN 15750
15760 ZM(12) = ZZ(3)
15770  VTAB 16: PRINT "ERROR PERCENT ";:ZZ(3) = ZM(13):ZZ(4) = 1:ZZ(5) = 50:ZZ(6) = 0: GOSUB 10100: IF
    ZE%(0) = 1 THEN 15770
15780 ZM(13) = ZZ(3)
15790  GOTO 15300
15800  HOME : VTAB 3: PRINT "ANALYSER"
15810  VTAB 6: PRINT "INTEGRATION TIME (SECONDS) ";:ZZ(3) = ZM(21):ZZ(4) = .01:ZZ(5) = 1E4:ZZ(6) = 0: GOSUB
    10100: IF ZE%(0) = 1 THEN 15810
15820 ZM(21) = ZZ(3)
15830  VTAB 9: PRINT "MEASUREMENT DELAY ": GOSUB 15995:ZZ(3) = ZM(11):ZZ(4) = 0:ZZ(5) = 1E5:ZZ(6) = 0: GOSUB
    10100: IF ZE%(0) = 1 THEN 15830
15840 ZM(11) = ZZ(3)
15850  VTAB 14: PRINT "INITIAL HARMONIC ";:ZZ(3) = ZM(25):ZZ(4) = 1:ZZ(5) = 16:ZZ(6) = 1: GOSUB 10100: IF
    ZE%(0) = 1 THEN 15850
15860 ZM(25) = ZZ(3)
```

```
15B70  VTAB 18: PRINT "AUTO INTEGRATE  OFF=0": PRINT "CH1(L)=1,CH2(L)=2,CH2(S)=3,CH2(S)=4":ZZ(3) = ZM(2
    6):ZZ(4) = 0:ZZ(5) = 4:ZZ(6) = 1: GOSUB 10100: IF ZE%(0) = 1 THEN 15B70
15BB0 ZM(26) = ZZ(3)
15900  VTAB 6: CALL  - 95B: VTAB B: PRINT "INPUT VOLTAGE RANGE  AUTO=0": PRINT "30MV=1,300MV=2,3V=3,30V
    =4,300V=5":ZZ(3) = ZM(27):ZZ(4) = 0:ZZ(5) = 5:ZZ(6) = 1: GOSUB 10100: IF ZE%(0) = 1 THEN 15900
15910 ZM(27) = ZZ(3)
15920  VTAB 13: PRINT "INPUT COUPLING ": PRINT "DC=0,AC=1,FREQUENCY TO CHANGE=XXX":ZZ(3) = ZX%(1):ZZ(4)
     = 0:ZZ(5) = 999:ZZ(6) = 0: GOSUB 10100: IF ZE%(0) = 1 THEN 15920
15930 ZM(49) = ZZ(3):ZM(29) = ZM(49): IF ZM(49) > 1 THEN ZM(29) = 0
15950  VTAB 2B: PRINT "INPUT (FRONT=0,REAR=1,BOTH=2) ";:ZZ(3) = ZM(50):ZZ(4) = 0:ZZ(5) = 2:ZZ(6) = 1: GOSUB
    10100: IF ZE%(0) = 1 THEN 15950
15960 ZM(50) = ZZ(3):ZM(30) = ZM(50): IF ZM(50) > 1 THEN ZM(30) = 0
15990  GOTO 15300
15995  PRINT "(S=SECONDS,C=CYCLES) ";:II = 24: PRINT "CYCLES ";: GET ZD$(0): IF ZD$(0) = "S" THEN  HTAB
    22: VTAB 10: PRINT "SECONDS";:II = 23
15996  RETURN
16000  HOME : VTAB 3: PRINT "SWEEP(S)...# OF MEASUREMENTS = ";ZM%
16010  VTAB 6: CALL  - 95B: PRINT "DC VOLTAGE SWEEP (Y/N) ? ";: GOSUB 10000:ZM(57) = 1: IF ZE%(0) = 1 THEN
    16010
16020  IF ZZ(3) = 1 THEN ZM(11B) = ZM(3):ZM(119) = ZM(3):ZM(120) = 0: GOTO 16100
16030  VTAB 9: PRINT "INITIAL DC VOLTAGE ";:ZZ(3) = ZM(3):ZZ(4) =  - 10.23:ZZ(5) = 10.23:ZZ(6) = 0: GOSUB
    10100: IF ZE%(0) = 1 THEN 16030
16040 ZM(11B) = ZZ(3)
16050  VTAB 12: PRINT "FINAL DC VOLTAGE ";:ZZ(3) = ZM(119):ZZ(4) =  - 10.23:ZZ(5) = 10.23:ZZ(6) = 0: GOSUB
    10100: IF ZE%(0) = 1 THEN 16050
16060 ZM(119) = ZZ(3)
16070  VTAB 15: PRINT "DC VOLTAGE STEP ";:ZZ(3) = ZM(120):ZZ(4) =  - 10.23:ZZ(5) = 10.23:ZZ(6) = 0: GOSUB
    10100: IF ZE%(0) = 1 THEN 16070
160B0 ZM(120) = ZZ(3)
160B5  IF  SGN (ZM(119) - ZM(11B)) <  > SGN (ZM(120)) THEN  VTAB B: PRINT "ARE YOU GOING TO CIRCLE INF
    INITY ?": GOTO 16030
160BB  IF ZM(120) = 0 THEN ZM(121) = 2:ZM(57) = 1:ZM(117) = 0: GOTO 16100
16090  VTAB 1B: PRINT "FILL ARRAY BETWEEN DC STEPS (Y/N)";: GOSUB 10000:ZM(121) = ZZ(3): IF ZM(121) = 2
     THEN 16100
16093 ZM(57) =  INT (1.5 + (ZM(119) - ZM(11B)) / ZM(120))
16095  VTAB 20: PRINT "DELAY BETWEEN DCV (/S) ";:ZZ(3) = ZM(117):ZZ(4) = 0:ZZ(5) = 1000:ZZ(6) = 0: GOSUB
    10100: IF ZE%(0) = 1 THEN 16095
16097 ZM(117) = ZZ(3)
16100  VTAB 6: CALL  - 95B: PRINT "FREQUENCY SWEEP (Y/N) ? ";: GOSUB 10000:ZM(56) = 1: IF ZE%(0) = 1 THEN
    16100
16105  IF ZZ(3) = 1 THEN ZM(34) = ZM(1):II = 34: GOSUB 21000:ZM(35) = ZM(1):II = 35: GOSUB 21000: GOTO
    16150
16110  VTAB 9: PRINT "FREQUENCY MINIMUM ";:ZZ(3) = ZM(35):ZZ(4) = 1E - 5:ZZ(5) = 65535:ZZ(6) = 0: GOSUB
    10100: IF ZE%(0) = 1 THEN 16110
16120 ZM(35) = ZZ(3):II = 35: GOSUB 17000
16130  VTAB 12: PRINT "FREQUENCY MAXIMUM ";:ZZ(3) = ZM(34):ZZ(4) = ZM(35):ZZ(5) = 65535:ZZ(6) = 0: GOSUB
    10100: IF ZE%(0) = 1 THEN 16130
16140 ZM(34) = ZZ(3):II = 34: GOSUB 17000
16150 ZM(55) = 1: IF ZM(34) > 32767 THEN ZM(25) = 1: GOTO 16200: REM NO HARMONIC POSSIBLE
16155  VTAB 6: CALL  - 95B: PRINT "HARMONIC SWEEP (Y/N) ? ";: GOSUB 10000: IF ZE%(0) = 1 THEN 16150
16160  IF ZZ(3) = 1 THEN ZM(122) = ZM(25):ZM(123) = ZM(25): GOTO 16200
```

```
16170  VTAB 9: PRINT "INITIAL HARMONIC # ";:ZZ(3) = ZM(122):ZZ(4) = 1:ZZ(5) =  INT (65535 / ZM(34)):ZZ(
    6) = 1: GOSUB 10100: IF ZE%(0) = 1 THEM 16170
16180 ZM(122) = ZZ(3)
16190  VTAB 12: PRINT "FINAL HARMONIC # ";:ZZ(3) = ZM(123):ZZ(4) = ZM(122):ZZ(5) =  INT (65535 / ZM(34)
    ):ZZ(6) = 1: GOSUB 10100: IF ZE%(0) = 1 THEN 16190
16195 ZM(123) = ZZ(3):ZM(55) = ZM(123) - ZM(122) + 1
16200  VTAB 6: CALL  - 958: PRINT "TIMED SWEEP (Y/N) ? ";: GOSUB 10000: IF ZE%(0) = 1 THEN 16200
16210  IF ZZ(3) = I THEN ZM(124) = 0:ZM(125) = ZM(124):ZM(126) = ZM(125): GOTO 16290
16220  GOSUB 18000: VTAB 9: PRINT ZD$(0): REM    CLOCK
16230  VTAB 12: PRINT "START MEASUREMENTS @ HH.MM ";:ZZ(3) = ZM(124):ZZ(4) = 0:ZZ(5) = 24:ZZ(6) = 0: GOSUB
    10100: IF ZE%(0) = 1 THEM 16230
16240 ZM(124) = ZZ(3)
16250  VTAB 15: PRINT "STOP MEASUREMENTS @ HH.MM ";:ZZ(3) = ZM(125):ZZ(4) = ZM(124):ZZ(5) = 99.59:ZZ(6)
     = 0: GOSUB 10100: IF ZE%(0) = 1 THEM 16250
16260 ZM(125) = ZZ(3)
16270  VTAB 18: PRINT "MEASUREMENT INTERVAL HH.MM ";:ZZ(3) = ZM(126):ZZ(4) = 0:ZZ(5) = 24:ZZ(6) = 0: GOSUB
    10100: IF ZE%(0) = 1 THEM 16270
16280 ZM(126) = ZZ(3)
16290 ZM(56) =  INT (ZM% / (ZM(55) * ZM(57))): GOTO 15300
16300  HOME : VTAB 3: PRINT "SCALE FACTORS:"
16310  VTAB 6: PRINT "// RESISTANCE STANDARD ";:ZZ(3) = ZM(51):ZZ(4) = .1:ZZ(5) = 1E9:ZZ(6) = 0: GOSUB
    10100: IF ZE%(0) = 1 THEM 16310
16320 ZM(51) = ZZ(3)
16330  VTAB 10: PRINT "// CAPACITANCE STANDARD ";:ZZ(3) = ZM(52):ZZ(4) = 0:ZZ(5) = 1E3:ZZ(6) = 0: GOSUB
    10100: IF ZE%(0) = 1 THEM 16330
16340 ZM(52) = ZZ(3)
16350  VTAB 14: PRINT "IMPEDANCE SCALE FACTOR ";:ZZ(3) = ZM(53):ZZ(4) = 1:ZZ(5) = 1E9:ZZ(6) = 0: GOSUB
    10100: IF ZE%(0) = 1 THEM 16350
16360 ZM(53) = ZZ(3)
16490  GOTO 15300
16500  HOME : VTAB 3: PRINT "MEASUREMENT MODE:"
16510  VTAB 5: CALL  - 958: PRINT "INPUT(S):    0=2/1": HTAB 14: PRINT "1=1": HTAB 14: PRINT "2=2": HTAB
    14: PRINT "3=(2-1)/1": HTAB 14: PRINT "4=1/(2-1)": HTAB 14: PRINT "5=1&2"
16520  VTAB 11:ZZ(3) = ZM(127):ZZ(4) = 0:ZZ(5) = 5:ZZ(6) = 1: GOSUB 10100: IF ZE%(0) = 1 THEM 16520
16525 ZM(127) = ZZ(3)
16530  VTAB 13: PRINT "OPERATOR:    0=UNITY": HTAB 14: PRINT "1=JW": HTAB 14: PRINT "2=1/JW": HTAB 14: PRINT
    "3=JW^2": HTAB 14: PRINT "4=1/JW^2"
16540  VTAB 19:ZZ(3) = ZM(116):ZZ(4) = 0:ZZ(5) = 4:ZZ(6) = 0: GOSUB 10100: IF ZE%(0) = 1 THEM 16540
16545 ZM(116) = ZZ(3)
16550  VTAB 20: PRINT "COORDINATES  0=A/B": HTAB 14: PRINT "1=R/THETA": HTAB 14: PRINT "2=LOG.R/THETA"
16560  VTAB 23:ZZ(3) = ZM(46):ZZ(4) = 0:ZZ(5) = 2:ZZ(6) = 0: GOSUB 10100: IF ZE%(0) = 1 THEM 16560
16565 ZM(46) = ZZ(3)
16570  GOTO 15300
16600  HOME : VTAB 3: PRINT "RETRIEVE SET-UP FILE"
16620  GOSUB 16680:ZZ(8) = 77: GOSUB 11300: GOTO 15000
16640  HOME : VTAB 3: PRINT "SAVE SET-UP FILE TO DISK"
16660  GOSUB 16680:ZZ(8) = 77: GOSUB 11400: GOTO 15000
16680 X =  FRE (0): GOSUB 11500: PRINT : PRINT "FILE NAME WILL BE PRECEDED BY OMSS(P)-": PRINT : INPUT
    "ENTER FILE NAME = OMSS(P)-";ZO$(0):ZF$ = "OMSS(P)-" + ZO$(0):ZO$(0) = ZF$: RETURN
16700  HOME : VTAB 3: PRINT "EXECUTE SET-UP FILE"
16710  FOR II = 1 TO 6: GOSUB 17000: NEXT II
```

```
16720 II = 14: GOSUB 17000: IF ZN(14) = 1 THEN  FOR II = 11 TO 13: GOSUB 17000: NEXT II
16730 II = 20: GOSUB 16900
16740 II = 21: GOSUB 17000:II = 24: IF ZN(23) > 0 THEN II = 23
16750  GOSUB 17000:II = 25: GOSUB 17000:II = 26: GOSUB 17000
16760  FOR II = 27 TO 30: FOR JZN = I TO 2: GOSUB 17100: NEXT JZN: NEXT II
16770 II = 34: GOSUG 17000:II = 35: GOSUB 17000:II = 46: GOSUB 17000
167B0 ZN(45) = 0201: IF ZN(127) > 0 THEN ZN(45) = 0100: IF ZN(127) > 1 THEN ZN(45) = 0200: IF ZN(127) >
    2 THEN ZN(45) = 0100
16790 II = 45: GOSUB 17000:II = 6B: GOSUB 16900
16B00 JZN = 0:II = B5:ZN(B5) = 1: GOSUB 17200: REM DISPLAY
16B02 JZN = 1:ZN(B5) = 0: GOSUB 17200
16B04 JZN = 2:ZN(B5) = 1: GOSUB 17200
16B06 JZN = 3:ZN(B5) = 1: GOSUB 17200
16B10 JZN = 1:II = B6:ZN(B6) = 0: GOSUB 17200: REM DISPLAY
16B11 JZN = 2:ZN(B6) = 0: GOSUB 17200
16B12 JZN = 3:ZN(B6) = ZN(116): GOSUB 17200
16B13 JZN = 4:ZN(B6) = 0: GOSUB 17200
16B14 JZN = 5:ZN(B6) = 0: GOSUB 17200
16B16 II = 10B: GOSUB 17000:II = 109: GOSUB 17000
16B20  GOTO 1000
16900  RESTORE : FOR I = 1 TO II: READ M$: NEXT I:N$ = ":'" + M$ + "'": GOSUB 21000: RETURN
17000  RESTORE : FOR I = I TO II: READ N$: NEXT I:N$ = ":'" + N$ +  STR$ (ZN(II)) + "'": GOSUB 21000: RETURN

17100  FOR JZN = 1 TO 2: RESTORE : FOR I = 1 TO II: READ M$: NEXT I:N$ = ":'" + N$ +  STR$ (JZN) + "," +
     STR$ (ZN(II)) + "'": GOSUB 21000: NEXT JZN: RETURN
17200  RESTORE : FOR I = 1 TO II: READ N$: NEXT I:N$ = ":'" + M$ +  STR$ (JZN) + "," +  STR$ (ZN(II)) +
    "'": GOSUB 21000: RETURN
IB000  REM CLOCK
1B010 ZZ(3) =  PEEK ( - 163B4) - I2B: REM KEY PUSN
19020  IF ZZ(3) = 1 THEN  GOTO 1000: REM  ABORT
1B0B0  IF ZZ(3) = 19 THEN IB220: REM   STATUS
1B090  IF ZZ(3) = 20 THEN ZN(47) = 999: REM  TERNINATE
1B100  IF ZZ(3) = 21 THEN ZN(47) = 0
1B190  RETURN
1B200  REM TIME
1B220 II = 1:N$ = ":'?TN0'": GOSUB 24000:ZZ(3) = ZZ(II):N$ = ":'?TN1'": GOSUB 24000:ZZ(4) = ZZ(II):ZD$(
    0) = "TINE IS " +  STR$ (ZZ(3)) + ":":N$ =  STR$ (ZZ(4)): IF ZZ(4) < 9 THEN N$ = "0" + N$
1B240 ZD$(0) = ZD$(0) + M$: VTAB 1: HTAB 2B: PRINT ZD$(0): RETURN : REM  READ CLOCK
19900  REM CHAIN SUBROUTINE
19920  HOME : VTAB 9:NPZ = 1: PRINT "LOADING DNSS."ZD$(0)
19940  PRINT  CHR$ (4);"BLOAD CHAIN,A520,S"SBZ;",D1,V"VBZ
19960  RETURN
20000 ZZZ = 12
20010 ZD$(4) = "∂" +  CHR$ (95) +  CHR$ (ZZZ + 64):ZD$(5) = "∂" +  CHR$ (95) + "?" +  CHR$ (ZZZ + 32) +
    ":"
20020 ZD$(6) =  CHR$ (4) + "IN$0":ZD$(7) =  CHR$ (4) + "PR$0"
20030 ZD$(B) =  CHR$ (4) + "PR$3":AA$ = "∂" +  CHR$ (95) + "(:'":BB$ = "X'∂?;∂H:"
20900  RETURN
21000  REM  SEND DATA TO FRA
21030  PRINT ZD$(B): PRINT ZD$(5)
21040  PRINT N$
21050  PRINT ZD$(6)
```

```
21470  PRINT ZD$(7)
21500  RETURN
24000  REM DATA RETRIEVE
24030  PRINT ZD$(8): PRINT ZD$(5)
24040  PRINT  CHR$ (13): PRINT M$: GOSUB 28500: PRINT ZD$(7): PRINT ZD$(6): RETURN
28500  PRINT  CHR$ (13);ZD$(4);":": PRINT ZD$(7): VTAB 23
28501  ON II - 1 GOTO 28504,28506,28508
28502  INPUT ZZ(1): PRINT ZD$(8): RETURN
28504  INPUT ZZ(1),ZZ(2): PRINT ZD$(8): RETURN
28506  INPUT ZZ(1),ZZ(2),ZZ(3): PRINT ZD$(8): RETURN
28508  INPUT ZZ(1),ZZ(2),ZZ(3),ZZ(4): PRINT ZD$(8): RETURN
29000  REM KEITHLEY MODEL 192 SET-UP
29200 ZD$(0) = M$ + "ROKOQOOS3MOZON1"
29220  VTAB 23
29240  PRINT ZD$(8): PRINT AA$;ZD$(0);BB$: PRINT ZD$(7): INPUT ZD$(0): PRINT ZD$(6): VTAB 23: PRINT "0"
29260 ZZ(3) =  VAL ( MID$ (ZD$(0),5)): RETURN
```

Appendix B

DIFFUSION IN AN ANGULAR CRACK

This appendix gives the solution concentration as a function of time and position in an angular crack. The mathematical representation of the crack is shown in Figure B.1. A crack tip rupture and dissolution provides the concentration C = 1 up to the r = a cell element of the angular crack. In this case, r_m is the distance from the crack origin to the m^{th} cell segment and Δ is the distance between cell segments. Thus,

$$r_m = m\Delta \tag{B-1}$$

We need to solve for $c_m(t)$ where $c_m(t)$ = average concentration in $r_{m-1} < r < r_m$ at time t and

$$m = 1,2,3...$$

Let $c = c(a,r,t)$ be the solution of the standard diffusion equation

$$\frac{\partial c}{\partial t} = D \frac{1}{r} \frac{\partial}{\partial r} \left(r \frac{\partial c}{\partial r}\right) \tag{B-2}$$

where D = diffuaion coefficient with

$$c = \begin{cases} 1 \text{ for } r < a \\ 0 \text{ for } a < r \end{cases} \qquad \text{at} \qquad t = 0$$

Assuming only nearest neighbors interact over short time t givea

$$c_1(t) = c_2(0) + [c_1(0) - c_2(0)]\, J_{-}(1) \tag{B-3}$$

and for m = 2,3,4,...; the solution for the concentration aa a function of time and position along the crack is given by

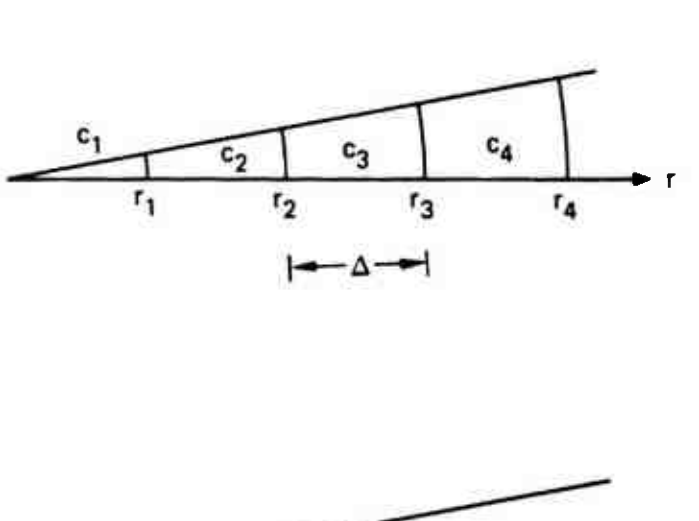

FIGURE B.1 MATHEMATICAL REPRESENTATION OF DIFFUSION IN AN ANGULAR CRACK

$$c_m(t) = c_{m+1}(0) + [c_m(0) - c_{m+1}(0)]\, J_-(m) + [c_{m-1}(0) - c_m(0)]J_+ (m-1)$$

(B-4)

where $J_-(m)$, a function of t as well aa m, is the average concentration in cell m just to the left of a unit jump in concentration at $r = r_m$ and $J_+(m)$ ia the average concentration in cell (m+1) juat to the right of the unit jump at $r = r_m$. That is,

$$J_-(m) = \frac{\int_{(m-1)\Delta}^{m\Delta} c(m\Delta, r, t)\, r\, dr}{\int_{(m-1)\Delta}^{m\Delta} r\, dr} \qquad \text{(B-5)}$$

$$J_+(m) = \frac{\int_{(m+1)\Delta}^{m\Delta} c(m\Delta, r, t)\, r\, dr}{\int_{m\Delta}^{(m+1)\Delta} r\, dr} \qquad \text{(B-6)}$$

Approximate valuea valid for $\sqrt{Dt}/\Delta << 1$ are

$$J_-(m) = 1 - \frac{\sqrt{Dt}}{\Delta} \frac{2m}{(2m-1)\sqrt{\pi}} \qquad \text{(B-7)}$$

$$J_+(m) = \frac{\sqrt{Dt}}{\Delta} \frac{2m}{(2m+1)\sqrt{\pi}} \qquad \text{(B-8)}$$

The derivation of solution (B-4) ia given aa follows.

Let $\bar{c}$ = Laplace transform of c; therefore,

$$\bar{c} = \int_0^\infty e^{-pt}\, c\, dt \qquad \text{(B-9)}$$

Then the transform of the basic problem is

$$D\left(\frac{d^2\bar{c}}{dr^2}\right)+\left(\frac{1}{r}\frac{d\bar{c}}{dr}\right)-p\bar{c}=-c_{oo} \qquad \text{(B-10)}$$

where c_{oo}, a function of r, is the initial value of c:

$$c_{oo}=\begin{cases}1 & r<s\\ 0 & a<r\end{cases}$$

Solving for $r < a$ yields

$$\bar{c}=AI_o(qr)+BK_o(qr)+1/p \qquad \text{(B-11)}$$

where I_o and K_o are the modified Bessel functions; $q=\sqrt{p/D}$; and A and B are constants of integration. Now $B = 0$ because $K_o \to \infty$ as $r \to 0$.

Solving for $a < r$ gives

$$\bar{c}=HI_o(qr)+GK_o(qr) \qquad \text{(B-12)}$$

where H and G are constants of integration and $H = 0$ because $I_o \to \infty$ as $r \to \infty$.

Both $\bar{c}$ and $d\bar{c}/dr$ are continuous at $r = a$. Therefore,

$$AI_o(qa)+1/p=GK_o(qa) \qquad \text{(B-13)}$$

$$AI_o'(qs)=GK_o'(qa) \qquad \text{(B-14)}$$

Then

$$A = \frac{qaK_o'(qa)}{p} \tag{B-15}$$

$$G = \frac{qa\, I_o'(qa)}{p} \tag{B-16}$$

by use of $K_o(x)I_o' - I_o(x)K_o'(x) = 1/x$. Therefore,

$$\bar{c} = \begin{cases} \frac{1}{p} - \frac{qa\, K_1(qa)\, I_o(qr)}{p} & r < a \\ \frac{qa\, I_1(qa)\, K_o(qa)}{p} & a < r \end{cases} \tag{B-17}$$

(B-18)

Early time approximation is as follows:

$$\frac{\sqrt{Dt}}{\Delta} << 1 \sim \frac{1}{q\Delta} << 1 \sim \frac{1}{qa} << 1$$

Then

$$K_o(qa) \doteq K_1(qa) \doteq \sqrt{\frac{\pi}{2qa}}\, e^{-qa} \tag{B-19}$$

$$I_o(qa) \doteq I_1(qa) \doteq \frac{e^{qa}}{\sqrt{2\pi qa}} \tag{B-20}$$

$$\bar{c} \doteq \begin{cases} \frac{1}{p} - \frac{1}{2p}\sqrt{\frac{a}{r}}\, e^{-q(a-r)} & r < a \\ \frac{1}{2p}\sqrt{\frac{a}{r}}\, e^{-q(r-a)} & a < r \end{cases} \tag{B-21}$$

(B-22)

Inversion of the transforms gives

$$c = \begin{cases} 1 - \frac{1}{2}\sqrt{\frac{a}{r}}\ \operatorname{erfc}\frac{a-r}{2\sqrt{Dt}} & r < a \qquad \text{(B-23)} \\ \frac{1}{2}\sqrt{\frac{a}{r}}\ \operatorname{erfc}\frac{r-1}{2\sqrt{Dt}} & a < r \qquad \text{(B-24)} \end{cases}$$

With $J_+(m)$ and $J_-(m)$ defined after equation (B-4) and with $I_+(m)$ and $I_-(m)$ being the integrals of the concentration in those definitions, one finds

$$J_+(m) = \frac{I_+(m)}{\int_{m\Delta}^{(m+1)\Delta} r\,dr} = \frac{2}{(2m+1)\Delta^2}\ I_+(m)$$

$$I_+(m) = \int_{m\Delta}^{(m+1)\Delta} \frac{1}{2}\sqrt{\frac{a}{r}}\ \operatorname{erfc}\frac{r-a}{2\sqrt{Dt}}\ r\,dr \qquad \text{(B-25)}$$

where $a = m\Delta$. The order of accuracy is $1/Q$. Approximations correct to this order can be found as follows:

$$J_-(m) = 1 - \frac{2}{(2m-1)\Delta^2}\ I_-(m)$$

$$I_-(m) = \int_{(m-1)\Delta}^{m\Delta} \frac{1}{2}\sqrt{\frac{a}{r}}\ \operatorname{erfc}\frac{a-r}{2\sqrt{Dt}}\ r\,dr \qquad \text{(B-26)}$$

Let $Q = \Delta/2\sqrt{Dt}$. Then $Q >> 1$ by assumption. Integrations are needed to order of accuracy $1/Q$.

Function ierfc(x) is defined by

$$\text{ierfc}(x) = \int_x^\infty \text{erfc}(x)\,dx = \frac{1}{\sqrt{\pi}} e^{-x^2} - x\,\text{erfc}(x) \qquad \text{(B-27)}$$

$$I_+(m) = \int_a^{a+\Delta} \frac{1}{2}\sqrt{ar}\ \text{erfc}\ \frac{r-a}{2\sqrt{Dt}}\,dr \qquad a = m\Delta \qquad \text{(B-28)}$$

Let $x = (r - a)/2\sqrt{Dt}$. Then $r = a\,(1 + x/mQ)$ and

$$I_+(m) = \int_o^Q \frac{1}{2}\,a\,\sqrt{1 + x/mQ}\,\text{erfc}(x)\ \frac{a}{mQ}\,dx$$

$$= \frac{a^2}{2mQ} \int_o^Q \sqrt{1 + x/mQ}\ \text{erfc}(x)\,dx$$

$$= \frac{m\Delta^2}{2Q}\,[H_+(m) + K_+(m)]$$

where

$$H_+ = \int_0^1 \sqrt{1 + x/mQ}\ \text{erfc}(x)\,dx$$

$$K_+ = \int_o^Q \sqrt{1 + x/mQ}\ \text{erfc}(x)\,dx$$

H_+ can be approximated by

$$H_+ = \int_o^1 [1 + \frac{1}{2}\frac{y}{mQ} + \ldots]\ \text{erfc}(x)\,dx$$

$$\doteq \int_0^1 \text{erfc}(x)\,dx$$

and to lowest (Q^0) order

$$H_+ = -\text{ierfc}(x)\Big|_0^1$$

$$= \frac{1}{\sqrt{\pi}} - \text{ierfc}(1) \qquad \text{(B-30)}$$

For H_- we get

$$H_- = \int_I^Q \sqrt{1 + x/mQ}\ \text{erfc}(x)\ dx$$

$$= \sqrt{1 + x/mQ}\ (-\text{ierfc}(\infty)) \int_1^Q - \int_1^Q (-\text{ierf}(x))\ \frac{1}{2mQ}\ (1 + \frac{x}{mQ})^{-1/2} dx$$

Then

$$H_- = \text{ierfc}(1) \qquad \text{(B-31)}$$

to lowest order. Therefore,

$$I_+(m) = \frac{m\,\Delta^2}{2\,Q\sqrt{\pi}}$$

$$J_+(m) \doteq \frac{m}{(2m+1)Q\sqrt{\pi}}$$

For $I_-(m)$ we get

$$I_-(m) = \int_{a-\Delta}^{a} \frac{1}{2}\sqrt{ar}\ \ \text{erfc}\ \frac{a - r}{2\sqrt{Dt}}\ dr$$

where

$$a = m\Delta$$
$$Q = \Delta/2\sqrt{Dt}$$

Then, with $z = (a - r)/2\sqrt{Dr}$, $r = a(1 - x/mQ)$. Thus,

$$I_{-}(m) = \frac{a^2}{2mQ} \int_0^Q \sqrt{1 - x/mQ}\ \operatorname{erfc}(x)\, dx$$

$$I_{-}(m) = \frac{a^2}{2mQ} \frac{1}{\sqrt{\pi}} \tag{B-32}$$

to lowest order, as before.

$$J_{-}(m) = \frac{m}{(2m - 1)Q\sqrt{\pi}} \tag{B-33}$$

Appendix C

DC TRANSMISSION LINE MODEL

```
1       REM "SCC TL DC  16/April/1985
2       REM "Transmission Line Model for Stress Corrosion Cracking
3       REM "BY M.C.H.McKubre
10      PRINT  CHR$ (13); CHR$ (4);"SAVE SCC TL DC#6O"
500     DIM Zn(9,200),Zm(26)
520      F = 96478
600     DATA14,.IDC,AMPS,0,.WIDTH,CM,10,.HEIGHT,CM,5,.LENGTH,CM,.1,
        .ANGLE,RAD.,.02,.BULK.pH,--,6,.RHO-E,OHM-CM,20,.RHO-S,OHM-CM,1E-5,
        .GAMMA,CM,1E-4,#.E-/ATOM,2,INTERVAL,SEC.,3600,NUMBER,SEGMENTS,20,
        TOLERANCE,MV,.1,MAX.ITER.,LOOPS,99
620     DATA 26,IO.M/M^A+,A.CM-2,1E-3,V..M/M^A+,VOLT,0,IO.M/MO,A
        .CM-2,1E-5,V..M/MO,VOLT,.1,IO.H/H2,A.CM-2,1E-5,V..H/H2,VOLT,.2,
        K,----,1E-6,MONOLAYER,COUL/CM2,1E-4,N*F*MW*RHO,COUL/CM^3,8.4E7,D,
        CM2.S-1,2E-5,PASSIVE.1,A.CM-2,1E-6,?,?,0
700     RESTORE : READ II: FOR I = 1 TO II: READ ZQ$,ZT$,Zm(I): NEXT I:
        READ IJ: FOR I = 1 + II TO IJ: READ ZQ$,ZT$,Zm(I): NEXT I:N% = Zm(12)

1000    TEXT : HOME : VTAB 3: PRINT "PROGRAM OPTIONS ARE:: PRINT
1010     PRINT : PRINT "1....SET UP NEW CONSTANTS"
1020     PRINT : PRINT "2....CALCULATE STEADY STATE"
1030     PRINT : PRINT "3....INITIALGUESS OF V"
1040     PRINT : PRINT "4....SAVE ARRAY  TO  DISK"
1050     PRINT : PRINT "5....SEND ARAY TO PIPELINE"
1090     PRINT : PRINT : PRINT "WELL ? ";: GET ZQ$: IF ZQ$ = "0" THEN  HOME :
        VTAB 15: PRINT "PROGRAM EXITED - GOTO 1000 TO RESUME": END
1100    IF  VAL (ZQ$) > 5 THEN 1000
1120    ON  VAL (ZQ$) GOTO 1500,2000,3000,4000,5000
1140    GOTO 1000
1500    GOSUB 1510: GOTO 1000
1510    HOME : VTAB 2: PRINT "SET-UP CONSTANTS – PAGE#1"
1520    RESTORE : READ II: FOR I = 1 TO II: READ ZQ$,ZT$,J: VTAB (3 + I): HTAB 4:
        PRINT I;"  ";ZQ$;: HTAB 20: PRINT Zm(I);: HTAB  2: PRINT ZT$: NEXT I
1540    VTAB 23: INPUT "HIT # TO MODIFY ";ZQ$:
         IF  VAL (ZQ$) < 1 OR  VAL (ZQ$) > II THEN 1600
1560     II =  VAL (ZQ$): FLASH : VTAB (II + 3): HTAB (1): PRINT "=>": VTAB 22: RESTORE :
        READ N: FOR I = 1 TO II: READ ZQ$,ZT$,N: NEXT I: NORMAL : PRINT
        "CHANGE ";ZQ$;: INPUT " TO ";ZQ$: IF ZQ$ <  > "" THEN Zm(II) =  VAL (ZQ$)
1580    VTAB 22: HTAB 32: PRINT ZT$: GOTO 1500
1600     HOME : VTAB 2: PRINT "SET-UP CONSTANTS -- PAGE#2"
1620    RESTORE : READ II: FOR I = 1 TO II: READ ZQ$,ZT$,J: NEXT I: READ IJ:
        FOR I = II + 1 TO IJ: READ ZQ$,ZT$,N: VTAB (3 + I - II): HTAB 4: PRINT I;"
        ";ZQ$;: HTAB 20: PRINT Zm(I);: HTAB 32: PRINT ZT$: NEXT I
1640    VTAB 23: INPUT "IIIT # TO MODIFY ";ZQ$: IF  VAL (ZQ$) = 0 THEN  RETURN
1650     IF  VAL (ZQ$) < II OR  VAL (ZQ$) > IJ THEN 1510
1660    IJ =  VAL (ZQ$): VTAB 22: RESTORE : READ N: FOR I = 1 TO II: READ ZQ$,ZT$,N: NEXT I:
        READ N: FOR I = II + 1 TO IJ: READ ZQ$,ZT$,N: NEXT I: NORMAL : PRINT "CHANGE
        ";ZQ$;: INPUT " TO ";ZQ$: IF ZQ$ <  > "" THEN Zm(IJ) =  VAL (ZQ$)
1680    VTAB 22: HTAB 32: PRINT ZT$: GOTO 1600

2000    HOME : VTAB 2: PRINT "CALCULATING STEADY STATE CONDITIONS"
2010    PRINT  CHR$ (13); CHR$ (4);"PR#1": PRINT  CHR$ (15):
        PRINT  CHR$ (9);"132N": PRINT  CHR$ (12)
2012    RESTORE : READ II: FOR I = 1 TO II: READ ZQ$,ZT$,J: PRINT I;") ";ZQ$;" = ";Zm(I);" ";ZT$:
        NEXT I: READ IJ: FOR I = II + 1 TO IJ: READ ZQ$,ZT$,J: PRINT I;") ";ZQ$;" = ";Zm(I);" ";ZT$:
        NEXT I: PRINT : PRINT "VERSION: ";: LIST 10
2014     ZQ$ = "    /    ": PRINT "LOOP";ZQ$;"NQ";ZQ$;"G";ZQ$;"SI";ZQ$;"I";ZQ$;"V":ZQ$ = "    "
```

```
2020  :SI = Zm(1)
2040  N% = Zm(12): REM "# OF SEGMENTS
2044  C = 77.4: REM "F/.5RT
2046  T = 0: REM "TIME=0
2100  Zn(0,0) = 0:Zn(7,0) = I0 ^(- Zm(6)):Zn(8,0) = Zn(7,0) ^Zm(I0) / Zm(21): FOR N = I TO N%:
      FOR M = 0 TO 6:Zn(M,N) = 0: NEXT M:Zn(7,N) = Zn(7,0):Zn(8,N) = Zn(8,0):Zn(9,N) = I:
      NEXT N: REM "INITIALISE ARRAY
2120  IF Zn(1,0) = 0 THEN Zn(1,0) = (Zm(I6) + Zm(20)) / 2: REM "INITIAL GUESS
2200  LL = 0:G = 32:NQ = 0: REM "LOOP COUNTER & INITIAL VSTEP (MV)
2220  S1 = Zm(1):I = 0:LL = LL + I: FOR N = I TO N%
2240  GOSUB 10000:TI = Zn(4,N) + Zn(5,N) + Zn(6,N):
      REM "CALCULATE INTERFACIALCURRENTS
2250  Zn(2,N) = Zm(8) * (Zm(4) / N%) / (Zm(2) * Zm(3)): REM "RS
2260  Zn(3,N) = Zm(7) / (2 * Zm(2) * (N% + 1 - N) *  TAN (Zm(5))): REM "RE
2270  Zn(0,N) = Zn(0,N - 1) + Zn(2,N) * (SI - TI): REM "VS
2280  Zn(1,N) = Zn(1,N - 1) - Zn(3,N) * (SI - TI): REM "VE
2290  I = I + TI: REM "MOVING SUM I
2299  NEXT N
2300  IF  ABS (G) < Zm(13) THEN 2500: REM "SUCCESSFUL ITERATION
2301  ZQ$ = "  ": PRINT LL;ZQ$;NQ;ZQ$;G;ZQ$;SI;ZQ$;I;ZQ$;Zn(1,0)
2305  GOSUB 9000: REM "READ KEYBOARD
2310  IF I < SI THEN 2400
2320  REM "VOLTAGE TOO LARGE
2330  IF NQ = 1 THEN G = G / 2
2340  NQ = - 1: REM "LAST LOOP FLAG
2350  Zn(I,0) = Zn(I,0) - G / I000: GOTO 2220
2400  REM "VOLTAGE TOO SMALL
2410  IF NQ = - 1 THEN G = G / 2
2420  NQ = 1:Zn(1,0) = Zn(1,0) + G / I000: GOTO 2220
2500  REM "SUCCESSFUL ITERATION TO FIND DC CONDITION @ TIME T
2520  PRINT : PRINT " V = ";Zn(1,0);" VOLTS,  I/I.SUM = ";Zm(1);"/";I" AMPS";",  ERROR =
      ";G;"MV,  TIME = ";LT;" HOURS,  LENGTH = ";Zm(4);" CM": PRINT " CRACK GROWTH =
      ";DL / Zm(11);" CM/S,  TIP PH = "; - LOG (Zn(7,N%)) /  LOG (10): PRINT
2540  LT = LT + Zm(11) / 3600: REM "TIME
2549  PRINT "BEFORE DELTA-C":ZQ$ = "  ": FOR N = 0 TO N% STEP N% / 5:
      FOR M = 0 TO 6:PRINT Zn(M,N);ZQ$;: NEXT M: PRINT N: NEXT N: PRINT : PRINT
2560  FOR N = 1 TO N%: GOSUB 11000: NEXT N: REM "NOW SOLVE
      FOR DELTA-CONCENTRATIONS
2580  Zm(4) = Zm(4) + DL: FOR N = 1 TO N%: FOR M = 7 TO 8:Zn(M,N) = Zn(M,N) * ((Zm(4) - DL)
      / Zm(4)) ^2: NEXT M:Zn(9,N) = Zn(9,N) * (Zm(4) - DL) / Zm(4): NEXT N: REM "C
      SPREAD-OUT WITH CRACK GROWTH
2599  PRINT "BEFORE DIFFUSION":ZQ$ = "  ": FOR N = 0 TO N% STEP N% /
      5:PRINTZn(0,N);ZQ$;Zn(1,N);ZQ$;: FOR M = 4 TO 9: PRINT Zn(M,N);ZQ$;: NEXT M: PRINT
      N: NEXT N:PRINT : PRINT
2600  REM "CALCULATE DIFFUSION
2620  ZZ(0) = (N% / Zm(4)) * (Zm(24) * Zm(11) * 3.14) ^.5: REM CHI
2640  FOR N = N% TO 1 STEP  - 1: GOSUB 12000  NEXT N
2699  PRINT "AFTER  DIFFUSION":ZQ$ = "  ": FOR N = 0 TO N%: FOR M = 1 TO 3 STEP 2: PRINT
      Zn(M,N);ZQ$;: NEXT M: FOR M = 4 TO 9: PRINT Zn(M,N);ZQ$;: NEXT M: PRINT N: NEXT
      N: PRINT : PRINT
2920  LL = 0:G = 4:NQ = 0: GOTO 22

3000  HOME : VTAB 4: PRINT "INITIAL GUESS OF VDC = ";Zn(1,0): PRINT : INPUT "CHANGE
      TO";ZQ$: IF ZQ$ = "0" THEN 1000
3020  IF  VAL (ZQ$) <  > 0 AND  ABS ( VAL (ZQ$)) < 2 THEN Zn(1,0) =  VAL (ZQ$)
3040  GOTO 1000
```

```
5000    REM "OUTPUT DATA TO PIPELINE
5010    GOSUB 5020: GOTO 1000
5020    PRINT CHR$ (13); CHR$ (4);"PR#1": PRINT CHR$ (9);"132N": PRINT CHR$ (15)
5040    FOR N = 0 TO N%: FOR M = 0 TO 6: PRINT Zn(M,N);"  ";: NEXT M: PRINT N: NEXT N
5080    PRINT CHR$ (13); CHR$ (4);"PR#0": RETURN

9000    REM "READ KEYBOARD
9010    ZZ(3) = PEEK ( - 16384) - 128: POKE - 16386,0: IF ZZ(3) < 1 THEN RETURN
9020    PRINT CHR$ (13); CHR$ (4);"PR#0"
9030    IF ZZ(3) = 16 THEN PRINT "": GOSUB 1510: REM "CHANGE PARAMETERS
9040    IF ZZ(3) = 20 THEN POP : GOTO 1000
9090    PRINT CHR$ (13); CHR$ (4);"PR#1": IF ZZ(3) = 16 THEN GOSUB 9100
9099    RETURN
9100    REM "PRINT PARAMETERS
9110    RESTORE : READ II: FOR I = 1 TO II: READ ZQ$,ZT$,J: PRINT I;") ";ZQ$;" = ";Zm(I);" ";ZT$:
        NEXT I: READ IJ: FOR I = II + 1 TO IJ: READ ZQ$,ZT$,J: PRINT I;") ";ZQ$;" = ";Zm(I);" ";ZT$:
        NEXT I: PRINT : RETURN
9999    PRINT CHR$ (13); CHR$ (4);"SAVE SCC TL DC#6A": END

10000   REM "INTERFACIAL ELECTRICS
10100   REM "METAL DISSOLUTION @ CRACK TIP DUE TO STRESS
10110   Zn(4,N) = 0: IF N < N% THEN 10200
10120   ZZ(0) = Zm(15) * Zm(9) * Zm(2) * TAN (Zm(5)):ZZ(1) = Zm(10):ZZ(2) = Zm(16):ZZ(3) =
        Zn(8,N): GOSUB 10800: REM "B-V 0=I0,1=N,2=V0,3=C
10140   Zn(4,N) = ZZ(5):DL = Zn(4,N) * Zm(11) / (Zm(23) * Zm(9) * Zm(5) * Zm(2)): IF DL < 0 THEN
        DL = 0: REM "DELTA-L
10200   REM "CHEMICAL PASSIVATION
10300   REM "HYDROGEN ION REDUCTION
10320   ZZ(0) = Zm(19) * 2 * Zm(2) * (Zm(4) / N%):ZZ(1) = 1:ZZ(2) = Zm(20):ZZ(3) = Zn(7,N): GOSUB
        10800: REM "B-V 0=I0,1=N,2=V0,3=C
10340   Zn(5,N) = ZZ(5)
10400   REM "METAL OXIDE REDUCTION
10410   ZZ(0) = Zn(9,N): IF ZZ(0) > 1 THEN ZZ(0) = 1
10420   ZZ(0) = ZZ(0) * Zm(17) * 2 * Zm(2) * (Zm(4) / N%):ZZ(1) = Zm(10):ZZ(2) = Zm(18):ZZ(3) =
        Zn(7,N): GOSUB 10800: REM "B-V 0=I0,1=N,2=V0,3=C
10440   Zn(6,N) = ZZ(5)
10500   REM "METAL DISSOLUTION ON CRACK WALLS
10510   ZZ(9) = (1 - Zn(9,N)): IF ZZ(9) < 0 THEN ZZ(9) = 0: REM "ACTIVE/PASSIVE
10520   ZZ(0) = Zm(15) * 2 * Zm(2) * (Zm(4) / N%):ZZ(1) = Zm(10):ZZ(2) = Zm(16):ZZ(3) = Zn(8,
        N): GOSUB 10800: REM "B-V 0=I0,1=N,2=V0,3=C
10540   ZZ(0) = (1 - Zn(9,N)): IF ZZ(0) < 0 THEN ZZ(0) = 0: REM THETA
10560   IF ZZ(0) > 0 THEN ZZ(6) = ZZ(5) * ZZ(0): GOTO 10590: REM "ACTIVE KINETICS
10580   ZZ(6) = SGN (ZZ(5)) * ABS (Zm(25) * 2 * Zm(2) * (Zm(4) / N%) * (1 - Zn(8,N)) / Zn(9,N)): IF
        ABS (ZZ(5)) < ABS (ZZ(6)) THEN ZZ(6) = ZZ(5): REM "PASSIVE DIFFUSION
10590   Zn(4,N) = Zn(4,N) + ZZ(6)
10600   RETURN
10800   REM "COMPUTE BUTLER-VOLMER I
10805   ZZ(2) = Zn(1,N - 1) - Zn(0,N - 1) - ZZ(2) + (2 / (Zm(10) * C)) * LOG (ZZ(3)): REM "ZETA
        INCLUDING CONC.
10810   ZZ(4) = ZZ(1) * C * (ZZ(2)): IF ABS (ZZ(4)) > 30 THEN ZZ(4) = SGN (ZZ(4)) * 30
10820   ZZ(5) = ZZ(0) * ( EXP (ZZ(4)) - EXP ( - ZZ(4)))
10830   ZZ(6) = Zm(2) * Zm(5) * (Zm(4) / N%) ^2 * (2 * N% - 2 * N + 1): REM "VOLUME
10839   IF N = N% AND ZZ(5) > 0 THEN 10849: REM "NO LIMIT TO M->MO @ TIP
10840   IF ABS (ZZ(5)) > ABS (99 * ZZ(1) * F * ZZ(3) * ZZ(6) / Zm(11)) THEN ZZ(5) = SGN (ZZ(5)) *
        99 * ZZ(1) * 96478 * ZZ(3) * ZZ(6) / Zm(11): REM "MAX DELTA-C
```

```
10849  REM "ZQ$ = "  ": FOR NN = 0 TO 6: PRINT ZZ(NN);ZQ$;: NEXT NN: PRINT N
10850  RETURN

11000  REM "INTERFACIAL CHEMISTRY
11020  ZZ(0) = Zm(2) * Zm(5) * (Zm(4) / N%) ^2 * (2 * N% - 2 * N + 1): REM "V
11040  ZZ(1) = Zn(4,N) * Zm(11) / (Zm(10) * F * ZZ(0)): IF ZZ(1) > Zn(8,N) / 2 THEN ZZ(1) =
       Zn(8,N) / 2: REM  "DELTA METAL IONS
11060  ZZ(2) = (Zn(5,N) + Zn(6,N)) * Zm(11) / (F * ZZ(0)): IF ZZ(2) > Zn(7,N) / 2 THEN ZZ(2) =
       Zn(7,N) / 2:REM "DELTA PROTONS
11080  ZZ(3) = Zn(6,N) * Zm(11) / (Zm(10) * Zm(22) * Zm(2) * (Zm(4) / N%)): IF ZZ(3) > Zn(9,N) / 2
       THEN ZZ(3) = Zn(8,N) / 2: REM "DELTA METAL OXIDE
11100  Zn(7,N) = Zn(7,N) - ZZ(2):Zn(8,N) = Zn(8,N) - ZZ(1):Zn(9,N) = Zn(9,N) - ZZ(3): REM:
       "ELECTROCHEMISTRY
11120  ZZ(9) = (Zn(8,N) - ZZ(8)) * F * Zm(10) / (Zm(23) * Zm(2) * (Zm(4) / N%) * 2): IF ZZ(9)
       >Zn(9,N) / 2 THEN ZZ(9) = Zn(9,N) / 2: REM "DELTA OXIDE
11140  ZZ(5) = Zn(9,N): IF ZZ(5) > 1 THEN ZZ(5) = 1: REM "MO ACTIVITY
11160  Zn(7,N) = (Zn(8,N) * Zm(21) / ZZ(5)) ^(1 / Zm(10)):Zn(8,N) = ZZ(5) * (Zn(7,N) ^Zm(10)) /
       Zm(21):Zn(9,N) = Zn(9,N) - ZZ(9): REM "CHEMISTRY
11600  RETURN

12000  REM
12020  ZZ(3) = 2 * (N% - N):ZZ(1) = (ZZ(3) + 3) / (ZZ(3) + 1): REM "V N-1/N
12040  ZZ(2) = (ZZ(3) - 1) / (ZZ(3) + 1): IF ZZ(2) < 0 THEN ZZ(2) = 0: REM "V N+1/N
12080  IF ZZ(0) > .5 THEN 12200
12100  REM "SHORT TIME
12120  FOR M = 7 TO 8:Zn(M,N) = Zn(M,N) * (1 - ZZ(0)) + ZZ(1) * ZZ(0) * (3 * Zn(M,N) + Zn(M,N -
       1)) / 4 + ZZ(2) * ZZ(0) * (3 * Zn(M,N) + Zn(M,N + 1)) / 8: NEXT M
12160  RETURN
12200  REM "LONG TIME
12220  FOR M = 7 TO 8:Zn(M,N) = ZZ(1) * (3 * Zn(M,N) + Zn(M,N - 1)) / 8 + ZZ(2) * (3 * Zn(M,N)
       +Zn(M,N + 1)) / 8: NEXT M
12260  RETURN
```

APPENDIX ?? DC Transmission Line Model